Supported Metal Catalyst for Degradation of Toxic Organic Pollutants in Industrial Effluent

Thesis submitted in the fulfilment of the requirement of
Master of Chemical Engineering

By
Soumyajit Das
Registration No. 135726 of 2016-17
Examination Roll No. M4CHE24003
Class Roll No. 002210302003

Under the supervision of
Dr. Shyamal Roy
Assistant Professor
CHEMICAL ENGINEERING DEPARTMENT
JADAVPUR UNIVERSITY
KOLKATA-700032

CERTIFICATE

This is to certify that the project report entitled "Supported metal catalyst for degradation of toxic organic pollutants in industrial effluent" being submitted by **Soumyajit Das**, M.E. Chemical Engineering Dept., Jadavpur University, **Examination Roll No. M4CHE24003**, **Registration No. 135726 of 2016-17**, is a record of research work carried out under my guidance and supervision in conformity with the rules and regulations of Jadavpur University. The result presented in this report has not been submitted, in part or full, to any other University or Institute.

DEAN
Faculty of Engineering & Technology
JADAVPUR UNIVERSITY
KOLKATA-700 032

Dipak Laha 30/5/24

Prof. Dipak Laha
Dean
Faculty of Engineering and Technology
Jadavpur University
Kolkata

30/5/24

Prof. Papita Das
Chemical Engineering Department
Jadavpur University
Kolkata

HEAD
CHEMICAL ENGINEERING DEPARTMENT
JADAVPUR UNIVERSITY
Kolkata-700 032

Shyamal Roy 30/05/2024

Dr. Shyamal Roy
Assistant Professor
Chemical Engineering Department
Jadavpur University
Kolkata

Assistant Professor
CHEMICAL ENGINEERING DEPARTMENT
JADAVPUR UNIVERSITY
Kolkata-700 032

ACKNOWLEDGMENT

I owe a great deal of gratitude to Dr. Shyamal Roy, Assistant Professor in the Department of Chemical Engineering at Jadavpur University, for his valuable guidance. I am also thankful to PhD scholars Mr. Avik Kr. Basu and Mr. Abhishek Siuli, Ms. Sushmita Maity, and Mr. Arijit Saha, M.E., Chemical Engineering. Dept., Jadavpur University, for their kind cooperation.

Soumyajit Das
31/05/2024

.....

Signature of the candidate

Master of Engineering,

Chemical Engineering Department

Jadavpur University

Kolkata

TABLE OF CONTENTS

Sl No.	Contents	Page No.
1.	**Introduction**	1
1.1.	Comparison of various Wastewater Treatment Techniques (WWT.T)	5
1.2.	Various Traditional Wastewater Treatment Methods	6
1.3.	Several treatment technologies	7
1.4.	Various methods for catalyst preparation	17
1.5.	Different types of reactors used for oxidation reactions	30
1.6.	Different types of Supports used for catalyst preparation	36
1.7.	Selection of metals	41
2.	**Literature Review**	45
3.	**Experimental Procedure**	74
3.1.	Synthesis of catalyst	74
3.1.1.	Excess Solution Impregnation Method	74
3.2.	Characterization Techniques	76
3.2.1.	Brunauer-Emmett-Teller (BET) Surface Area Measurement Technique	76
3.2.2.	Thermogravimetric analysis (TGA)	78

3.3. Oxidation reactor set up 81

3.4. Conversion measurements 82

4. **Results and Discussion** 85

4.1. Characterization Techniques 85

4.1.1. Brunauer-Emmett-Teller (BET) Surface Area Measurement Technique 85

4.1.2. Thermogravimetric analysis (TGA) 87

4.2. Effect of temperature on degradation of acetic acid 88

4.3. Effect of stirring speed (rpm) on acetic acid degradation 90

4.4. Effect of loading of metal on acetic acid degradation 91

4.5. Effect of initial concentration of acetic acid on the degradation of acetic acid 92

4.6. Modeling of the reaction: Power Law Model 93

4.7. Mechanism of the reaction 94

5. **Conclusions and future work** 96

5.1. Conclusions 96

5.2. Future Work 97

References 98

Appendix A

Appendix B

Appendix C

Biodata

LIST OF FIGURES

Fig. No.	Contents	Page No.
Fig.1.	Adsorption process	8
Fig.2.	A typical waste incineration plant.	9
Fig.3.	Schematic representation of the electrocoagulation process	11
Fig.4.	Ion exchange resin used in water treatment	12
Fig.5.	Wet air oxidation in a sludge treatment line	15
Fig.6.	Schematic diagram for catalyst synthesis by wet impregnation method	18
Fig.7	Flow chart of co-precipitation method	19
Fig.8.	Schematic of different stages of the sol-gel process. from precursor to aerogel	20
Fig.9.	Schematic illustration of template-assisted synthesis of Ag-/ZnO-PMOS	21
Fig.10.	Schematic diagram of ion exchange set up for adsorption of ammonium from wastewater	22
Fig.11.	Mechanochemical synthesis of C-ABC	23
Fig.12.	ALD process. schematic of one cycle of Al_2O_3 ALD growth	24
Fig.13.	Hydrothermal synthesis process	25
Fig.14.	Schematic diagram for the microemulsion method	26
Fig.15.	Schematic overview of electrodeposition for the electrochemical separation of organic/inorganic compounds from waste streams	27
Fig.16.	Flame spray pyrolysis apparatus	28
Fig.17.	Schematic of the spray drying process	29
Fig.18.	Diagram of layer-by-layer deposition of ABS material	29
Fig.19.	Schematic diagram of the pulsed laser deposition (PLD) set-up	30
Fig.20.	Schematic diagram of batch reactor	31
Fig.21.	Continuous stirred tank reactor (CSTR)	32
Fig.22.	Plug flow reactor	33

Fig.23.	Schematic view of the single-tube fixed-bed reactor	34
Fig.24.	Fluidized bed reactor for polyethylene production	35
Fig.25.	Schematic of two configurations of the tubular membrane reactor	35
Fig.26.	Schematic diagram of the fabricated microreactor	36
Fig.27.	Microstructure of Al_2O_3	37
Fig.28.	Crystal structure of SiO_2	38
Fig.29.	Representative zeolite frameworks, (with pore openings)	39
Fig.30.	Schematic diagram of the ESI method	75
Fig.31.	Excess Solution Impregnation (ESI)	75
Fig.32.	Underlying scientific principle of the BET technique	77
Fig.33.	BET Instrument	78
Fig.34.	TGA Instrument	80
Fig.35.	Three-necked bottle flask	81
Fig.36.	Schematic diagram of wet air oxidation	82
Fig.37.	Titration with Sodium Hydroxide	83
Fig.38.	Adsorption-Desorption curve	85
Fig.39.	TGA curve	87
Fig.40.	Effect of temperature on AA degradation	88
Fig.41.	Arrhenius's plot for the reaction	89
Fig.42.	Effect of rpm on AA degradation	90
Fig.43.	Effect of metal loading on AA degradation	91
Fig.44.	Effect of initial concentration of acetic acid on AA degradation	92
Fig.45.	The curve of rate of oxygen vs. concentration of acetic acid	93

LIST OF TABLES

Table No.	Content	Page No.
Table 1.	Impact of typical water contaminants	2
Table 2.	Post-reaction BET surface area for Cs-promoted Fe/Al_2O_3 catalysts	86
Table 3.	BET surface area of reduced catalysts as measured using N_2 physisorption	86
Table 4.	BET surface area of different catalyst	86

ABSTRACT

The study investigates the process of catalytic wet air oxidation (CWAO) of acetic acid by using a catalyst (iron with different weight percentages, supported on alumina), prepared by the Excess Solution Impregnation (ESI) method. Brunauer-Emmett-Teller (BET) surface area measurement and thermogravimetric analysis (TGA) were used for the characterization of the catalyst. The BET analysis yielded data on the catalyst's specific surface area, which was determined to be 77.97 m^2/g and the analysis offered information on the catalyst's adsorption capacity. The TGA analysis revealed insights into the catalyst's thermal stability and breakdown properties and results showed a total weight loss of -17.6 wt. % in the temperature range of 70^{o}C to 760^{o}C. The activation energy was found to be 95.901 kJ/mol. Various key reaction parameters, including temperature, mixing speed, metal loading, and initial acetic acid concentration, were varied to carry out the catalytic wet air oxidation of acetic acid. The maximum level of degradation of acetic acid was achieved under the optimum conditions of a temperature of 80°C, a mixing speed of 400 rpm, an iron loading of 1.5 wt.%, and an initial concentration of 1000 ppm. The introduction of a power law model to the reaction kinetics provided mechanistic insights into the CWAO process. The process of acetic acid oxidation by an iron catalyst, with the involvement of molecular oxygen, has been explained, emphasizing the mechanism of the reaction. The iron catalyst supported on alumina showed satisfactory performance in the catalytic wet air oxidation (CWAO) of acetic acid, with a maximum conversion rate of 88.5% under the most optimum conditions.

LIST OF ABBREVIATIONS

AC	: Activated carbon
ACBS	: Activated carbon beads
SAC	: Activated carbon from sewage sludge
AOPS	: Advanced oxidation processes
NH_3-TPR	: Ammonia-temperature programmed reduction
APBBRS	: Anaerobic packed bed biofilm reactors
ASBBRS	: Anaerobic structured bed biofilm reactors
ALD	: Atomic layer deposition
bcm	: Billion cubic meters
BMP	: Biochemical methane potential
BOD	: Biological oxygen demand
BPA	: Bisphenol A
BET	: Brunauer-emmett-teller
CNFS	: Carbon nanofibers
CWAO	: Catalytic wet air oxidation
COD	: Chemical oxygen demand
C-ABC	: Chitosan-activated bentonite composite
Cl-vocs	: Chlorinated volatile organic compounds
CIP	: Ciprofloxacin
COCM	: Cobalt oxide
WWT.T	: Comparison of various Wastewater Treatment Techniques
CSTRS	: Continuous stirred-tank reactors
CV	: Crystal violet
DFT	: Density functional theory
EC	: Electrocoagulation
EDX	: Energy-dispersive X-ray spectroscopy
EDX	: Energy-dispersive X-ray spectroscopy
ESI	: Excess solution impregnation method
FTIR	: Fourier transform infrared
FDM	: Fused deposition modeling
PMG	: Glyphosate
(HAADF-STEM)	: High-angle annular dark-field scanning transmission electron microscopy
HA	: Humic acid
HS	: Humic substance
HRT	: Hydraulic retention time
H_2-TPR	: Hydrogen-temperature programmed reduction
IOR	: Industrial organic raffinate
FE-NP	: Iron nanoparticle

LCA : Life cycle assessment
LHSV : Liquid hourly space velocity
MBR : Membrane bioreactor
MD : Membrane distillation
MOFS : Metal-organic frameworks
TM-S : Metal-to-semiconductor transition temperature
NF : Nanofiltration
NCIWRD : National Commission on Integrated Water Resources Development
FTO : New transformer oil
OLR : Organic loading rate
PMS : Peroxymonosulfate
POPS : Persistent organic pollutants
Pl : Photoluminescence spectroscopy
PFRS : Plug flow reactors
PWPO : Promoted wet peroxide oxidation
PSO : Pseudo-second-order
ROS : Reactive oxygen species
RR2 : Reactive red 2
SEM : Scanning electron microscopy
SEM : Scanning electron microscopy
SBET : Significant specific surface area
SRT : Sludge retention time
SCOD : Soluble chemical oxygen demand
SMX : Sulfamethoxazole
TGA : Thermogravimetric analysis
TCOD : Total chemical oxygen demand
TOC : Total organic carbon
TSS : Total suspended solids
TMP : Trans-membrane pressure
UF : Ultrafiltration
WTO : Waste transformer oils
WAO : Wet air oxidation
WO : Wet oxidation
XRD : X-ray diffraction

DEDICATED
TO
MY PARENTS

CHAPTER 1

INTRODUCTION

CHAPTER 1

INTRODUCTION

Water is essential for life on Earth, serving as the foundation for various ecological and human processes. Although there are abundant water resources, they remain largely inaccessible to humans due to their composition of salt water in oceans and seas and ice in glaciers. (97.2%) of Earth's water is found in oceans and seas in the form of saltwater and an additional 2.15% of the Earth's water is sequestered in glaciers with merely 0.65% of the total water mass classified as freshwater, representing a finite and crucial resource for human sustenance (Kurian, M., 2021). In recent decades, global freshwater resources have faced significant pollution due to rapid industrialization and urbanization. Both natural and man-made factors, including overexploitation of water for domestic, industrial, and irrigation purposes, contribute to this degradation. Unfortunately, the situation is expected to deteriorate further due to the cumulative effects of climate change and population growth (Carneiro et al., 2020). India, despite having the biggest worldwide freshwater asset, endures from inadequate water supply to meet its expanding requests. The National Commission on Integrated Water Resources Development (NCIWRD) ventures a water demand of 843 billion cubic meters (bcm) in 2025 and 1180 bcm in 2050, including different segments like water systems, drinking water, industry, and vitality. With the world's population expected to reach 9 billion by 2050, and India contributing 17.7% to the whole, the water shortage issue escalates. Alarmingly, more than 2.2 million people succumb annually to the lack of access to fresh drinking water globally (Manna and Sen, 2023). Water contamination occurs when a body of water is negatively impacted by the introduction of substantial quantities of substances. If the water becomes unsuitable for its intended purpose, it is considered polluted. The origin of water pollution, as indicated in Table 1, can be either a point source or a nonpoint source.

Point sources of water pollution occur when harmful substances are directly released into a water body from a single discharge point. On the other hand, nonpoint sources distribute pollutants across a wide area. For instance, water pollution of this kind happens when pesticides or fertilizers are washed from agricultural fields by rain and carried into a water body like a lake or river. While pollution from nonpoint sources is responsible for most contaminants in streams and lakes, it is significantly more challenging to manage. The presence of nutrients such as nitrates and phosphorus exceeding acceptable levels in freshwater ecosystems and the toxicity caused by pesticides remains a global concern.

Table 1. Impact of typical water contaminants (Roy et al., 2010)

POLLUTANT	PRIMARY SOURCE	EFFECTS
Organic Matter	Industrial wastewater and domestic sewage	Drains oxygen from the water as it breaks down, putting stress on or suffocating aquatic organisms.
Excess nutrients (nitrates, phosphorous)	Run-off from agricultural lands and urban areas	Promotes excessive algae growth through a process called eutrophication, which, upon decomposition, depletes oxygen in the water, harming aquatic life. Elevated nitrate levels in drinking water can also cause illness in humans.
Heavy metals	Industries and mining sites	Endures in freshwater habitats such as river sediments and wetlands for extended durations, accumulating within the bodies of fish and shellfish. It poses a threat to both aquatic organisms and humans.
Microbial contaminants (e.g., cryptosporidium, cholera and other bacteria, amoebae, etc.)	Domestic sewage, cattle, natural sources	Transmits infectious diseases via polluted water sources, leading to millions of cases of diarrheal diseases and intestinal parasites.

POLLUTANT	PRIMARY SOURCE	EFFECTS
Toxic organic compounds (oil, pesticides, some plastics, industrial chemicals)	Wide variety of sources, from industrial sites to automobiles to farmers and domestic gardeners	Manifests various toxic effects in aquatic animals and humans, ranging from mild immune suppression to acute poisoning or reproductive failure.
Dissolved salts (salinization)	Washed out of alkaline soils due to excessive irrigation or pulled into coastal aquifers as a result of over-extraction of groundwater.	Results in the accumulation of salt in soils, leading to crop damage or reduced yields. Additionally, it renders freshwater sources unfit for drinking.
Acid precipitation or acid run-off	Deposition of sulfate particles, mostly from coal combustion. Acid run-off from mine tailings and sites	Acidifies lakes and streams, which harms or kills aquatic organisms and leaches heavy metals such as aluminum from soils into water bodies.
Silt and suspended particles	Soil erosion and construction activities on watersheds	Diminishes the quality of water for both drinking and recreational purposes, while also deteriorating aquatic habitats by covering them with sediment, disrupting spawning activities, and hampering feeding processes.
Thermal pollution	Fragmentation of rivers by dams and reservoirs, slowing water and allowing it to warm. Industrial uses such as cooling towers	Affects oxygen levels and decomposition rate of organic matter in water column. May shift the species composition of a river or lake

Industrial effluents contain a variety of pollutants, including organic compounds, heavy metals,

nutrients, and suspended solids. Inadequately processed effluents from industry pose risks to surface water quality, groundwater resources, and the environment as a whole. The collective effluent output reaches 500 million units daily. Nevertheless, conventional wastewater treatment methods encounter growing difficulties in handling complex contaminants arising from swift industrialization. Adherence to stringent discharge limits has emerged as a significant concern in this scenario, as highlighted by research studies (Zhang et al., 2020; Mishra et al., 2021). If not properly managed, the release of both industrial and domestic effluent poses a significant risk not only to the aquatic ecosystem (Sushma et al., 2018) but also to human health (Tran et al., 2018). To mitigate impacts on the environment and health of industry pollution, efficient wastewater treatment strategies are therefore required. There is a growing need for water treatment due to the increasing demand for water reuse and stricter water quality regulations. To meet these requirements, it is essential to treat various waste streams containing pollutants. The focus is particularly on water-containing organic compounds, which are commonly found in effluents from chemical, petrochemical, textile, and pharmaceutical processes (Roy et al. 2017). Water pollution arises from the synthesis and application of industrial products in various areas such as nutrition, transportation, accommodation, and energy production. Although often overlooked, chemical processes are vital for sustaining life and achieving a high standard of living. Essential products for modern life, including medications, cleaning agents, cosmetics, stabilizers, fertilizers, pesticides, fuel, batteries, polymers (such as thermoplastics, thermosetting resins, elastomers, and fibers), paints, and dyes, inevitably lead to pollution during their production, usage, and disposal (Roy et al., 2010).

Acetic acid, which is widely used in a range of industrial sectors like chemical manufacture, food processing, and pharmaceuticals, represents one of these pollutants. While valuable in many applications, acetic acid can become a significant environmental contaminant when

discharged into wastewater without adequate treatment. Its presence in industrial effluents not only poses risks to aquatic life and ecosystems but also threatens human health through the contamination of drinking water sources.

1.1. Comparison of various Wastewater Treatment Techniques (WWT.T)

The development of efficient and eco-friendly methods for the treatment of contaminated waters is an urgent necessity. Researchers worldwide have tried to tackle this growing problem by designing different wastewater treatment processes depending on their composition, that effectively remove pollutants either by one simple method or a combination of different methods sequentially. Wastewater treatment techniques (WWT.Ts) are commonly categorized into physical, chemical, and biological methods. Physical techniques encompass sedimentation (Lin et al., 2017), adsorption (Mustafa and Asmatulu, 2020), and membrane separation (Yang et al., 2018). Industries commonly utilize various WWT.Ts, including physicochemical methods (such as adsorption, reverse osmosis, coagulation, precipitation, and membrane separation), incineration, and advanced oxidation processes (like wet air oxidation and ozonation). Often, a combination of these techniques is employed to effectively treat wastewater. Conventional WWT.Ts such as chlorination, once considered a reasonably viable and practical method for water treatment purposes for many decades, have become nearly obsolete in recent times. This shift is primarily due to concerns over the potential adverse health effects of the by-products formed during the chlorination process. Additionally, the raised standards for drinking water parameters have also played a role in its diminishing usage. Conventional sewage treatment methods frequently face difficulties and require an exploration of alternatives to effectively remove acetic acid, as well as a range of pollutants from the

environment. Traditional water treatment methods have limitations when it comes to effectively removing many toxic organic pollutants.

1.2. Various Traditional Wastewater Treatment Methods

1.2.1. Primary Treatment

Primary treatment involves the physical separation of solid and floating materials from wastewater. This process typically employs sedimentation tanks, where heavier particles settle at the bottom due to gravity, forming sludge, while lighter materials float to the surface and are skimmed off. Primary treatment significantly reduces the organic load in wastewater by targeting suspended solids and gross pollutants. (Samer, M., 2015)

1.2.2. Secondary Treatment

Secondary treatment also known as 'Biological Treatment' focuses on the biological degradation of organic matter present in wastewater. The most common method used in secondary treatment is the activated sludge process, where microorganisms break down organic pollutants into simpler compounds through aerobic digestion. In this process, wastewater is mixed with activated sludge—a mixture of bacteria and other microorganisms—in aeration tanks, allowing microbial metabolism to occur. The treated water is then separated from the sludge through sedimentation, and the excess sludge is either recycled or disposed of. (Samer, M., 2015)

1.2.3. Tertiary Treatment

Tertiary treatment is an advanced stage of wastewater treatment aimed at further improving water quality by removing residual contaminants that may remain after primary and secondary

treatment processes. Various methods such as filtration, disinfection, and chemical treatment are employed in tertiary treatment. Filtration techniques like sand filtration and membrane filtration are effective in removing fine particles, pathogens, and dissolved organic matter. Disinfection methods such as chlorination, UV irradiation, and ozonation are utilized to kill or inactivate remaining pathogens, ensuring the safety of treated water. As a result, there is a clear demand for the development of new, compact, and more efficient treatment processes. These advanced technologies aim to address the challenges posed by the presence of complex organic pollutants in wastewater and the necessity for environmentally friendly and sustainable solutions. There is an urgency to find better methods to ensure water quality and promote water reuse in the face of increasing pollution and regulatory requirements. Various treatment technologies can be utilized based on the nature and volume of the wastewater effluent. These technologies aim to address the challenges posed by different levels of chemical oxygen demand (COD) and organic concentrations in the effluent.

1.3. Several treatment technologies

1.3.1. Adsorption

Absorption in wastewater treatment involves the adherence of contaminants dissolved or suspended in the wastewater onto a solid surface. The surface can be a porous material, such as activated carbon, or a biological medium like biofilms in a treatment tank. Pollutants are physically or chemically trapped in the absorbent material, thereby removing them from the wastewater. Many of its advantages include the removal of contaminants as absorption is an effective method of removing a wide range of pollutants from wastewater, including organic compounds, heavy metals, and certain dissolved gases. Different absorbent materials can be used depending on the specific contaminants present in the wastewater. This versatility allows

for specific treatment approaches to address different types of pollution. Absorption processes can achieve high removal efficiencies for specific pollutants, resulting in treated wastewater that meets regulatory standards for discharge into the environment. Absorption systems can be operated and maintained easily compared to some other wastewater treatment technologies. They may require minimal supervision and can be automated in some cases. The disadvantages include limited capacity as absorbent materials have a limited capacity to adsorb contaminants. Once this capacity is reached, the material needs to be regenerated or replaced, which can incur additional costs. Some absorbents may selectively adsorb certain pollutants over others, leading to incomplete removal of all contaminants present in the wastewater. In cases where the absorbent material becomes saturated with pollutants, regeneration processes may be required to restore its adsorption capacity. Regeneration processes can be energy-intensive or involve the use of chemicals, which adds complexity and cost to the treatment process. Disposal of spent absorbent materials after use can pose environmental challenges if the absorbed pollutants are not properly managed. This can include the risk of re-release of pollutants into the environment or the generation of hazardous waste.

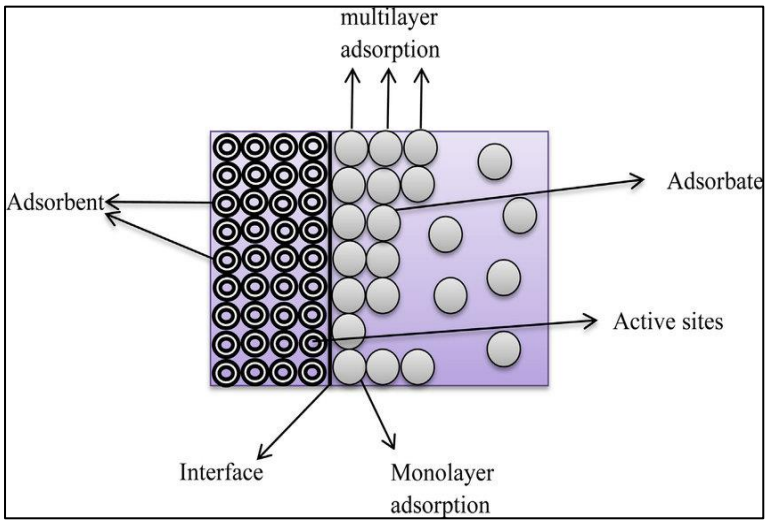


Fig.1. Adsorption process (Soliman et al. 2020)

1.3.2. Incineration

Incineration is a thermal treatment process that involves the controlled burning of waste materials at high temperatures. Organic substances in the waste are converted into ash, gases, and heat. Incineration may be applied to treat sludge generated during the wastewater treatment process. Sludge is the solid residue separated from wastewater during primary and secondary treatment processes. The advantages include volume reduction as incineration reduces the volume of sludge significantly, as organic matter is burned off, leaving behind ash, minimizing the need for storage and disposal space. Incineration effectively destroys pathogens present in sludge and reduces the risk of disease transmission associated with handling and disposal of untreated sludge. The heat generated during incineration can be recovered and used to produce steam or electricity.

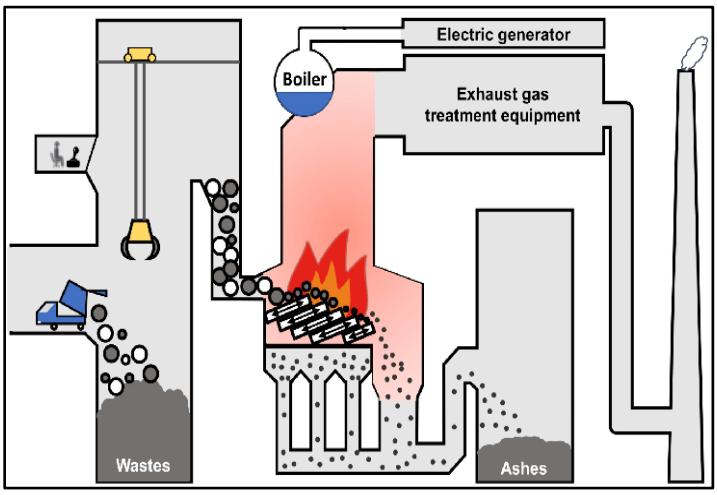


Fig.2. A typical waste incineration plant. (Kaneko et al, 2019)

Ash produced from incineration may contain valuable nutrients and minerals that can be recycled for various purposes, such as agricultural applications. The disadvantages include air emissions as incineration releases air pollutants such as nitrogen oxides, sulphur dioxide, heavy

metals, and particulate matter into the atmosphere, which can contribute to air pollution and have adverse health effects if not properly controlled. Although volume is reduced, incineration still produces ash residue, which requires proper disposal. Depending on the composition of the ash, it may need to be managed as hazardous waste, posing challenges for disposal and potentially requiring specialized treatment. Incineration facilities require significant capital investment and operational costs, including maintenance, monitoring, and compliance with emissions regulations.

1.3.3. Electrocoagulation Process

The electrocoagulation process works on the principle of passing an electric current through the wastewater between two electrodes (usually made of aluminum or iron). Coagulant species, such as metal hydroxide ions, are formed at the electrodes and they neutralize charged particles (both dissolved and suspended) in the wastewater, causing them to aggregate and form larger particles called flocs. The flocs can then be easily separated from the water through settling, flotation, or filtration processes, thereby removing contaminants from the wastewater. The advantages include the effective removal of contaminants. Electrocoagulation can effectively remove a wide range of contaminants from wastewater, including suspended solids, heavy metals, organic compounds, and certain pathogens. The electrocoagulation process does not rely on the addition of chemical coagulants unlike conventional coagulation processes as it generates coagulants in situ through electrochemical reactions, reducing the need for external chemical additives. Electrocoagulation can be applied to industrial effluents, municipal wastewater, and stormwater runoff. The flocs formed during electrocoagulation typically have larger particle sizes and settle more readily than those formed in conventional coagulation processes, leading to reduced sludge generation and easier sludge de-watering.

Electrocoagulation systems can be designed to operate at relatively low energy consumption levels, especially compared to other advanced treatment processes such as membrane filtration or UV disinfection. The disadvantages include operating costs as electrocoagulation eliminates the need for chemical coagulants, and it requires electricity to power the electrodes, which can contribute to operating costs. Electrodes may degrade over time due to corrosion or fouling, requiring periodic cleaning or replacement to maintain system performance. Scaling up electrocoagulation systems for large-scale wastewater treatment applications can be challenging and may require additional engineering considerations and infrastructure. Electrocoagulation systems may require skilled operators to monitor and control operating parameters such as current density, pH, and electrode spacing to ensure optimal treatment performance. While electrocoagulation is effective for removing suspended solids and some dissolved contaminants, it may be less efficient for highly soluble or non-ionic contaminants.

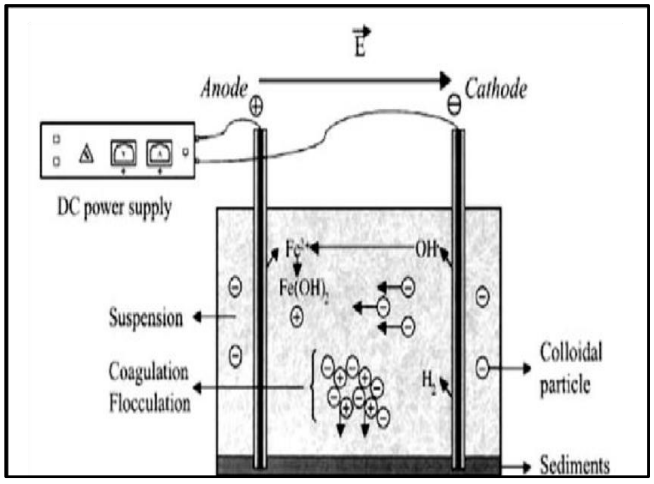


Fig.3. Schematic representation of the electrocoagulation process (Ni'am et al.)

1.3.4. Ion exchange resin

Ion exchange resin is a solid, insoluble material consisting of small beads or granules with a high surface area. These resins contain functional groups that can attract and exchange ions in

solution. In wastewater treatment, ion exchange resins are used to remove dissolved ions, such as heavy metals, nitrate, sulfate, and other contaminants, from water by exchanging them with ions of similar charge attached to the resin. The advantages include selective removal as ion exchange resins selectively remove specific ions from wastewater based on their chemical properties thus removing targeted removal of contaminants without affecting other water constituents. Ion exchange processes can achieve high removal efficiencies for targeted contaminants, resulting in treated water that meets regulatory standards for discharge or reuse. Ion exchange resins can be regenerated by eluting the bound ions from the resin, allowing for the reuse of the resin, and making it a cost-effective treatment option in the long term. The disadvantages include limited capacity as ion exchange resins have a finite capacity for ion exchange, after which they become saturated and require regeneration or replacement.

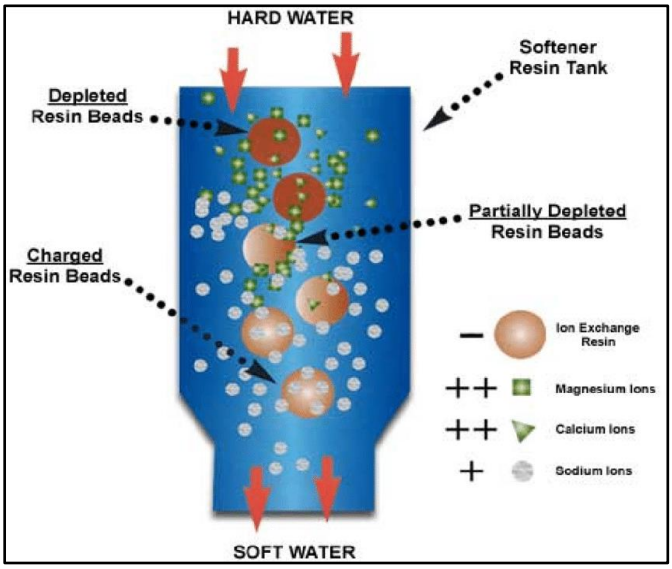


Fig.4. Ion exchange resin used in water treatment (Miklovicz et al 2014)

Regeneration of ion exchange resins produces a concentrated brine or regenerant solution containing the removed ions, which must be properly disposed of or treated to prevent

environmental impacts. Ion exchange systems may require careful monitoring and control of operating parameters such as flow rates, regeneration cycles, and bed depth to maintain optimal performance. Improper operation can lead to reduced efficiency or resin fouling. The initial capital investment for ion exchange systems, including the cost of the resin, vessels, pumps, and instrumentation, can be relatively high compared to some other treatment technologies.

1.3.5. Advanced oxidation processes (AOPs)

AOPs find application in various water treatment processes, including treating industrial effluents from distilleries, agrochemicals, pulp and paper facilities, textiles, oilfields, and metal-plating facilities. They are also used in managing hazardous effluents from hospitals and slaughterhouses, eliminating pathogens and persistent pharmaceutical residues from municipal wastewater treatment plants, and removing heavy metals such as arsenic and chromium from water. The categorization of AOPs depends on the method used to generate the transient hydroxyl radical. The integration of a catalyst has also been explored in conjunction with various oxidizing agents, to lower operating temperatures and pressures, and/or address pollutants that remain resilient to non-catalytic liquid-phase oxidation methods. Both homogeneous and heterogeneous catalysts have found successful applications in AOPs. Heterogeneous systems offer clear advantages over homogeneous ones, including easy catalyst separation for reuse, elimination of the need for secondary treatments to remove dissolved metals from treated water, and resilience under extreme operating conditions. Furthermore, heterogeneous systems are effective across a broader pH range, including the typical pH levels found in natural water and wastewater (pH 2–9). The presence of active, stable, and efficient catalysts is pivotal in eliminating pollutants in AOPs. Various catalysts, such as transition metal oxides, hydrotalcite-like compounds, metal-exchanged clays, and zeolites, have been

documented in the literature (Kurian et al. 2021). Wet air oxidation (WAO) is an advanced oxidation process (AOP) used to treat wastewater containing organic pollutants that are difficult to decompose by conventional biological treatment methods. It operates under high temperature and pressure conditions, typically from 150°C to 320°C and pressures from 10 to 200 atm, depending on the specific application and reactor design. The process begins by introducing wastewater into a reaction vessel, where it is pressurized and heated. Oxygen is then introduced into the system, either as pure oxygen or as air, to act as the oxidizing agent. The combination of high temperature, pressure, and oxygen promotes rapid oxidation reactions, breaking down complex organic molecules found in wastewater into simpler, more biodegradable compounds. Oxidation reactions in WAO mainly involve electron transfer from organic pollutants to oxygen molecules, leading to the formation of intermediate reactive oxygen species (ROS) such as hydroxyl radical (•OH), superoxide radicals ($\bullet O^{2-}$), and peroxide radicals ($\bullet O_2^{-2}$). These highly reactive species attack and break the chemical bonds of organic compounds, leading to their breakdown into smaller molecules such as carbon dioxide, water, and simple organic acids. The concept of AOPs was subsequently broadened to encompass other above-mentioned physical-chemical processes as well as methods employing different potent oxidizing agents such as $SO_4\bullet^-$ and Cl• (Parvulescu et al., 2021). WAO is particularly effective in treating wastewater streams containing a variety of organic contaminants, including pharmaceuticals, pesticides, aromatic hydrocarbons, and industrial chemicals. It can achieve high removal efficiency of organic pollutants, reducing their concentration to meet regulatory standards for discharge or reuse. The advantages include effective against complex pollutants as WAO can effectively treat wastewater containing complex organic pollutants that are resistant to biodegradation, including pesticides, pharmaceuticals, and industrial chemicals. It achieves high removal efficiency of organic pollutants, resulting in a significant reduction in chemical oxygen demand (COD) and wastewater toxicity. WAO applies to a variety of

wastewater streams, including those with high contaminant concentrations or fluctuating composition. Compared to other treatment methods, WAO typically produces less sludge, thereby reducing the need for subsequent sludge treatment and disposal. The high temperature and pressure used in WAO can effectively inactivate pathogens present in wastewater, thereby supporting the disinfection process. The high temperatures and pressures in WAO can be exploited to harvest energy through processes such as cogeneration, thereby increasing the overall efficiency of the process.

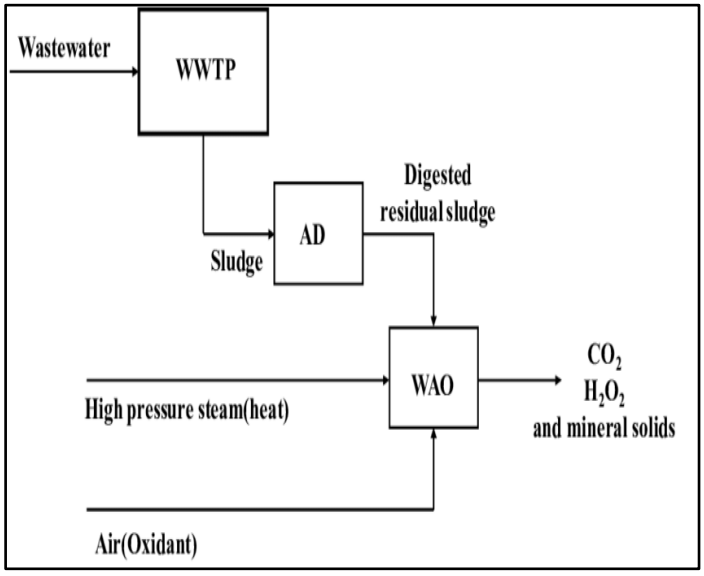


Fig.5. Wet air oxidation in a sludge treatment line (Cheng et al. 2019)

WAO requires significant energy input to reach and maintain high temperatures and pressures, making it potentially costly and energy-intensive compared to some other treatment methods. The corrosive nature of the reaction environment in WAO can pose challenges for reactor materials and require specialized corrosion-resistant materials, increasing equipment costs. Operating WAO reactors at high temperatures and pressures carry inherent safety risks, requiring stringent safety measures, monitoring, and maintenance protocols. WAO systems can be complex to design, operate, and control, requiring skilled personnel and sophisticated

instrumentation for proper performance and safety. While WAO can degrade many organic pollutants, it may not completely mineralize all compounds, leading to the formation of intermediate by-products that may still be toxic or recalcitrant. The energy consumption and potential emissions associated with WAO systems can contribute to their environmental footprint, especially if fossil fuels are used for heating.

1.3.6. Catalytic wet air oxidation

In CWAO, a catalyst is added to the WAO system to enhance oxidation reactions and improve the decomposition efficiency of organic pollutants. Catalysts typically promote the formation of reactive oxygen species (ROS) and accelerate the oxidation of organic compounds at lower temperatures and pressures than traditional WAO processes which save energy and reduce operating costs. Catalysts used in CWAO may vary depending on the specific application and target contaminants. Common catalysts include transition metal oxides, supported metal catalysts, and heterogeneous acids. These catalysts can enhance oxidation reactions by providing active sites for adsorption and activation of organic molecules, thereby accelerating their decomposition. CWAO is especially useful for treating wastewater streams with lower concentrations of organic pollutants or for applications where energy efficiency and cost-effectiveness are important considerations. It offers similar benefits to WAO, such as high organic contaminant removal efficiency and the ability to completely mineralize pollutants into harmless by-products (Roy, S., 2017). CWAO offers several advantages including enhanced oxidation efficiency as the presence of a catalyst accelerates oxidation reactions, leading to faster degradation of organic pollutants compared to traditional WAO processes. CWAO can operate at lower temperatures and pressures than conventional WAO, reducing energy consumption and operating costs. The catalyst can improve the selectivity of oxidation

reactions, targeting specific organic compounds for degradation while minimizing the formation of unwanted by-products. Faster oxidation kinetics in CWAO can result in shorter treatment times, increasing the throughput and efficiency of wastewater treatment systems. CWAO typically generates less sludge compared to other treatment methods, reducing the need for subsequent sludge handling and disposal. CWAO can be used to treat wastewater streams from industries such as pharmaceuticals, chemical manufacturing, petrochemicals, and manufacturing textile and garment production, where there are high concentrations of organic pollutants. CWAO can be used in municipal wastewater treatment plants to remove persistent organic pollutants, pharmaceutical residues, and other contaminants. CWAO can be used to treat leachate generated from landfills which often contain complex organic compounds and toxic substances that require advanced treatment for safe disposal or reuse. CWAO can be applied to treat contaminated groundwater, especially in cases where the contamination is due to industrial activities or organic chemical spills. CWAO can be integrated into waste-to-energy processes to treat organic-rich waste streams, such as sewage sludge or organic industrial waste, while energy recovery of oxidation reactions.

1.4. Various methods for catalyst preparation.

1.4.1. Impregnation

Impregnation is a method in which a support material (such as activated carbon, alumina, or silica) is impregnated with a solution containing metal precursors. The support is then dried and calcined to decompose the precursor and form the catalyst. Impregnation allows for precise control over metal loading and distribution on the support. Incineration can destroy a wide range of highly contaminated wastes and greatly reduce the amount of material that must be disposed of in a landfill. (Girish, C.R. 2018)**.**

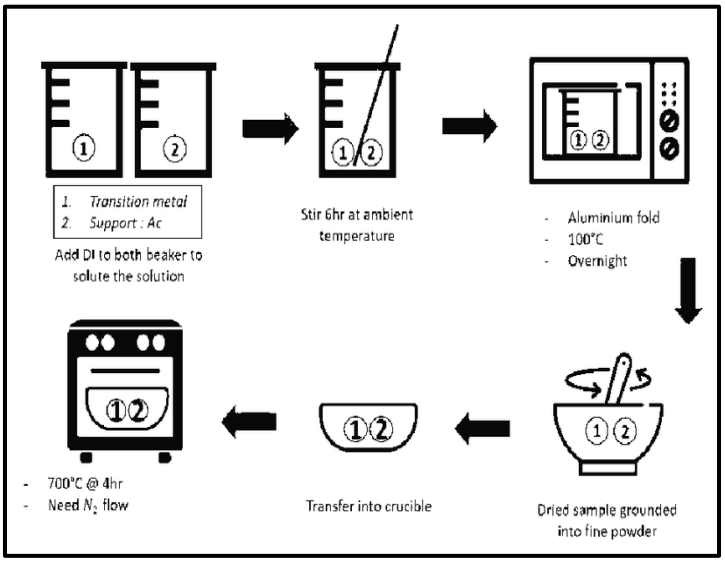


Fig.6. Schematic diagram for catalyst synthesis by wet impregnation method

(Binti et al. 2021)

1.4.2. Co-precipitation

Co-precipitation involves the simultaneous precipitation of metal ions and the support material from a solution containing their respective precursors. Co-precipitation is a synthesis technique where multiple components precipitate simultaneously from a solution, forming a solid compound. The process begins with the preparation of an aqueous solution containing the desired metal ions or precursors. A precipitating agent is then added to this solution, reacting with the metal ions to form insoluble compounds that precipitate out. As the precipitating agent is introduced, the solution becomes supersaturated, leading to the nucleation and growth of solid particles. Controlling the conditions such as pH, temperature, and concentration is crucial to influence the characteristics of the precipitated particles. Once the precipitate forms, the mixture is typically left to age, allowing the precipitate to undergo further structural and compositional changes that enhance its properties. The precipitate is then separated from the solution through methods like filtration or centrifugation and is washed to remove any residual

soluble impurities. After washing, the precipitate is dried to eliminate moisture and often subjected to calcination, a high-temperature treatment that induces further chemical and structural changes, such as increased crystallinity or the formation of specific phases. This method can produce catalysts with high dispersion of active species, but it may require careful control of pH and precipitation conditions to achieve the desired properties. (Hou et al. 2017)

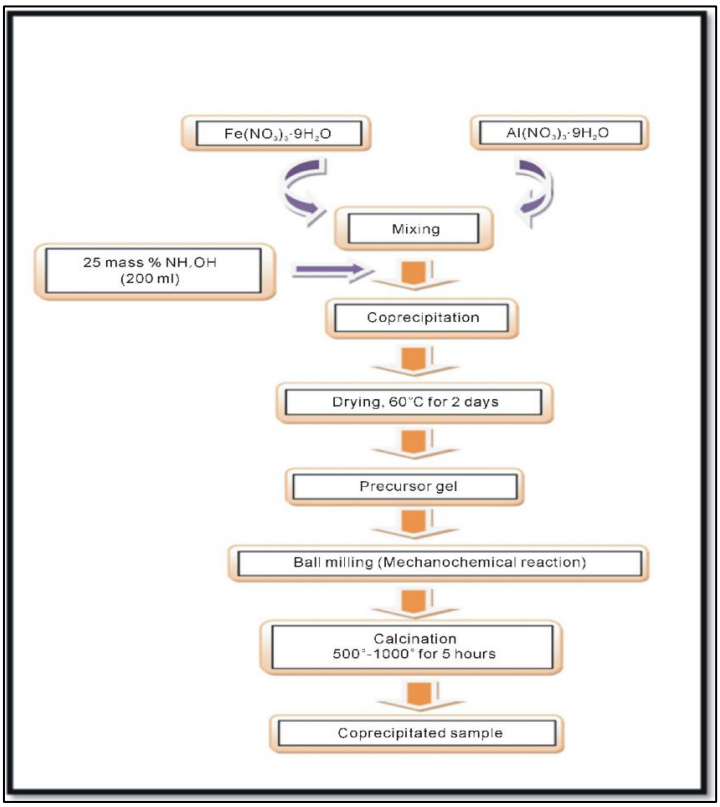


Fig.7. Flow chart of co-precipitation method (Singh et al. 2018)

1.4.3. Sol-gel Synthesis

Sol-gel synthesis involves the hydrolysis and condensation of metal alkoxides or metal salts in a solution to form a gel, which is then dried and calcined to form the catalyst. Sol-gel synthesis offers control over catalyst composition, particle size, and morphology, making it suitable for the preparation of homogeneous and tailored catalysts. (Danks et al. 2016)

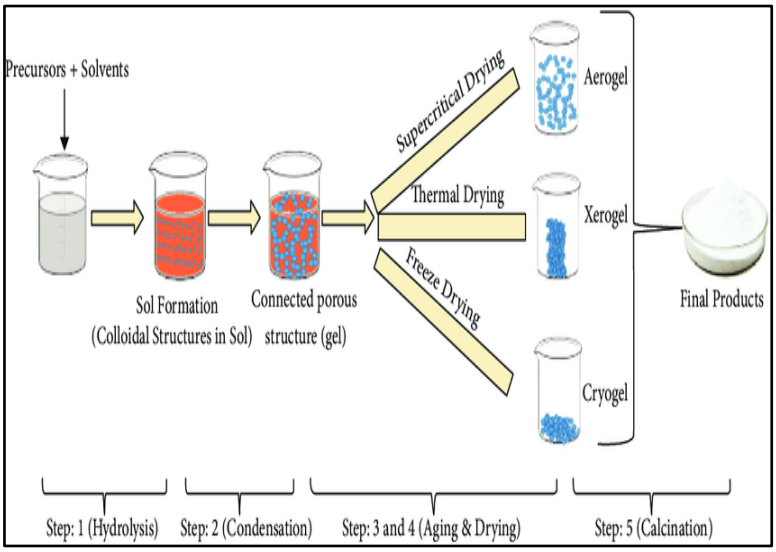


Fig.8. Schematic of different stages of sol-gel process. from precursor to aerogel (Bokov et al. 2021)

1.4.4. Template-Assisted Synthesis

Template-assisted synthesis involves using sacrificial templates, such as micelles or porous materials, to control the structure and morphology of the catalyst during synthesis. This method utilizes a template or scaffold to guide the formation of materials with specific shapes, sizes, and morphologies within which the material can form, allowing for precise control over the architecture of the final product. The process begins with the selection of a suitable template, which can be either hard or soft, such as rigid materials like silica, alumina, or polymers, and soft materials like surfactants, micelles, or biological molecules. Next, material precursors, including metal ions, monomers, or other chemical species, are introduced into the template. This step can be performed through various methods like infiltration, adsorption, or deposition, depending on the nature of both the template and the precursor. The precursors are then subjected to a chemical reaction, such as hydrolysis, polymerization, or reduction, to form the desired material within or around the template. Once the material has formed, the template is removed, typically through chemical dissolution, thermal decomposition, or selective etching,

leaving behind the structured material. This removal process must be tailored to the stability and nature of both the template and the material. The final product may then undergo additional processing steps, such as annealing, to improve properties like crystallinity and stability. After the deposition of active species, the template is removed to leave behind a catalyst with well-defined pores and surface characteristics. (Kaur et al. 2022)

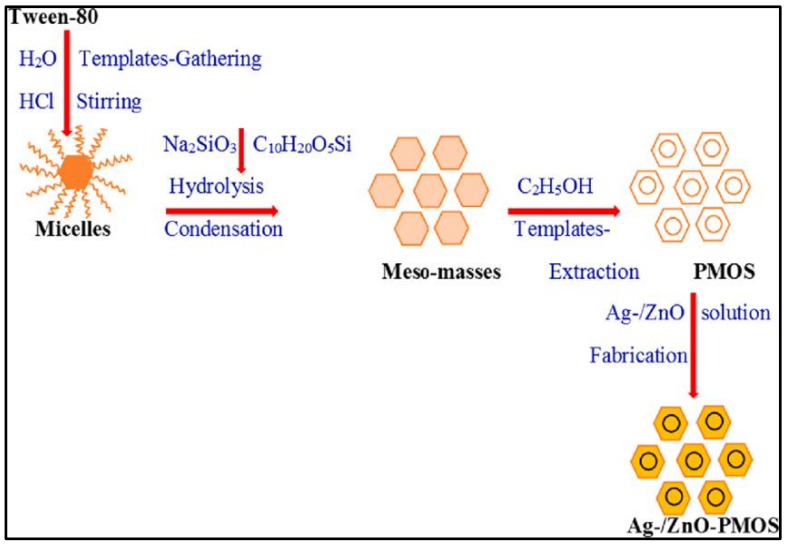


Fig.9. Schematic illustration of template-assisted synthesis of Ag-/ZnO-PMOS (Kumar et al. 2020)

1.4.5. Ion Exchange

Ion exchange is a process which involves the replacement of ions on a support material with metal ions from a solution containing metal precursors. It is often used for the preparation of heterogeneous catalysts with controlled metal loading and distribution. (Bashir et al. 2019)

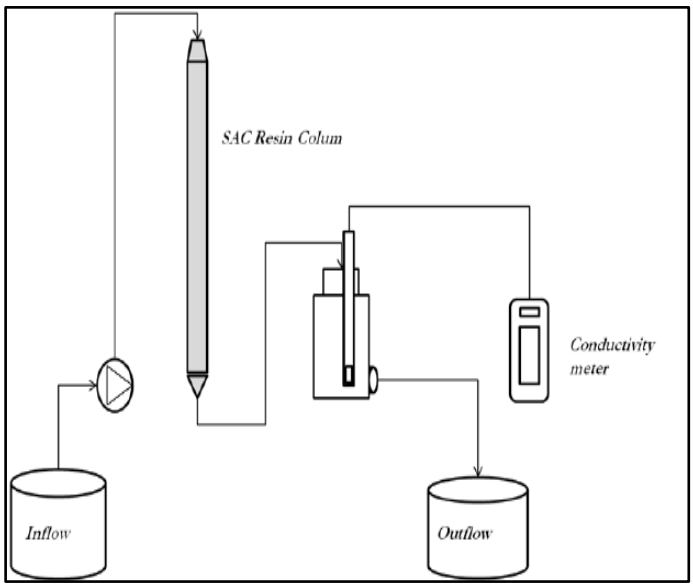


Fig.10. Schematic diagram of ion exchange set up for adsorption of ammonium from wastewater (Owusu-Agyeman, Isaac. 2012)

1.4.6. Mechanochemical Synthesis

Mechanochemical synthesis is a process that involves the use of mechanical energy, such as grinding or milling, to induce chemical reactions between solid reactants. Mechanochemical synthesis starts with the mechanical activation of reactants. This is usually achieved by placing the solid reactants in a ball mill or similar device, where they are subjected to repeated impact, friction, and shear forces. The mechanical energy imparted to the reactants leads to the breaking of chemical bonds and the formation of new ones, effectively driving the reaction forward. The energy can also increase the surface area of the reactants, enhance their reactivity, and sometimes create defects or amorphous regions that further facilitate the reaction. This method can be used to prepare catalysts with high surface area and reactivity, but it may require longer processing times and specialized equipment. (Amrute et al. 2021)

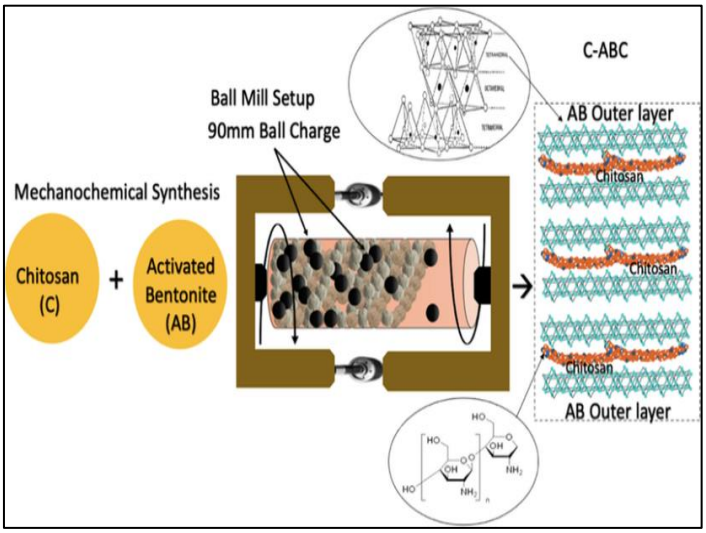


Fig.11. Mechanochemical synthesis of C-ABC (Duraisamy et al. 2022)

1.4.7. Atomic Layer Deposition (ALD)

ALD is a thin film deposition technique that allows for precise control over the thickness and composition of catalyst layers on a substrate. It involves the sequential use of gas phase chemical processes to deposit atomic layers of material onto a substrate, allowing for the controlled growth of films with atomic-level thickness precision. The process begins with the exposure of the substrate to a chemical precursor, which reacts with the surface to form a monolayer in a self-limiting manner, ensuring uniform coverage. This is followed by a purge step to remove excess precursor and reaction byproducts. The substrate is then exposed to a second precursor, which reacts with the initial monolayer to form a new layer of the desired material, followed by another purge step. This cycle of precursor exposure and purging is repeated multiple times, with each cycle depositing a single atomic layer, allowing for precise control over film thickness. ALD can be used to prepare catalysts with uniform and well-defined structures, but it may require high vacuum conditions and sequential deposition steps. (Zhang, B. and Qin, Y. 2018)

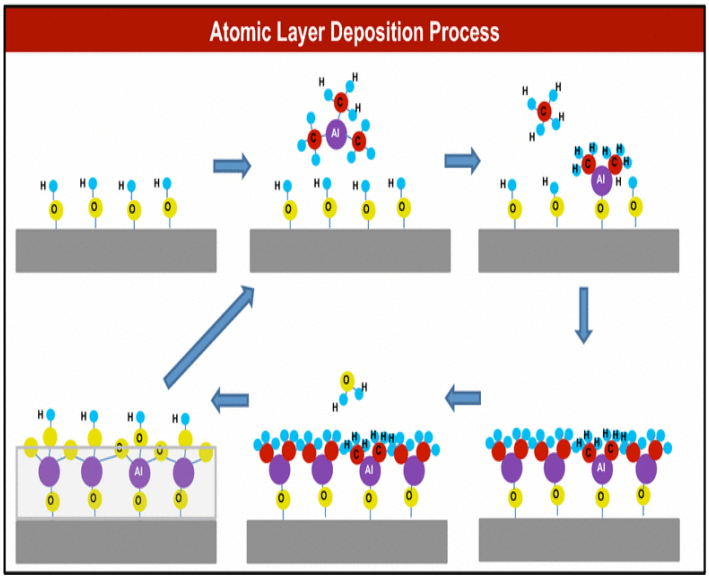


Fig.12. ALD process. schematic of one cycle of Al_2O_3 ALD growth

(Marquardt et al. 2015)

1.4.8. Hydrothermal Synthesis

Hydrothermal synthesis involves the preparation of catalysts under high-temperature and high-pressure conditions in an aqueous solution. The hydrothermal synthesis process begins with the preparation of an aqueous solution containing the desired reactants or precursors. These precursors can include metal salts, oxides, or other inorganic compounds, depending on the material to be synthesized. The solution is then transferred into an autoclave, a high-pressure sealed vessel. The autoclave is heated to a temperature typically ranging from 100°C to 300°C, depending on the specific requirements of the reaction. Under these conditions, water remains in a liquid state due to the high pressure, which can range from a few atmospheres to several hundred atmospheres. Within the autoclave, the high temperature and pressure conditions facilitate the dissolution of the precursors and promote the nucleation and growth of crystals. These conditions also allow for the formation of phases that are unstable or difficult to produce at atmospheric pressure and room temperature. The duration of the hydrothermal process can

vary from a few hours to several days, depending on the desired crystal size and properties. This method can lead to the formation of crystalline or amorphous materials with controlled particle size and morphology. (Feng, S.H. and Li, G.H., 2017)

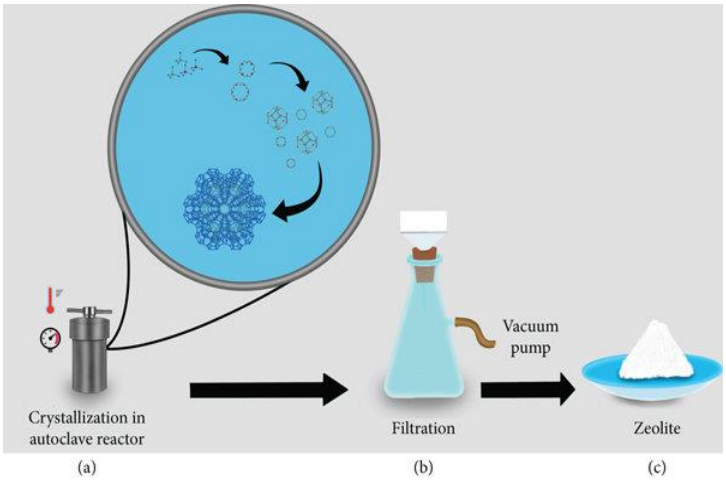


Fig.13. Hydrothermal synthesis process. (Magalhaes et al. 2022)

1.4.9. Microemulsion Technique

The microemulsion technique involves the formation of stable microemulsions consisting of water, oil, and surfactants. In this process, a microemulsion is formed by combining water, oil, surfactant, and sometimes a co-surfactant, resulting in nanoscale droplets dispersed within a continuous phase. These confined droplets serve as reaction vessels for the nucleation and growth of nanoparticles, which occurs once the desired precursors or reactants are incorporated. The microemulsion environment provides excellent control over reaction conditions, leading to high yields and reproducibility. Catalyst precursors are dissolved or dispersed in the microemulsion, allowing for the synthesis of nanoparticles or supported catalysts with narrow size distributions and high surface areas. (Muzaffar et al. 2013)

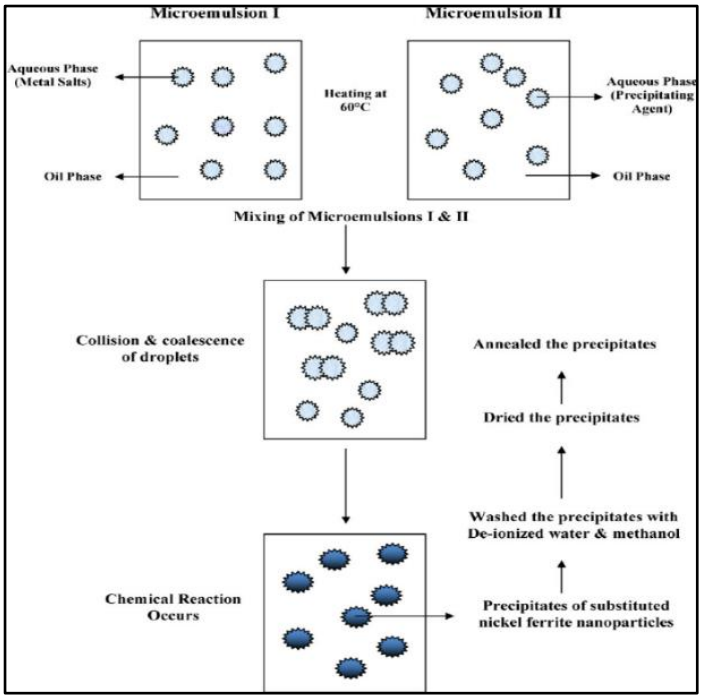


Fig.14. Schematic diagram for the microemulsion method. (Ashiq et al. 2011)

1.4.10. Electrodeposition Method

Electrodeposition involves the electrodeposition of metal ions onto a conductive substrate to form a catalyst layer. This method is often used for the preparation of electrocatalysts for fuel cells and electrolysers. The electrical current causes the dissolution of the anode, typically made from materials like aluminum or iron, into the water. These dissolved metal ions then react with the pollutants to form insoluble compounds or coagulants. These coagulants aggregate to form flocs, which can be easily separated from the water by sedimentation or flotation. Electrocoagulation is effective in removing a wide range of contaminants, including heavy metals, suspended solids, and organic compounds, making it a versatile solution for water purification. (Kale et al. 2021)

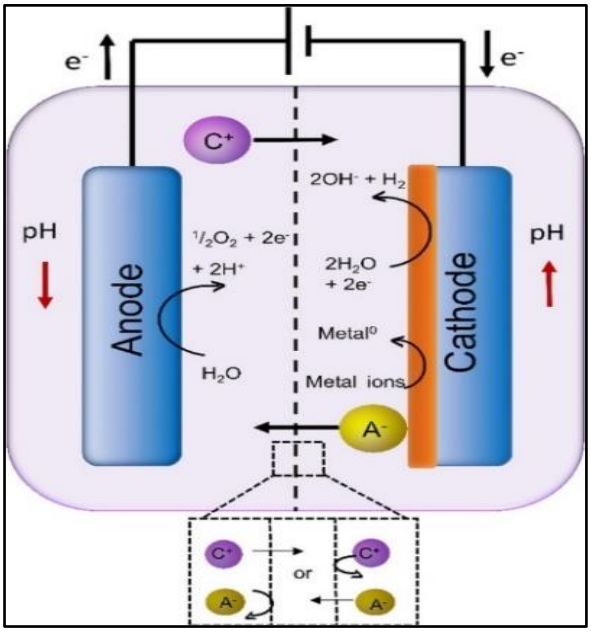


Fig.15. Schematic overview of electrodeposition for the electrochemical separation of organic/inorganic compounds from waste streams. (Gao et al. 2022)

1.4.11. Flame Spray Pyrolysis

Flame spray pyrolysis involves the combustion of precursor solutions or suspensions in a flame to produce catalyst nanoparticles. The process involves the combustion of a precursor solution or suspension in a flame, resulting in the formation of fine particles that are subsequently deposited onto a substrate. FSP is typically performed using a burner system where the precursor solution is atomized and introduced into a high-temperature flame, typically fueled by a combustible gas such as hydrogen or methane. The intense heat of the flame decomposes the precursor molecules into their constituent atoms or small clusters, which then nucleate and grow into nanoparticles as they cool and solidify in the surrounding air. This method can yield catalysts with high purity, narrow size distributions, and controlled stoichiometry, making it suitable for various catalytic applications. (Teoh et al. 2010)

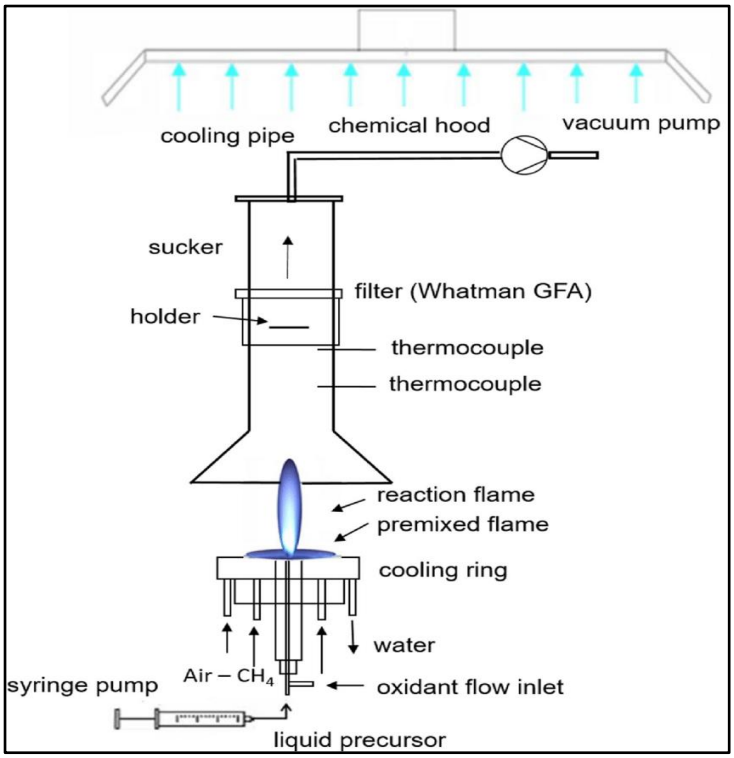


Fig.16. Flame spray pyrolysis apparatus (De Iuliis et al. 2019)

1.4.12. Spray Drying

Spray drying is a process that involves the atomization of a solution or suspension into droplets, which are then dried in a hot gas stream to form catalyst particles. In spray drying, the liquid feed is typically pumped to a spray nozzle, where it is atomized into small droplets. These droplets are then dispersed into a drying chamber, where they come into contact with hot air or gas. The high temperature of the drying gas causes rapid evaporation of the liquid from the droplets, leaving behind solid particles. The dried particles are collected from the bottom of the drying chamber, often in the form of a fine powder.

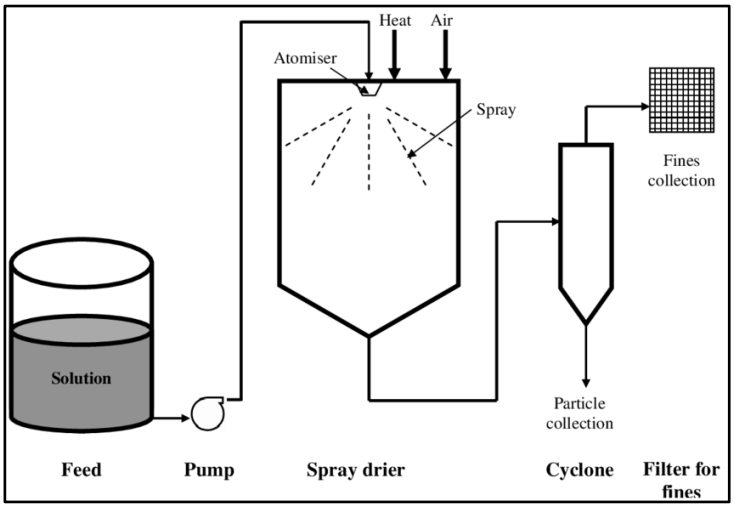


Fig.17. Schematic of the spray drying process. (Burey et al., 2008)

This method can produce catalysts with controlled particle size, morphology, and porosity and is widely used for the preparation of supported catalysts. (Okuyama et al. 2006).

1.4.13. Layer-by-Layer Deposition

Layer-by-layer deposition involves the sequential adsorption of oppositely charged species onto a substrate to form a multilayered catalyst structure.

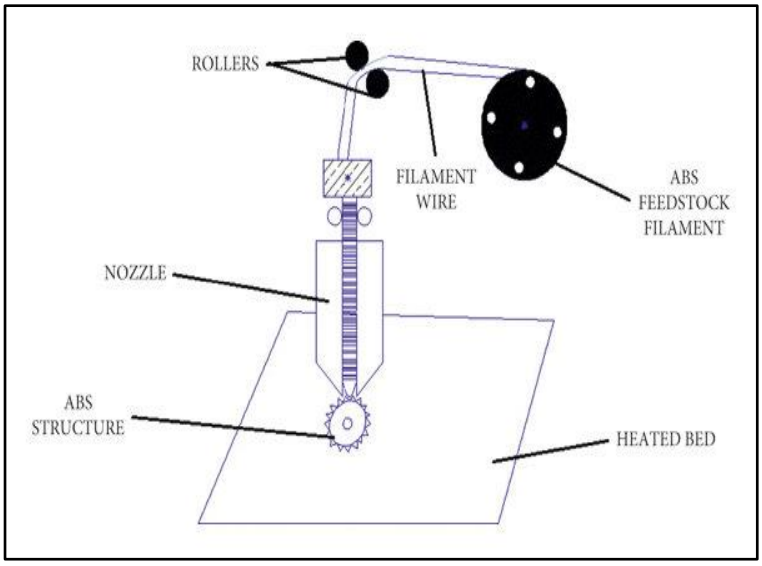


Fig.18. Diagram of layer-by-layer deposition of ABS material (Chohan et al., 2022)

This method allows for precise control over catalyst composition, thickness, and functionality and is often used for the preparation of catalysts for surface reactions and sensors. (Xiao et al. 2016)

1.4.14. Pulsed Laser Deposition

Pulsed laser deposition involves the ablation of a target material by a pulsed laser beam to deposit thin films onto a substrate. This method can produce catalysts with controlled stoichiometry, crystallinity, and orientation and is commonly used for the preparation of thin film catalysts for electronic and photonic applications. (Shepelin et al. 2023)

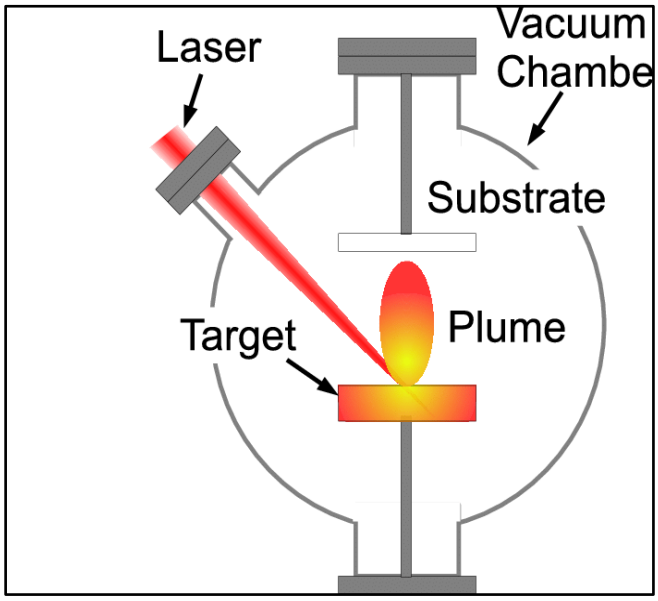


Fig.19. Schematic diagram of the pulsed laser deposition (PLD) set-up. (Cozzens et al.)

1.5. Different types of reactors, used for oxidation reactions.

1.5.1. Batch Reactors

Batch reactors are closed vessels where reactants are added together and allowed to react without the addition of new reactants or removal of products during the reaction. They are commonly used in laboratories and small-scale production processes where precise control

over reaction conditions is important, and where the reaction volume is relatively small. (Nanda, S., 2008)

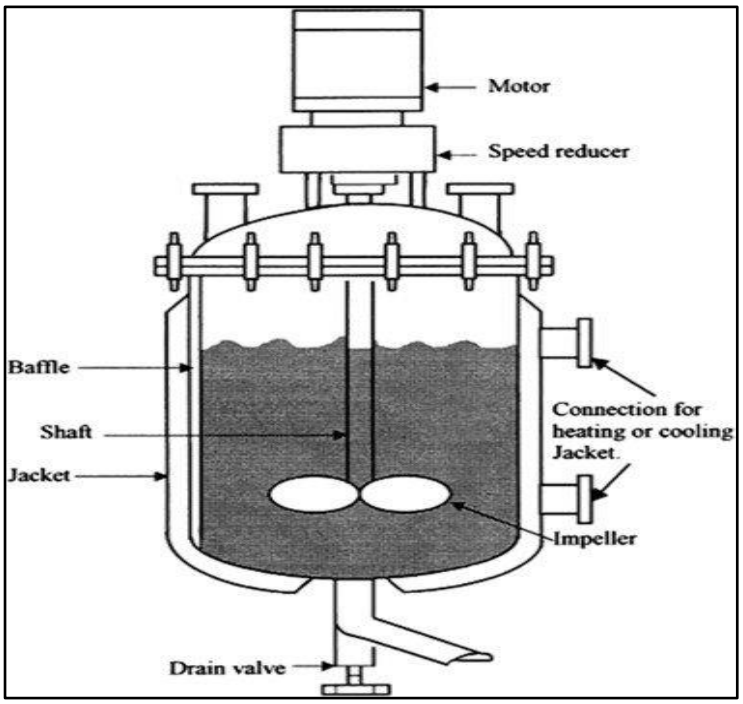


Fig.20. Schematic diagram of batch reactor. (Ahmed, Enas. 2013)

1.5.2. Continuous Stirred-Tank Reactors (CSTRs)

CSTRs are tanks equipped with agitation systems to maintain a uniform mixing of reactants and products. Reactants are continuously fed into the reactor, while products are simultaneously removed. These reactors consist of a cylindrical vessel with an agitator or stirrer to ensure uniform mixing of reactants. In a CSTR, reactants are continuously fed into the reactor, and the product stream is continuously removed, maintaining a steady-state operation. This continuous flow of reactants and products allows for precise control over reaction conditions, residence time, and product quality.

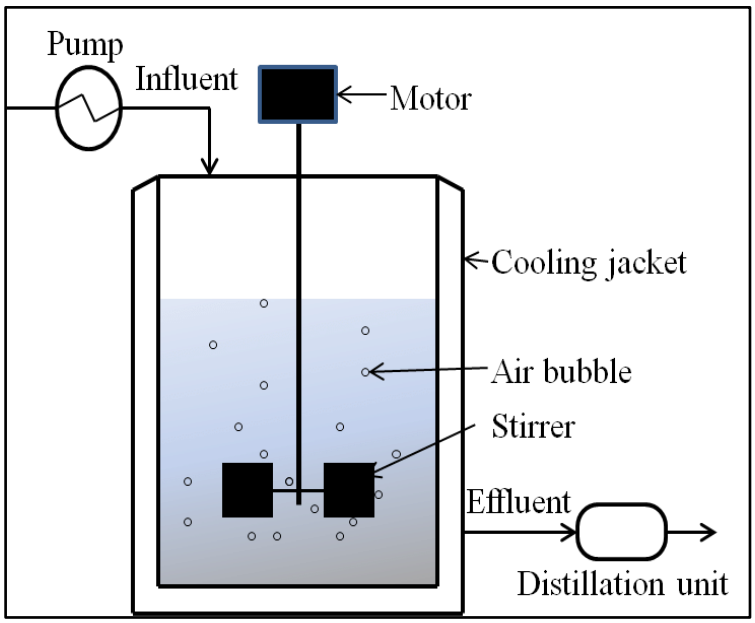


Fig.21. Continuous stirred tank reactor (CSTR) (Bhatia et al. 2017)

CSTRs are employed in industries where steady-state operation is desired. They are suitable for reactions where the reaction rate is relatively slow or where there are no significant changes in reaction conditions over time. (Mason, D.R. and Piret, E.L. 1951)

1.5.3. Plug Flow Reactors (PFRs)

PFRs are tubular reactors where reactants flow through the reactor without mixing along the length of the tube. The reactants are typically introduced at one end of the tube and flow through it, while products are removed at the other end. Unlike Continuous Stirred Tank Reactors (CSTRs), PFRs maintain a plug flow regime, where reactants enter one end of the reactor and flow through it without any lateral mixing. This unique flow pattern allows for precise control over residence time distribution and reaction kinetics, making PFRs particularly suitable for processes with complex reaction mechanisms or requiring specific residence times.

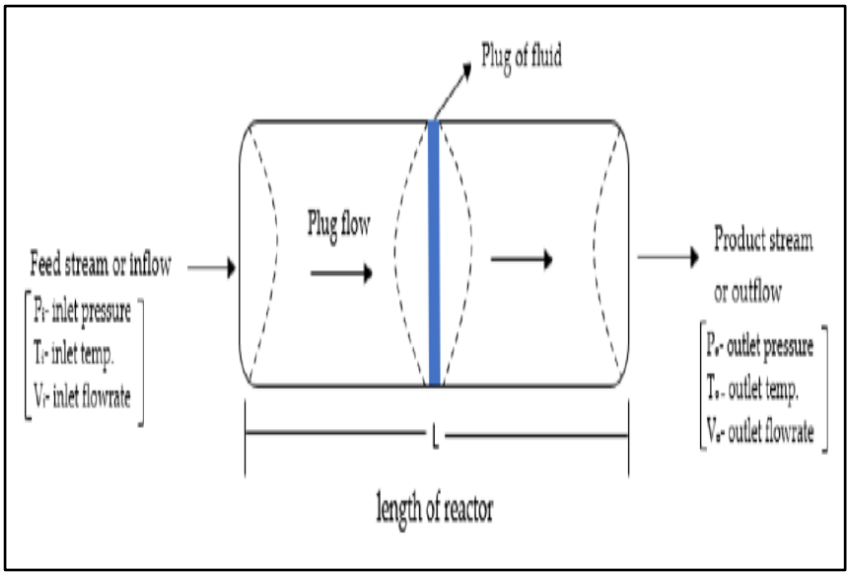


Fig.22. Plug flow reactor (Abu et al. 2023)

PFRs are ideal for reactions with fast kinetics or reactions where the residence time of the reactants in the reactor needs to be precisely controlled. They are commonly used in industries where high throughput and efficient heat and mass transfer are essential. (Nanda, S., 2008)

1.5.4. Fixed-Bed Reactors

Fixed-bed reactors consist of a packed bed of solid catalyst particles through which reactants flow. The reaction occurs on the surface of the catalyst particles. These reactors employ a bed of solid particles that are fluidized by a gas or liquid flowing through them. The fluidization of the bed creates a high degree of mixing and intimate contact between the reactants and catalysts, resulting in enhanced heat and mass transfer rates, as well as improved reaction kinetics. They are widely used in heterogeneous catalytic oxidation reactions where the catalyst promotes the oxidation reaction. In petroleum refining, FBRs are used for catalytic cracking of heavy hydrocarbons into lighter fractions, while in petrochemical processes, they are employed for the synthesis of olefins and aromatics from hydrocarbons. In pharmaceutical

manufacturing, FBRs are utilized for continuous flow synthesis of pharmaceutical intermediates and active pharmaceutical ingredients (APIs), offering advantages in terms of productivity, efficiency, and quality control. In environmental engineering, FBRs are used for processes such as catalytic combustion and waste gas treatment, where they can effectively remove pollutants from exhaust streams. Fixed-bed reactors offer a high surface area for catalytic reactions and are suitable for continuous operations in large-scale industrial processes. (Andrigo et al. 1999)

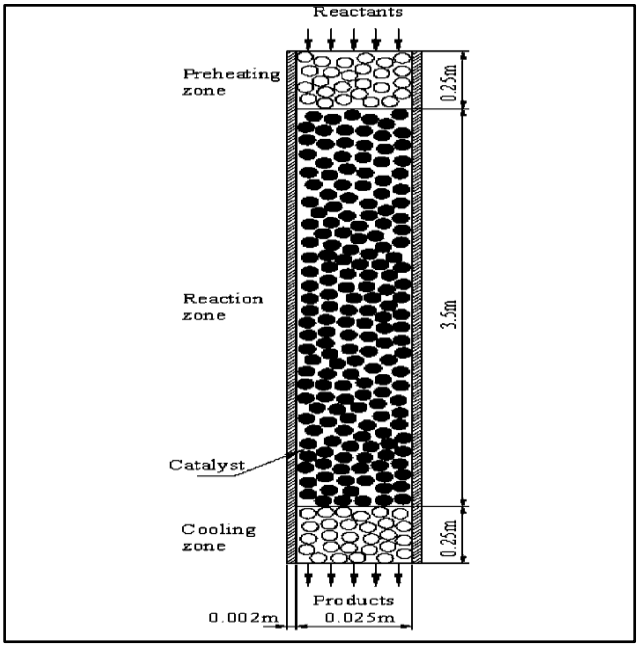


Fig.23. Schematic view of the single-tube fixed-bed reactor (Jiang et al. 2014)

1.5.5. Fluidized Bed Reactors

Fluidized bed reactors use an upward flow of gas to suspend and fluidize a bed of solid particles, typically catalysts. This creates a fluid-like behavior of the bed. Fluidized bed reactors are employed in oxidation reactions where intimate contact between reactants and

catalysts is crucial. They are suitable for reactions requiring high surface area contact between reactants and catalysts. (Grace et al. 2016)

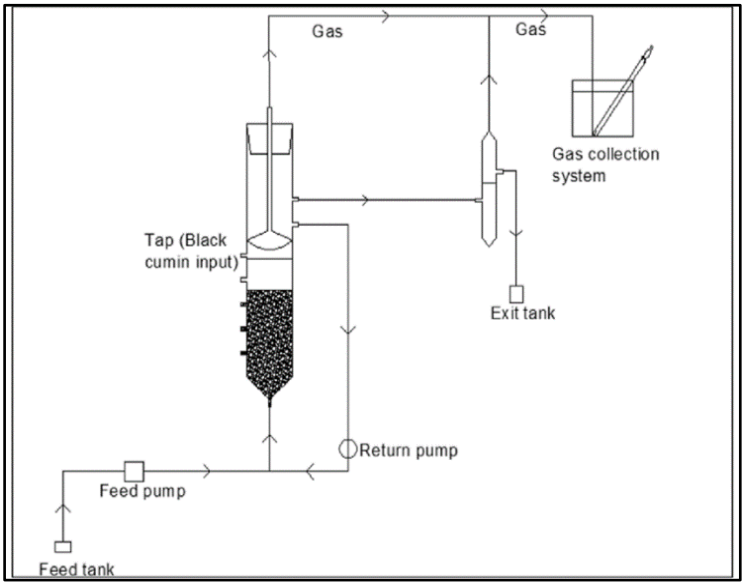


Fig.24. Fluidized bed reactor for polyethylene production. (Dursun et al. 2022)

1.5.6. Membrane Reactors

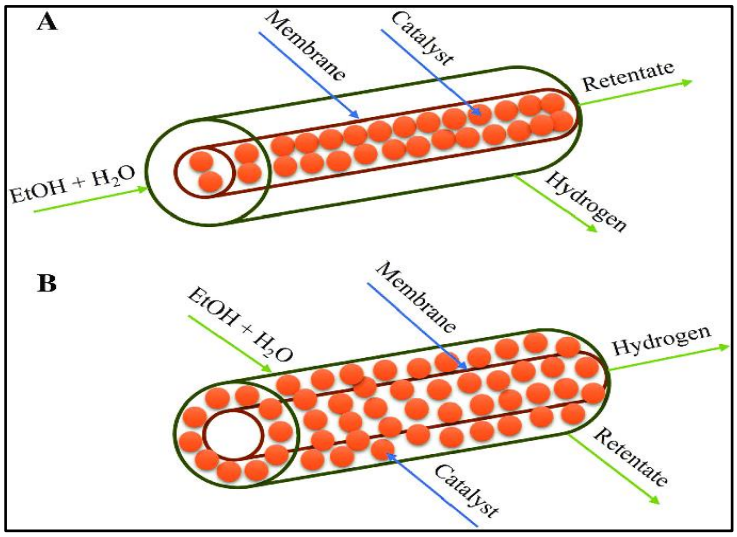


Fig.25. Schematic of two configurations of the tubular membrane reactor (Taghizadeh et al. 2019)

Membrane reactors are used in oxidation reactions where product separation is difficult. They offer benefits such as improved selectivity, improved reaction rates, and simplified downstream processing. (Sirkar et al. 1999)

1.5.7. Microreactors

Microreactors are miniature reactors with small reaction volumes. They offer benefits such as rapid mixing, improved heat transfer, and improved safety. Microreactors are commonly used in research and development of oxidation reactions, as well as for high-throughput testing. They allow precise control of reaction conditions and are suitable for reactions requiring small amounts of reagents. (Yao et al. 2015)

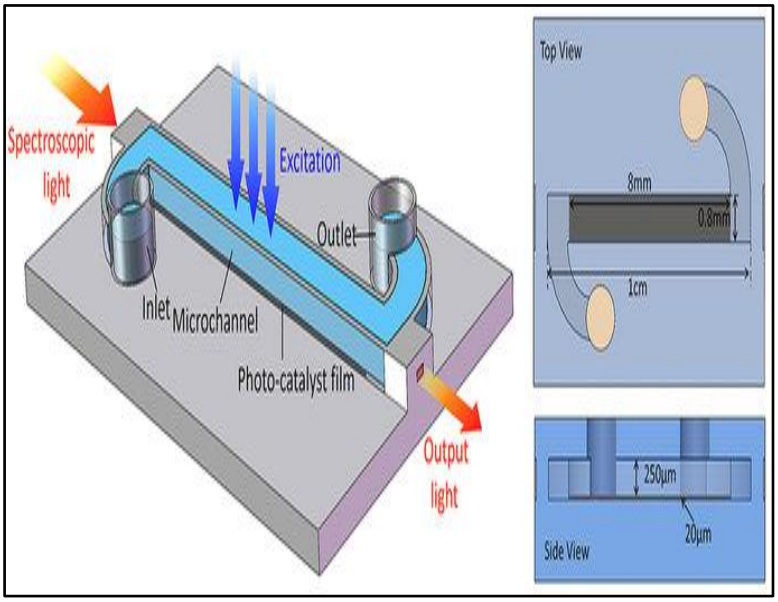


Fig.26. Schematic diagram of the fabricated microreactor (Li et al.)

1.6. Different types of Supports used for catalyst preparation

1.6.1. Alumina (Al_2O_3)

Alumina is a versatile support known for its high surface area, mechanical strength, and excellent thermal stability. It exists in different phases. Gamma-alumina is used as the most common for catalytic applications due to its high surface area and porosity. Alumina supports are widely employed in oxidation reactions such as the oxidation of alcohols, aldehydes, and hydrocarbons. They provide a stable platform for the deposition of active metal species, promoting catalytic activity and resistance to sintering at high temperatures.

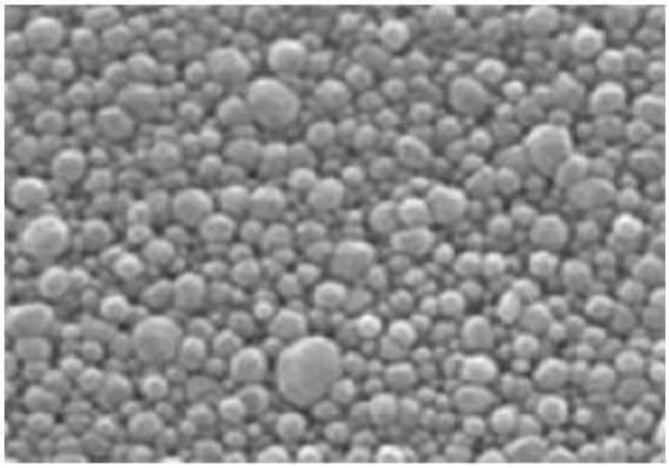


Fig.27. Microstructure of alumina. (Al-Sanabani et al. 2014)

1.6.2. Silica (SiO_2)

Silica is valued for its high surface area, chemical inertness, and thermal stability. It is available in various forms, including amorphous silica and mesoporous silica, offering pore sizes and surface properties. They are used in reactions involving polar or acidic reactants due to their inert nature and resistance to leaching. Silica, or silicon dioxide (SiO_2), is widely used as a support material across various fields, including catalysis, chromatography, and drug delivery, owing to its advantageous properties. In catalysis, silica serves as a support for heterogeneous

catalysts, providing a large surface area that enhances the dispersion and efficiency of catalytic active sites. This makes it ideal for processes such as hydrogenation and acid-base catalysis. In chromatography, silica gel is a common stationary phase in both column chromatography and thin layer chromatography (TLC), where its excellent adsorption properties facilitate the separation of compounds based on polarity. Beyond these applications, silica is also used as an adsorbent for moisture control and purification, and as a component in composite materials to improve mechanical and thermal properties. The benefits of silica as a support material are manifold: it provides a high surface area, thermal stability, and chemical inertness, which are essential for maintaining the integrity of supported substances and preventing unwanted reactions.

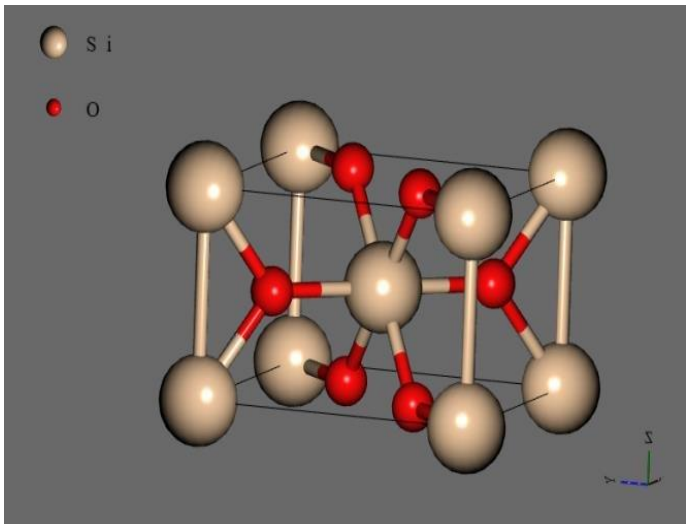


Fig.28. Crystal structure of SiO_2 (Ganbaatar et al. 2021)

1.6.3. Titania (TiO_2)

Titania exhibits excellent thermal stability, surface acidity/basicity, and photocatalytic properties. It exists in different crystal phases, with anatase and rutile being the most common for catalytic applications. Titania supports are utilized in photocatalytic oxidation reactions,

such as the degradation of organic pollutants and water purification. They are also employed in selective oxidation reactions where surface properties play a crucial role in catalysis and where light activation of the catalyst is desirable.

1.6.4. Zeolites

Zeolites are crystalline aluminosilicate materials with a regular pore structure and high surface area. Their framework structure provides acidic sites, making them useful for catalyzing various reactions. Zeolite supports are employed in oxidation reactions, where shape selectivity, pore size, and acidity are crucial for controlling reaction pathways and product selectivity. They find applications in petrochemical processes, fine chemical synthesis, and environmental catalysis.

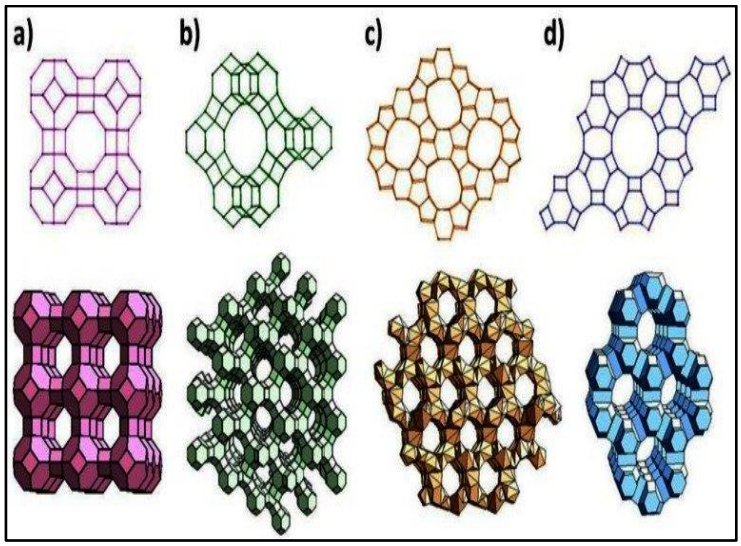


Fig.29. Representative zeolite frameworks, (with pore openings). (a) zeolite A (3D, 4.2 Å); (b) zeolite Y (3D, 7.4 Å); (c) Zeolite L (1D, 7.1 Å); (d) ZSM-5 (silicalite) (2D, 5.3 × 5.6 Å, 5.1 × 5.5 Å) D—dimensions of channel system. (Zheng et al. 2012)

1.6.5. Carbon Materials

Carbon-based supports, including activated carbon, carbon nanotubes, and carbon black, offer high surface area, surface chemistry, and electrical conductivity. Carbon supports find applications in oxidation reactions where unique properties such as electron transfer, adsorption, and confinement effects are desirable. They are used in environmental catalysis, energy storage, and electrochemical applications.

1.6.6. Mixed Metal Oxides

Mixed metal oxides consist of two or more metal cations combined with oxygen atoms, exhibiting synergistic effects that enhance catalytic activity and selectivity. Mixed metal oxide supports are utilized in oxidation reactions where specific redox properties or interactions between different metal species are advantageous. They are employed in automotive catalysis, fuel processing, and fine chemical synthesis. The selection of suitable support for catalyst preparation is crucial as it significantly influences the catalyst's performance in oxidation reactions. The support material should be chemically stable under the reaction conditions, especially if harsh reaction conditions such as high temperature or corrosive environments are involved. Commonly used stable supports include alumina (Al_2O_3), silica (SiO_2), and titania (TiO_2). A high surface area of the support provides more active sites for catalyst deposition, which can enhance catalytic activity. Porous materials like alumina and silica often offer high surface areas and are thus commonly used as catalyst supports. The pore structure of the support influences mass transfer within the catalyst and accessibility of reactants to active sites. Supports with a well-defined pore structure, including a mix of both micropores and macropores, are desirable to facilitate mass transport. The support should have sufficient mechanical strength to withstand the forces exerted during catalyst preparation, handling, and

use in the reactor. Brittle supports may lead to attrition and loss of catalyst activity over time. The support material should retain its properties at high temperatures to prevent structural changes or sintering of active catalytic sites during reaction conditions involving elevated temperatures. The support should not chemically interfere with the catalytic reaction or interact unfavorably with reactants, intermediates, or products. It should be inert under reaction conditions to avoid unwanted side reactions. If the catalyst requires the addition of promoters or modifiers to enhance its catalytic performance, the support should be compatible with these additives and should facilitate their dispersion and stabilization on the catalyst surface. The cost and availability of the support material are important practical considerations, especially for large-scale industrial applications. Commonly used supports such as alumina and silica are relatively cost-effective and readily available. Considering these factors, alumina (Al_2O_3) and silica (SiO_2) are among the most commonly used supports for catalyst preparation in oxidation reactions due to their favorable properties such as high surface area, thermal stability, and chemical inertness. The choice of support material depends on various factors such as reaction conditions, reactant properties, desired catalytic performance, and scalability to industrial production. Each support offers unique properties that can be tailored to optimize the activity, selectivity, and stability of the catalyst in oxidation reactions.

1.7. Selection of metals

The selection of metals is a complex decision-making process that requires a thorough understanding of the specific requirements of the application and the properties of the metals under consideration. The selection of metals for catalysis depends on various factors, including the mode of the reaction (oxidation, reduction, etc.), the nature of the reactants, and the desired catalytic performance.

1.7.1. Oxidation Reactions

For oxidation reactions, metals with higher oxidation states or metals that readily undergo oxidation themselves can be effective catalysts. Commonly used metals for oxidation reactions include Platinum (Pt), Palladium (Pd), Gold (Au), Silver (Ag), Iron (Fe), and Ruthenium (Ru). These metals can catalyze various oxidation reactions, including alcohol oxidation, olefin epoxidation, and selective oxidation of organic compounds.

1.7.2. Reduction Reactions

For reduction reactions, metals capable of donating electrons or undergoing reduction themselves are often used as catalysts. Commonly used metals for reduction reactions include Platinum (Pt), Palladium (Pd), Rhodium (Rh), Raney Nickel (Ni), Cobalt (Co), and Copper (Cu). These metals can catalyze reduction reactions such as hydrogenation, hydrosilylation, and nitro group reduction.

1.7.3. Hydrogenation Reactions

Hydrogenation reactions involve the addition of hydrogen atoms to unsaturated compounds. Metals capable of adsorbing and activating hydrogen are often used as catalysts. Commonly used metals for hydrogenation reactions include Platinum (Pt), Palladium (Pd), Nickel (Ni), Ruthenium (Ru), and Rhodium (Rh). These metals are effective catalysts for hydrogenation reactions, including the hydrogenation of alkenes, alkynes, and carbonyl compounds.

1.7.4. Dehydrogenation Reactions

Dehydrogenation reactions involve the removal of hydrogen atoms from organic compounds. Metals capable of activating C-H bonds are often used as catalysts. Commonly used metals for

dehydrogenation reactions include Platinum (Pt), Palladium (Pd), Rhodium (Rh), Ruthenium (Ru), and Iron (Fe). These metals can catalyze dehydrogenation reactions such as alkane dehydrogenation and alcohol dehydrogenation.

1.7.5. Hydrogen Transfer Reactions

Hydrogen transfer reactions involve the transfer of hydrogen atoms between reactants. Metals with varying redox properties are often used as catalysts. Commonly used metals for hydrogen transfer reactions include Palladium (Pd), Platinum (Pt), Nickel (Ni), Ruthenium (Ru), and Rhodium (Rh). These metals can catalyze hydrogen transfer reactions such as hydrogenation-dehydrogenation reactions and transfer hydrogenation reactions.

1.7.6. Oxygen Transfer Reactions

Oxygen transfer reactions involve the transfer of oxygen atoms between reactants. Metals capable of activating molecular oxygen or oxygen-containing species are often used as catalysts. Commonly used metals for oxygen transfer reactions include Manganese (Mn), Iron (Fe), Cobalt (Co), Vanadium (V), and Molybdenum (Mo). These metals can catalyze oxygen transfer reactions such as epoxidation, oxidation, and oxygenation reactions. The selection of metals for catalysis depends on the specific requirements of the reaction, including the desired selectivity, activity, stability, and cost considerations. Additionally, metal catalysts are often supported on high-surface-area materials such as alumina, silica, or carbon to improve their dispersion and stability during the reaction.

CHAPTER 2
LITERATURE REVIEW

CHAPTER 2

LITERATURE REVIEW

Akhter et al. (2021), performed the electrocoagulation (EC) method, utilizing electric current between iron or aluminum electrodes, a promising solution for wastewater treatment to treat industrial discharge, which if untreated contaminated water into the environment annually, posing risks to ecosystems. The authors studied that the EC method effectively destabilizes pollutants, though its efficacy depends on factors like pH, operation time, and electrode materials. The authors informed that EC proved to be energy-efficient and cost-effective compared to alternative methods, despite facing challenges like electrode passivation. The researchers compare its efficiency with other treatment approaches and suggest strategies for improvement. Anushree et al. (2020) explored the critical role of water in our existence and the escalating concern for water quality due to heavy industrial wastewater discharge. The growing interest in wastewater treatment technologies is because of health and environmental priorities. CWAO stands out as an effective technique for organic matter oxidation at elevated temperatures and pressures. Successful commercialization hinges on finding catalysts with high activity under mild conditions. The rational design of nano-structured materials, particularly ceria-based nanocatalysts, holds promise for advancing CWAO. The researchers delve into the synthesis, characterization, and application of ceria-based nanocatalysts, highlighting their notable oxygen storage capacity. They also discussed the reaction mechanism and addressed future research directions, the chapter outlines both challenges and opportunities associated with the CWAO process. Archila, K. (2020), et al. studied the influence of different active phases (Fe, Ni, and Ni–Fe) of mixed oxides in the catalytic wet air oxidation (CWAO) of Crystal Violet, a synthetic dye widely used in various industries. The authors synthesized mixed oxide catalysts, comprising Fe, Ni, and Ni–Fe supported on a solid

substrate, using specific methods, and performed characterization through various techniques such as X-ray diffraction (XRD), scanning electron microscopy (SEM), and Brunauer-Emmett-Teller (BET) surface area analysis. The researchers conducted CWAO experiments under controlled conditions and evaluated the catalytic activity of each mixed oxide catalyst based on the degradation efficiency of crystal violet and the formation of intermediate by-products. They also studied the impact of the active phase on the catalyst's selectivity and stability during the CWAO process. The results revealed that the presence of different active phases significantly influenced the performance of the mixed oxide catalysts in the CWAO of Crystal Violet The researchers reported that catalysts containing Fe and Ni individually exhibited distinct catalytic activities and selectivity towards specific degradation products. Additionally, the Ni–Fe mixed oxide catalyst demonstrated a synergistic effect, surpassing the individual Fe and Ni catalysts, and exhibited superior Crystal Violet degradation efficiency with reduced formation of harmful by-products. Moreover, the stability and recyclability of the mixed oxide catalysts were assessed, providing insights into their potential for long-term application in CWAO processes. Overall, this study highlights the importance of the active phase in mixed oxide catalysts for CWAO applications and demonstrates the significance of tuning the catalyst composition to achieve enhanced catalytic performance in the treatment of dye-contaminated effluents. Ashiq et al. (2011), synthesized spinel nickel ferrite with varying levels of antimony substitution ($NiFe_2{-}xSb_xO_4$) using the reverse microemulsion method. The authors performed characterization via XRD, FTIR, TGA/DTGA, SEM, AFM, Mossbauer Spectroscopy, and DC electrical resistivity measurements confirmed single spinel phase formation with crystallite sizes ranging from 8–38nm. The authors reported that particle sizes observed through AFM and SEM ranged from 5–45nm and 10–45nm respectively, suitable for high-density recording media, and Mossbauer spectra revealed distinct Zeeman patterns and a doublet at higher substitution levels. The authors also reported that DC electrical resistivity demonstrated

temperature-dependent behavior, indicating a metal-to-semiconductor transition temperature (TM–S), suggesting potential for switching applications. The researchers studied that resistivity increased with Sb-content, indicating the potential for use in microwave devices.

Baloyi & Moma (2020) synthesized and tested cordierite monoliths coated with Al/Zr pillared bentonite clay powder as catalysts for the catalytic wet air oxidation (CWAO) of phenol in aqueous solutions within a plug flow reactor. The authors performed EDS, SEM, BET, and XRD as various characterization techniques and reported effective deposition of Al/Zr pillared bentonite clay on cordierite monolith channel walls, even after ultrasound treatment it showed good mechanical stability. The authors reported high catalytic performance with 100% phenol conversion and 91% total organic carbon reduction during continuous oxidation experiments lasting 140 hours. The authors identified aromatic ring intermediates and short-chain carboxylic acids formed during the CWAO of phenol and also proposed a kinetic model, considering internal and external diffusion limitations, to describe the reaction. Bao et al. (2019) combined CWAO and membrane separation for efficient water treatment by employing Mo-based nanocrystal decorated ceramic membranes (Mo/Al_2O_3) under ambient conditions. The authors employed in-situ hydrothermal and calcination methods to prepare the catalytic membrane and performed characterization by using XRD, XPS, and FESEM and tested for the degradation of organics (safranine O and humic acid) in a membrane filtration system. The authors investigated the effects of calcination temperature, catalyst loading amount, and trans-membrane pressure (TMP) and reported that higher calcination temperature and increased pressure could decrease performance however the catalyst loading amount had a minor impact. A one-time loading membrane calcined at 300 °C demonstrated over 90% removal efficiency within 40 minutes in a recycled filtration system with an initial safranine O concentration of 10 mg L^{-1}. The authors employed chemical quenching and radical quantification experiments and identified reactive oxygen species (ROS), mainly $1O_2$ and O^{2-}.

Bao et al. (2019), developed a pore-functionalized ceramic membrane with isotropically impregnated cobalt oxide (CoCM) by an in-situ self-sacrificed template method for the degradation of sulfamethoxazole (SMX) through peroxymonosulfate (PMS) activation under a dead-end membrane filtration mode. The authors characterized through FESEM, AFM, XRD, and XPS and reported uniform impregnation of Co_3O_4 into the macropores throughout the ceramic membrane without pore blocking. The authors also reported that the formation of Co-O-Al bonding inhibited cobalt leaching during filtration and the Co-OH hydroxyl group played a crucial role in radical generation. The authors reported that CoCM exhibited improved pure water permeability due to a decreased contact angle and both contact time and PMS dosage influenced the catalytic degradation of SMX. They also reported that CoCM demonstrated superior antifouling properties during humic acid (HA) removal. Stability and regeneration of CoCM were investigated, and a radical quenching experiment provided a quantitative estimation of sulfate radical concentration. The study proposed a mechanism for PMS activation and organics removal in CoCM, highlighting the synergistic coupling of catalytic Co_3O_4 and membrane separation. Bhatia et al. (2023) explored the treatment of highly alkaline and toxic industrial organic raffinate (IOR) containing pyridine and its derivatives using a combination of catalytic wet air oxidation and a biological process. The authors employed a 1 wt. % platinum catalyst for CWAO to degrade toxic compounds in the IOR into biodegradable intermediates. The researchers performed a characterization of the catalyst and reported that CWAO-treated effluent exhibited complete degradation of pyridine with non-toxicity. Further biological treatment of the effluent ensured compliance with discharge limits. The authors reported that the catalyst demonstrated reusability for four cycles. This integrated approach offers an effective solution for addressing toxic organic pollutants in wastewater. Bhatia et al (2023) synthesized a 1 wt. % platinum catalyst to investigate the treatment of highly alkaline and toxic industrial organic raffinate containing pyridine and its derivatives through a

combination of catalytic wet air oxidation and a biological process. They also conducted scanning electron microscopy, energy-dispersive X-ray spectroscopy, and X-ray diffraction analysis for characterization of the catalyst. Complete degradation of pyridine in the CWAO-treated effluent exhibited non-toxicity and was confirmed by High-pressure liquid chromatography. The biological method as post-treatment resulted in a final effluent meeting the discharge limit. They also reported the reusability of catalysts for four cycles, providing an effective solution for addressing toxic organic pollutants in wastewater. Bhoite and Vaidya, 2018 explored catalytic wet air oxidation as a promising method to enhance the biodegradability of biomethaned distillery spent wash. The authors performed oxidation of distillery effluent, characterized by high biological oxygen demand (BOD) (8100 mg/L) and chemical oxygen demand (COD) (40,000 mg/L), using a ferrous sulfate catalyst under optimized conditions (temperature. 175 °C, oxygen partial pressure. 1.1 MPa, catalyst loading. 32 mg/L). Subsequent adsorption over activated carbon and anaerobic digestion with acclimatized biomass resulted in a 73% reduction in COD and a significant increase in the BOD/COD ratio. The application of a two-step power-law model accurately described the kinetics of COD conversion. The study concludes that CWAO, combined with complementary treatments, provides an effective solution for the pretreatment and valorization of biomethaned distillery wastewaters. Bokov et al. (2021), used the sol-gel process, a prominent wet chemical method for synthesizing metal oxide nanoparticles and various nanostructures. The researchers employed molecular precursors like metal alkoxides dissolved in water or alcohol, yielding a gel through hydrolysis or alcoholysis, subsequently dried and calcined. The authors also reported that the method was cost-effective and had precise control over chemical composition owing to low reaction temperatures making it widely applicable in ceramics molding and as an intermediate for metal oxide thin films across optical, electronic, energy, and biosensing realms. Furthermore, sol-gel-derived materials find utility in diverse industries, including

surface coating, insulation, and specialized textile production. The authors reported that grinding dried gels yields nanoparticles, enhancing their industrial versatility and applicability. Bourassi et al. (2023) reported the catalytic degradation tests on sulfamethoxazole and tetracycline using platinum (Pt) supported on cerium oxide (Ce) and mixed cerium and zirconium oxides (Ce-Zr). Pt/Ce-Zr catalyst showed 98 % tetracycline elimination at 50 °C under atmospheric pressure and 92 % removal at room conditions. They also reported that the Pt/Ce test enabled 77 % sulfamethoxazole elimination and reached 45 % sulfamethoxazole mineralization. Conventional wastewater treatment plants are often ineffective in eliminating emerging contaminants, leading to persistent threats in the receiving environment. The authors reported that the Pt/CeZr catalyst demonstrated high efficiency, achieving 98% TET elimination at 50 °C under atmospheric pressure and 92% removal at room conditions. The authors revealed that Pt/Ce exhibited 77% SM elimination and 45% SM mineralization. Toxicity assessments confirmed the environmental viability of the treated solution using CWAO. The study highlights an eco-energetic, eco-friendly, and efficient approach for treating wastewater containing pharmaceutical pollutants. Burey et al. (2008), reported that hydrocolloid gel particles, ranging from micron to sub-micron sizes, hold significant appeal across various industries including food, agriculture, pharmaceuticals, and chemicals due to their biocompatibility, natural perception, and soft-solid texture. The authors also reported that hydrocolloid gel particles have diverse industrial applications such as texturizers in confectionery and cosmetics, slow-release encapsulation agents for flavors, nutrients, and pharmaceuticals, as well as thickeners in soups and sauces. The researchers reported that essential properties like particle size, hardness, shape, texture, and molecular release rates dictate their suitability for specific applications, alongside considerations of physical form and compatibility with other components, and understanding and tailoring raw materials and process conditions are crucial for optimizing hydrocolloid gel particle properties. This review

outlines the materials utilized in hydrocolloid gel particle formation and the associated gel formation mechanisms. The researchers faced a significant challenge in controlling particle properties like release profiles, strength, and detectability within products in their production. The authors evaluated an alternative technique to traditional methods and proposed a model for controlling particle size and subsequent properties. The researchers identified key properties of hydrocolloid gel particles and performed characterization methods for evaluating the properties, thus providing insights for further advancements in their industrial applications. Carneiro et al. (2020), investigated the biodegradation of antibiotic compounds, sulfamethoxazole (SMX) and ciprofloxacin (CIP), common emerging contaminants in sewage, known for contributing to antimicrobial resistance. The authors assessed operational parameters like organic loading rate (OLR), hydraulic retention time (HRT), and sludge retention time for their impact on biodegradation in anaerobic fixed bed reactors. The authors found that sulfamethoxazole (SMX) and ciprofloxacin (CIP) biodegradation decreased with increasing organic loading rate (OLR) and and reduction in hydraulic retention time (HRT) led to enhanced liquid-phase mass transfer coefficients but decreased antibiotic-biomass contact time, impacting reactor performance negatively. The researchers reported that anaerobic structured bed biofilm reactors (ASBBRs) exhibited superior biomethane production and biodegradation kinetics compared to anaerobic packed bed biofilm reactors (APBBRs). Cometabolic biodegradation of SMX and CIP was linked to hydrogenotrophic methanogenesis, particularly involving the Methanobacterium genus, in co-culture with fermentative bacteria. Overall, the study demonstrates the effectiveness of anaerobic fixed bed biofilm reactors in mitigating antibiotic contamination, thereby preventing environmental dissemination. Chai et al. (2023), addressed the scarcity of studies on the life cycle assessment (LCA) of industrial wastewater treatment, particularly using catalytic wet air oxidation (CWAO) technology, with a focus on actual industrialized data. The authors employed Simapro 9.0 software and

established an LCA model for the treatment of high-concentration organic wastewater by CWAO. It comprehensively analyzed the environmental impact across the construction, operation, and demolition phases. Key findings indicate that marine ecotoxicity, mineral resource consumption, and global warming are significant environmental factors. The operation phase, attributed to high power consumption and emissions, has the most substantial impact on the environment. Sensitivity analysis highlights electricity consumption as a major factor affecting abiotic depletion and freshwater aquatic ecotoxicity, while global warming is primarily influenced by pollutant emissions during the operation phase. The authors performed Monte Carlo simulations which revealed slightly higher uncertainty in abiotic depletion and toxicity-related impact categories. Cheng et al. (2019), studied the importance of sludge treatment in water treatment and reported that traditional methods suffer from issues like high sludge production and low solid content, hindering environmental and economic benefits. The researchers discussed various oxidation methods like Fenton reagent oxidation, ozone oxidation, wet air oxidation, and supercritical water oxidation mechanisms highlighting their effects on sludge dry yield and dewatering, along with the advantages and disadvantages of each technology. Advanced oxidation technologies offer promise by reducing sludge production and enhancing dewatering performance. Chohan et al. (2022), investigated the impact of various parameters, including nozzle temperature, infill pattern, and printing speed, on surface roughness and thickness in fused deposition modeling (FDM) using acrylonitrile butadiene styrene (ABS). The authors employed Taguchi L9 orthogonal array and ANOVA methods and reported that printing speed has the most significant influence on surface roughness, with a contribution of 83.41%, while nozzle temperature accounts for 9.04%. The researchers also reported that lower printing speed improves surface finish, while thickness and outer dimensions remain consistent across printed samples. De Julius et al. (2019), investigated the feasibility of using laser-induced incandescence for TiO_2 nanoparticles in flame spray

synthesis. The authors examined the fluorescence, flame emission, and incandescence signals and reported that time-resolved spectral measurements on TiO_2 nanoparticles revealed fluorescence at low laser fluences and incandescence at higher fluences, with a fluence threshold for breakdown phenomena. The researchers then conducted laser-induced incandescence spectral measurements on the flame spray at different heights above the burner and acquisition delay times, demonstrating the potential and challenges of this diagnostic tool in flame spray synthesis. Dükkancı and Gündüz (2008) studied the effectiveness of the catalysts in the oxidation of organic acids like butyric acid and maleic acid, which are commonly found in various industrial wastewaters. The researchers synthesized noble metal catalysts, such as platinum (Pt), palladium (Pd), and ruthenium (Ru) supported on TiO_2 to enhance their catalytic activity in the CWAO process. The researchers performed CWAO experiments under controlled conditions, and the oxidation kinetics of butyric acid and maleic acid were studied. The influence of various operational parameters, including temperature, pressure, and initial acid concentration, on the reaction rate and efficiency was analyzed to optimize the CWAO process. Furthermore, the study investigated the selectivity of the noble metal catalysts towards the conversion of butyric acid and maleic acid into intermediate by-products and eventually into harmless end-products. The researchers assessed the stability and durability of the noble metal catalysts during the CWAO process to understand their potential for practical application in wastewater treatment. In conclusion, this study provides valuable insights into the application of noble metal catalysts supported on TiO_2 for the CWAO of butyric acid and maleic acid solutions. The findings contribute to the development of efficient and sustainable solutions for the treatment of organic acid-containing industrial wastewater. Duraisamy et al. (2022), explored the degradation of waste transformer oils (wTOs) using a novel approach involving magnetic treatment followed by a biopolymer-clay micro-composite, chitosan-activated bentonite composite (C-ABC), as an adsorbent. The authors reported that the C-ABC

composite, being biocompatible and possessing exceptional adsorption properties, effectively restores the dielectric characteristics of wTOs to levels comparable to brand-new transformer oil (fTO). Comparative analysis with conventional adsorption materials highlights the superior reclamation efficacy of the C-ABC micro composite. The researchers confirmed that interactions between chitosan and activated bentonite significantly enhance dielectric properties by CIE chromaticity coordinates study. The researchers performed Energy-dispersive X-ray (EDX) spectroscopy and scanning electron microscopy (SEM) to reveal elemental composition and topography changes in C-ABC. Fourier transform infrared (FTIR) analysis and Statistical analysis demonstrate improved dielectric breakdown voltage for treated oils. Mathematical models and response surface analysis highlight interactive effects between process and response variables. SWOT analysis underscores the method's environmental friendliness, affordability, and efficacy, making it a promising solution for wTO remediation. Feijoo et al. (2023), explored the growing concern about contaminants in water streams, which has led to an increased research focus on advanced oxidation processes. The authors reported that advanced oxidation processes generate oxidative radicals, particularly hydroxyl, sulfate, chlorine, and iodine radicals and these oxidative radicals prove effective in decomposing stubborn compounds. The authors synthesized different types of free radicals generated using different techniques, elucidating the principles, mechanisms, and environmental/economic aspects related to each method. The study reported the growing concerns of antibiotics as an emerging contaminant in water, posing risks to both the environment and human health due to their large production and consumption. The authors investigated various methods including biological, physical, and chemical methods for removing antibiotics from wastewater and reported that the advanced oxidation process (AOP) effectively degrades antibiotics in aquatic environments due to its fast reaction rate and strong oxidation ability. The authors discussed a brief overview of the principles, characteristics, main influencing factors, and applications of

the AOPs such as Fenton or Fenton-like reactions, ozonation, catalytic ozonation, photocatalytic oxidation, electrochemical oxidation, and ionizing radiation, analyzing their current use in degrading antibiotics in water and wastewater. Feng et al. (2023) synthesized a copper-based catalyst with excellent hydrothermal stability with TiO_2 as support to ensure long-term fixation of copper and reduce catalyst leaching for oxidative decomposition experiment of m-cresol, a coal chemical wastewater that is the most bio-toxic and the most difficult to decompose. The authors used the one-pot sol-gel method to ensure the super-dispersion and uniform distribution of copper nano-particles on the support, allowing them to retain more active sites for a long time. The authors reported good stability and catalytic activity of the catalyst prepared by this method and the catalytic effect does not decrease significantly after 10 cycles of use. The authors reported that at 140°C, 2 MPa, and 2 hr, m-cresol with a concentration of up to 1000 mg L^{-1} could be completely degraded, and the COD removal rate could reach 79.15%. Gao et al. (2022), studied different electrochemical technologies, as it is a promising solution, enabling simultaneous pollutant removal and resource recovery while minimizing chemical input and water consumption. The authors provided an overview of various electrochemical technologies for separating and recovering organics and inorganics from wastewater such as electrodeposition, electrodialysis, membrane electrolysis, electrochemical oxidation, capacitive deionization, and bio-electrochemical systems. The authors reported that dealing with persistent pollutants in wastewater often requires high energy input and chemical additions, particularly for organometallic complexes that hinder removal efficiency. The researchers faced challenges including material cost and longevity, process efficiency and selectivity, and complexity of wastewater matrices. Geng et al. (2020) used the redox-precipitation method for a range of $MnCeO_x$ catalysts, developed for the catalytic wet air oxidation (CWAO) of phenol. The authors reported that $Mn_9Ce_1O_x$ showed maximum activity and stability, achieving an 88.1% Total Organic Carbon (TOC) conversion in 60

minutes at 70 °C and stable for over five runs and at 50 °C, phenol conversion was 84.2% and the TOC conversion was 73.8%. The study reported the roles valence state of Mn and Ce modification in the catalyst's performance thus revealing that Ce optimization enhanced the activity of catalysts and stability by preserving the catalyst structure and preventing the reduction of Mn^{4+} and Mn^{3+} to Mn^{2+}. Gizaw and Habtu (2022) investigated the degradation of reactive red 2 mono azo dye using a catalytic wet air oxidation process with a copper oxide-loaded activated carbon catalyst (CuO/AC). The authors derived the activated carbon (AC) from water hyacinth root via physicochemical activation and prepared CuO/AC through wet impregnation. The researchers performed various characterization techniques including Fourier transform infrared (FTIR), scanning electron microscope (SEM), X-ray diffraction (XRD), and thermogravimetric analysis (TGA). The authors studied the operating parameters such as catalyst dose (2–6 g/L), reaction temperature (70°C–120°C), and oxygen partial pressure (1–3 bar) for their influence on reactive red 2 (RR2) dye decolorization and chemical oxygen demand (COD) conversion within a reaction time of 10–120 min. The authors reported that at maximum conditions (6 g/L catalyst dose, 120 °C reaction temperature, 3 bar oxygen partial pressure) complete dye decolorization (100%) and 88.57% COD conversion was achieved within 120 min. Dye decolorization percentages were reduced in the presence of free radical scavengers (sodium bicarbonate and methanol), and the performance of the reused catalyst declined. The treated dye solution exhibited low phytotoxicity (62.67% germination index of Lepidium nativism seeds) compared to the untreated dye solution (34.80%). González et al. (2023) studied different operating conditions of humid air oxidation and catalytic humid air oxidation for the treatment of highly concentrated methyl diethanolamine wastewater streams from an amine plant in acid gas recovery of a gasoline refinery. The authors reported that wet air oxidation treatment demonstrated excellent removal efficiency of methyl diethanolamine, sulfide, chemical oxygen demand, and total organic carbon (99%, 95%, 65%,

and 38%, respectively). The authors used activated petroleum coke materials produced under different conditions from refineries as catalysts. The author informed that wet air catalytic oxidation using activated petroleum coke effectively removed methyl diethanolamine under milder operating conditions while maintaining comparable wastewater treatment removal performance compared to non-catalytic experiments. This technology significantly improved the biodegradability of treated wastewater (25-70% range). Gopakumar et al. (2023) focused on the catalytic oxidation of NO to NO_2 for industrial nitric acid (Ostwald process) using silver-enhanced manganese over a zirconia catalyst under industrially relevant conditions (10% NO, 6% O_2, and 15% H_2O). The authors reported that converting homogeneous gas-phase NO oxidation reactions to catalysts significantly reduces space requirements and capital expenditures. However, there is still no industrial catalyst for this process. The authors reported that the manganese catalyst can operate at low temperatures in both dry and wet conditions and concentrations relevant to industrial catalytic oxidation of NO compared to unformed manganese. Gupta and Verma, (2021) found CWAO as an effective technique for the complete mineralization of glyphosate (PMG) in wastewater using iron nanoparticle (Fe NP)-dispersed carbon nanofibers (CNFs) decorated over activated carbon beads (ACBs). The authors reported that the catalyst exhibits a high BET-specific surface area, good Fe-loading, high thermal stability, and graphitic characteristics contributing to efficient CWAO. The experimental data demonstrated that complete PMG degradation was achieved at 220 °C and 25 bar within 6 hours using a catalyst dose of 0.75 g/L, with a turnover frequency indicating efficient Fe metal site activity. Chemical oxygen demand removal reached 80% in 6 hours. The process, initiated by hydroxyl radicals, converted PMG to non-toxic byproducts, and the treated water showed no toxicity. The scalable Fe-CNF/ACB catalyst and CWAO technology hold the potential for treating other recalcitrant organic compounds like herbicides, pesticides, and pharmaceuticals. Gupta et al. (2022) devised a two-step process for the sequential mineralization of glyphosate,

a widely used herbicide known for its environmental impact. The process involves CWAO using iron nanoparticle-tipped carbon nanofibers (Fe-CNF/ACB) as the catalyst, followed by microbial degradation. The authors reported that Fe-CNF/ACB exhibited a high specific surface area, excellent thermal stability, and increased exposure of Fe nanoparticles, resulting in ~70% degradation of glyphosate (100 mg/L) in 2 hours at 220 °C, 25 bar-air pressure, and 0.75 g/L catalyst dose. They also reported that subsequent microbial degradation by Providencia vermicola, isolated from industrial wastewater, completed the mineralization in the next 2 hours at 37 °C, achieving a 100% reduction in total organic carbon content. The non-toxicity of Fe-CNF/ACB towards the bacterial strain simplifies the sequential remediation process by eliminating the need to remove the spent catalyst before microbial degradation. This two-step approach demonstrates efficiency in degrading and mineralizing toxic, bio-refractory pollutants in wastewater. Gutiérrez-Sánchez et al. (2023) investigated the catalytic activity of degrading the antibiotic ciprofloxacin in catalytic wet air oxidation (CWAO) of activated carbon from sewage sludge (SAC) loaded with iron nanoparticles (FeSAC). The authors employed various characterization techniques of FeSAC catalysts such as N_2 adsorption/desorption, scanning electron microscopy, X-ray fluorescence spectroscopy, X-ray photoelectron spectroscopy, and thermogravimetric analysis. The CWAO reactions were performed in a batch reactor at different conditions, different temperatures (120°–140°C), total pressures (10–30 bar), and catalyst dosages (0.1–0.7 g/L). The authors reported that temperature and catalyst dosage significantly influenced antibiotic removal, with a catalyst dosage of 0.7 g/L resulting in >99% ciprofloxacin degradation and >60% CO_2 degradation within 2 h at 140 °C and 20 bar and achieved selectivity. The FeSAC catalyst showed high stability with low loss of active phase (Fe) under the tested conditions. The authors proposed a potential equation to describe the decomposition of ciprofloxacin with a calculated activation energy of 53.8 kJ/mol. The authors also performed density functional theory (DFT)

calculations to show which compounds are least degraded by CWAO in terms of electronic energy and demonstrate the degradation mechanism of ciprofloxacin. Hammedi et al. (2023), conducted the catalytic wet air oxidation (CWAO) of p-hydroxybenzoic acid (p-HBA) in a batch reactor at 140°C, 50 bar over Ru-based catalysts on four mesoporous supports. TiO_2, CeO_2–TiO_2, ZrO_2–TiO_2, and La_2O_3–TiO_2, prepared via the sol-gel method and then impregnated with 3 wt.% Ru pre-cursors. N_2-sorption, XRD, XPS, H_2–TPR, NH_3-TPD, TEM, and HAADF-STEM, were employed as various characterization techniques. They also reported that cerium-containing catalysts (Ru/CeTi) showed a significant specific surface area (SBET), abundant surface-active oxygen, and Lewis acidity sites. Fresh Ru catalysts with cerium exhibited higher activity than those with TiO_2, Zr-Ti, and La-Ti. The study suggested that acidic sites and surface oxygen trap p-HBA molecules and increase catalytic properties through interactions with Ru particles via the cerium redox process (Ce^{3+}/Ce^{4+}). They reported that the presence of cerium increases surface-active oxygen and prevents carbon deposition on Ru catalyst surfaces. The authors studied the kinetic data of p-HBA oxidation which followed the pseudo-second-order (PSO) model. Javid et al. (2023) performed wet air oxidation (WAO) of the PPE blends at temperatures ranging from 300°C to 350°C and initial air pressures of 30 bar and 60 bar, respectively. The authors reported that total suspended solids (TSS) were reduced by up to 99%, and total chemical oxygen demand (tCOD) and soluble chemical oxygen demand (sCOD) were significantly reduced to 360 mg/L and 110 mg/L, respectively. The authors reported volatile fatty acids (acetic acid and propionic acid) as the main products and ammonia nitrogen (NH_3-N), with maximum concentrations of 1117 mg/L, 975 mg/L, and 18 mg/L, respectively. The authors also reported that Nitrogen and oxygen were the most abundant gaseous products, reaching 72% (w/w) and 14% (w/w), respectively. The authors performed semi-batch WAO processing at 300°C and 350°C to achieve comparable waste reductions. The result suggests that non-catalytic WAO is a viable solution for PPE waste treatment. Jing et al.

(2015) synthesized a catalyst using hollow microspheres made of $NiCo_2O_4$ (NCO) spinel for catalytic wet air oxidation to remove humic substance (HS) at atmospheric pressure and low temperature. The authors reported that treatment with NCO at 90°C resulted in a 93.4% decrease in total organic carbon concentration after 24 hours. NCO showed solid-state redox couples, a large surface area (66.88 m^2/g) the main reason for its ability to mineralize adsorbed HS on its surface, numerous surface oxygen species, a low reduction temperature, dissolved oxygen filling oxygen vacancies and restoration of NCO to its original state. Kaneko et al. (2021), introduced a method for predicting in-furnace images and sensor signal readings in a waste incineration plant. The approach utilizes a deep dynamical model based on Kalman Variational Auto-Encoders, incorporating various process signals, control inputs, and time-series sequences of in-furnace image data. The goal is to enable automatic control systems to anticipate abnormalities in incoming waste, preventing potential instabilities during and after combustion. The experimental results using real plant data demonstrated that the proposed strategy offers enhanced prediction accuracy for both process signals and in-furnace images compared to Long Short-Term Memory neural networks. Khatri and Garg (2021) explored the efficacy of an activated carbon (AC) supported copper catalyst in the catalytic wet oxidation (CWO) of pretreated high-strength biomethaned spent wash (BMSW) from alcohol distilleries. Before wet oxidation (WO) treatment, the BMSW underwent centrifugation to remove suspended solids. The authors reported that at 220°C, CWO treatment achieved substantial chemical oxygen demand and colour removals of 72% and 97%, respectively, from the centrifuged BMSW (catalyst dose = 3.4 g L^{-1}, reaction time = 3 h). The researchers identified acetic acid, a major methane precursor in large concentrations in the treated liquid samples. Kinetic expressions for WO and CWO processes were developed, and the recovered catalyst could be reused twice in CWO runs. Biochemical methane potential (BMP) tests indicated significant biogas production from the treated BMSW. Overall, the study suggests that CWO

of BMSW holds potential as a treatment method before disposal in the environment. Kurian, M. et al. (2017) investigated the use of iron-doped nanoceria as a catalyst for the CWO of chlorinated organics under mild conditions. The authors reported that mild conditions that involve lower temperatures and pressures not only improve the safety aspects of the process but also reduce energy consumption. The authors reported that iron-doped nanoceria catalyst effectively degraded chlorinated organic compounds, thus reducing their concentration in the wastewater. They also evaluated the catalytic activity, stability, and efficiency of iron-doped nanoceria for the mild CWO of chlorinated organics catalyst, indicating its potential for long-term use in CWO applications and providing a greener and more sustainable approach to wastewater treatment. Kumar et al. (2020) synthesized Silver and ytterbium-doped bismuth vanadate ($Ag_xYb_yBi_{z-xy}VO_4$) composites via solid-state reaction at 950°C for 6 hours in an open-air atmosphere. The authors examined the impact of dopant concentration on morphology, optical properties, and dye degradation efficiency using various techniques including X-ray Diffraction (XRD), energy-dispersive X-ray (EDX) spectroscopy, thermogravimetric analysis (TGA), scanning electron microscopy (SEM), photoluminescence (PL) spectroscopy, Fourier transform infrared (FTIR), and UV–Visible spectroscopy.

The authors reported that SEM analysis revealed irregular-shaped particles with some grain-like structures, EDX confirmed the presence of V, Bi, Ag, Yb, and O in the doped materials., TGA indicated stability at room temperature, FTIR results suggested the formation of vanadium pentoxide-based materials and the presence of V–O bond. The authors calculated the optical band gaps to be 2.25 eV for V_2O_5 and 1.56 eV for the composites and reported that Nyquist plots showed higher charge transfer potential. Photoluminescence spectra exhibited bands in the red and red-to-infrared regions, suggesting potential for optical devices. The researchers achieved a remarkable dye degradation efficiency of 94.57% for crystal violet (CV) dye under solar-light irradiation within 120 minutes. The photoluminescent study revealed

emission bands at 1088 and 1045 nm, indicating the further potential for optical devices. Kurian (2021) explored the integration of advanced oxidation processes (AOPs) with nanomaterials for various environmental applications. AOPs are powerful techniques for the degradation of organic pollutants in water and air, utilizing highly reactive species to break down contaminants. Nanomaterials, with their unique properties and high surface area, have emerged as promising catalysts or adsorbents to enhance AOP efficiency. The review discussed various AOPs, such as photocatalysis, ozonation, the Fenton process, and the photo-Fenton process, and their mechanisms for generating reactive species. Nanomaterials, including metal oxides, metal nanoparticles, carbon-based materials, and metal-organic frameworks (MOFs), are examined for their catalytic and adsorption capabilities in AOP-based environmental applications. Furthermore, the review highlights the advantages of incorporating nanomaterials into AOPs, such as improved catalytic activity, enhanced mass transfer, and the ability to target specific pollutants. The role of nanomaterial properties, such as size, shape, and surface functionalization, in influencing AOP performance is discussed. Moreover, the review presents case studies on the application of nanomaterial-based AOPs for the degradation of various organic pollutants, such as dyes, pharmaceuticals, and emerging contaminants. The efficiency of these hybrid systems is compared with conventional AOPs, emphasizing the potential of nanomaterials to overcome limitations and increase the degradation rates of recalcitrant pollutants. Additionally, the review addresses the challenges and considerations related to the use of nanomaterials in AOPs, including potential toxicity and environmental impact. Proper nanomaterial characterization and recovery from treated wastewater are highlighted to ensure safe and sustainable application. In conclusion, this review provides valuable insights into the advancements and potential of integrating nanomaterials with AOPs for environmental remediation. It highlights the promising future of these hybrid systems in addressing complex environmental challenges and promoting sustainable water and air treatment solutions. Ma et

al. (2021) provided a comprehensive analysis of various AOPs employed in organic wastewater treatment, focusing on their mechanisms, influencing factors, and degradation products. The review delves into the underlying mechanisms of AOPs, including photocatalysis, ozonation, Fenton process, and photo-Fenton process, highlighting their effectiveness in generating highly reactive species capable of breaking down organic pollutants. The researchers analyzed various factors that influence the efficiency of AOPs, such as pH, temperature, catalyst type, and initial pollutant concentration to understand their impact on the overall treatment performance. They also assessed the formation of degradation products during AOP treatment, as the presence of by-products may be a concern for the environment and human health. Characterizing and identifying these by-products are essential for assessing the overall environmental impact of AOP-treated effluents. The review also evaluated the potential toxicity of AOP-treated effluents, emphasizing the importance of ecotoxicological assessments to ensure the safety of treated water before discharge. They also reported that the integration of AOPs with other treatment technologies, hybrid approaches, and the development of novel catalysts are potential strategies for enhancing the efficiency of organic wastewater treatment. In conclusion, this critical review offers valuable insights into the advancements and challenges of AOPs in organic wastewater treatment. It provides a foundation for further research and development of sustainable and efficient strategies to address the complexities of organic pollution in water resources. Makatsa et al. (2021) studied different reaction mechanisms-direct (without intermediates, directly forming CO_2 and H_2O) or indirect (involving the formation of intermediates), kinetics, and computational fluid dynamics (CFD) modeling like power law and Langmuir–Hinshelwood (to describe adsorption/desorption of reactants on the catalyst surface) for treating refractory organic compounds like phenol in wastewater. The authors identified acetic acid as a stable intermediate in phenol oxidation and reported that phenol conversion increases with higher temperature, pressure, and gas velocity but decreases with

increased liquid space velocity. The authors also cited the formation of hot spots, catalyst deactivation, and reactor thermal runaways as safety concerns. Pan et al. (2013) investigated the promoted wet peroxide oxidation (PWPO) process for the degradation of chlorinated volatile organic compounds (Cl-VOCs) using FeOCl supported on macro-microporous biomass-derived activated carbon as a catalyst. The authors derived activated carbon catalyst from biomass through a carefully optimized activation process, resulting in a hierarchical macro-microporous structure with a high surface area and enhanced adsorption capacity. The PWPO experiments were conducted under controlled conditions, and the catalytic performance of FeOCl supported on the activated carbon was evaluated by monitoring the degradation of various Cl-VOCs present in the wastewater. The study explored the efficiency of the catalyst in breaking down these challenging pollutants. The reaction mechanism involved in the PWPO process, particularly the role of FeOCl supported on the activated carbon, was elucidated to understand the catalytic activity and degradation pathways. The study also investigated the stability and reusability of the catalyst, assessing its potential for practical application in the long-term treatment of Cl-VOC-contaminated effluents. Furthermore, the influence of key operational parameters, such as reaction time, temperature, and H_2O_2 dosage, on the PWPO process is examined to optimize the treatment efficiency. In conclusion, this study demonstrates the effectiveness of FeOCl supported on macro-microporous biomass-derived activated carbon as a catalyst for PWPO in the treatment of Cl-VOCs. The hierarchical porous structure of the activated carbon, combined with the catalytic activity of FeOCl, results in the efficient degradation of these challenging pollutants, providing a promising approach for wastewater treatment. Roy and Saroha (2014) investigated the use of a ceria-promoted γ-Al_2O_3 supported platinum catalyst for the catalytic wet air oxidation (CWAO) of oxalic acid, a common organic pollutant found in industrial wastewater. The authors examined the catalyst's composition, comprising platinum supported on γ-Al_2O_3 with ceria as a promoter for its

efficiency in facilitating the oxidation of oxalic acid. The researchers investigated the kinetic behavior of the CWAO process using the ceria-promoted catalyst, providing insights into the reaction rate and reaction mechanism. They also analyzed the influence of various operational parameters, such as temperature, pressure, and initial oxalic acid concentration, on the oxidation rate to optimize the process conditions. Furthermore, the study assessed the catalyst's deactivation overtime during the CWAO process, elucidating the factors contributing to its loss of activity. They compared the performance of the ceria-promoted γ-Al_2O_3 supported platinum catalyst with other catalysts commonly used in CWAO applications, providing valuable information on its catalytic activity and selectivity. They also addressed the environmental implications of the CWAO process for oxalic acid degradation considering the potential formation of by-products and their impact on water quality. In conclusion, this study sheds light on the application of ceria promoted γ-Al_2O_3 supported platinum catalyst for CWAO, offering valuable insights into its kinetic behavior, deactivation mechanisms, and potential for efficient oxalic acid degradation in industrial wastewater treatment. Sassi et al. (2017) explored the application of a catalytic wet air oxidation (CWAO) process over Al-Fe pillared clays, which were synthesized using microwave irradiation. The synthesis of pillared clays using microwave irradiation offers several benefits, including improved energy efficiency and shorter reaction times. The catalytic properties of Al-Fe pillared clays have shown promise in effectively degrading various pollutants found in wastewater. The CWAO process, which utilizes both air and a catalyst, facilitates oxidation reactions that convert toxic organic compounds into less harmful substances. Through investigation, the efficiency and stability of the Al-Fe pillared clay catalyst have been assessed, indicating its potential for long-term use in wastewater treatment. Furthermore, the impact of key operational parameters, such as temperature, pressure, and catalyst loading, has been evaluated to optimize the performance of the CWAO process. Overall, these findings highlight the effectiveness of the CWAO process

using microwave-synthesized Al-Fe pillared clays as a sustainable and viable solution for wastewater treatment, contributing to the preservation of our environment and water resources. Shan et al. (2023) synthesized carbon-supported Pt-Pb/XC-72R and Pt-Pb/EC-300 catalysts for CWAO of phenol wastewater by using a Pt-M alloy structure (M=Pb, Cu) in which Pt, mainly present in the form of PtO and M in the form of M^{2+}. The authors reported Pt-Pb/XC-72R to be highly active and stable against phenol CWAO even at 100 °C with an initial TOC conversion rate being 91.1% and could be maintained above 75% for 5 consecutive cycles, whereas Pt-Pb/EC-300 rapidly deactivated after 5 cycles, and the TOC conversion rate decreased from 91.2% to 47.1%. The authors reported that the Pb^{2+} concentration of Pt-Pb/XC-72R is much higher than that of Pt-Pb/EC-300, and the higher Pb^{2+} concentration promotes surface oxidation and prevents the oxidation of PtO during the CWAO process which improves stability. The authors also found that for Pt-Pb/EC-300, both PtO and PbO are oxidized during the reaction, resulting in inactivation. The authors replaced Pt-Pb with Pt-Cu to reduce the use of lead for environmental reasons and reported that the catalytic performance can be further improved by increasing Cu^{2+}. Singh et al. (2018) explored alternatives to the conventional aqueous ion-exchange method for the synthesis of Cu/zeolite Y catalysts used in the catalytic wet peroxide oxidation of quinoline in a continuous fixed-bed reactor. The authors investigated various synthesis routes such as aqueous ion exchange (CuYAIE), wet-impregnation (CuYIMP), and precipitation-impregnation (CuYPI). The authors employed characterization techniques to reveal the significant impact of preparation methods on the synergy between copper-support interfaces. CuYAIE and CuYIMP promoted isolated Cu^{1+}/Cu^{2+} species and reported that CuYPI exhibited large crystallites of CuO on its external surface. They also reported that CuYPI demonstrated hierarchical porosity and increased surface area and both CuYAIE and CuYIMP displayed comparable mineralization and H_2O_2 stoichiometric efficiencies, with higher catalytic activities than CuYPI. The study concluded that isolated

sites, rather than high surface area, played a crucial role in H_2O_2 activation. The authors synthesized CuYIMP, through wet-impregnation, exhibited high operational stability, with over 60% mineralization under specific conditions. The authors reported that copper leaching was influenced by factors such as liquid hourly space velocity (LHSV) and particle size. The system followed the Eley-Rideal mechanism, and kinetic parameters were calculated based on this mechanism. The researchers reported that wet-impregnation was identified as a more effective method than aqueous ion exchange for synthesizing Cu/zeolite Y catalysts with desirable catalytic properties. Sun et al. (2022) explored the potential of Catalytic Wet Air Oxidation (CWAO) coupled desalination technology for the efficient degradation of high salinity and high organic wastewater. The presence of chloride in wastewater poses challenges for Advanced Oxidation Processes (AOPs). The researchers introduced a novel chlorine ion-resistant catalyst, $LaFe_{0.85}Ru_{0.15}O_{3-\delta}$ for CWAO treatment of chlorine ion wastewater. The researchers reported that $LaFe_{0.85}Ru_{0.15}O_{3-\delta}$ exhibited chlorine ion resistance regardless of Cl^- concentration, and no Ru dissolution occurred after the reaction. Structural verification through various techniques confirmed the catalyst's composition. Kinetic data and density functional theory (DFT) indicated that Fe is the site of acetic acid oxidation and chloride ion adsorption. The authors reported that the presence of Fe in $LaFe_{0.85}Ru_{0.15}O_{3-\delta}$ facilitated the adsorption of chlorine ions, protecting the Ru site and other active oxygen species, and ensuring catalytic activity. This study is crucial for developing chloride-resistant catalysts in CWAO. Sushma and Saroha (2019), assessed the efficacy of fresh and used noble and non-noble metal-based catalysts for CWAO of industrial organic raffinate under mild operating conditions. The evaluation, based on COD removal, includes monitoring catalyst stability over repeated experiments. The authors performed various characterization techniques of fresh and used catalysts revealing that, at low operating conditions, the non-noble metal ceria-promoted manganese catalyst showed potential to replace expensive noble metals such as platinum. The

authors also calculated the biodegradability of the industrial organic raffinate and CWAO effluent in terms of the BOD/COD ratio. Tekin et al. (2023), employed catalytic wet air oxidation with lanthanum cobalt oxide ($LaCoO_3$) as a catalyst for the efficient treatment of synthetic sugar industry wastewater in a single process and identified reaction temperature and theoretical air percentage as crucial parameters. The authors reported 91% total organic carbon (TOC) and 87% chemical oxygen demand (COD) removals in optimum conditions, indicating high mineralization. The authors studied the kinetics using pseudo-homogeneous and heterogeneous models and with the pseudo-homogeneous approach, a second-order reaction was indicated. The author reported that the presence of mass transfer limitations was only observed for oxygen as a gas reactant according to the surface concentration calculations for heterogeneous models. Mars–van Krevelen model provided accurate fits for sucrose and TOC oxidation among all heterogeneous models, thus highlighting the effectiveness of the catalytic wet air oxidation process. Wang et al focused on achieving high performance under ambient pressure (AP-CWAO) for treating high-salt wastewater, involving hydrophobic modification using polytetrafluoroethylene (PTFE) on hollow microspheres $NiCo_2O_4$ (HM-$NiCo_2O_4$) to enhance O_2 transfer and salt resistibility. The authors reported that in a 10 g/L NaCl solution under ambient pressure at 80 ℃, PHM- $NiCo_2O_4$ catalyzed O_2 to achieve approximately 70% mineralization of bisphenol A (BPA) within 240 minutes, whereas HM- $NiCo_2O_4$ achieved only about 50% mineralization under the same conditions thus showing enhanced performance compared to the unmodified version (HM- $NiCo_2O_4$).The authors performed density functional theory calculations and molecular dynamics simulations to confirm that PTFE modification improved the O_2 transfer and salt resistibility of HM-$NiCo_2O_4$. The degradation of BPA in the presence of O_2 was attributed to various reactive oxygen species (HO•, $•O^{2-}$, and $1O_2$), generated based on the Mars-van Krevelen mechanism. Verma et al. (2021) employed the process of catalytic wet air oxidation (CWAO) to treat coking wastewater (CWW), a highly

polluting effluent. The authors explored the degradation of pollutants such as COD, phenol, and cyanide in CWW and investigated parameters including initial pH, temperature, air partial pressure, catalyst mass loading, and treatment time, using various catalysts in batch mode. The authors reported copper chloride to be the most effective catalyst for pollutant degradation and the optimum conditions for organic compound degradation were identified at a temperature of 130 °C, air partial pressure of 8.8 MPa, catalyst mass loading of 3 g/L, and treatment time of 6 hours. The highest percentage reduction of COD, phenol, and cyanide was achieved at 160 °C, 12.2 MPa air partial pressure, 5 g/L catalyst mass loading, and 6 hours treatment time, with reductions of 97.32%, 97.94%, and 99.87%, respectively. The authors also conducted kinetic studies to determine rate constants and reaction orders for COD, phenol, CN, CW, and air partial pressure. Wang et al. (2020) synthesized highly active and stable nano-hybrid bimetallic catalysts consisting of $Na_2Mo_4O_{13}$ and MoO_3 (NM) (hydrothermal method) and Au-Pd (one-pot deposition reduction method) for ambient condition-catalytic wet air oxidation (AC-CWAO) of organic dyes (Brilliant Green, Safranine O, and Methylene Blue) using air as the sole oxidant in aqueous solutions. The authors reported that Au-Pd (1.1)/NM-400 with an Au/Pd mass ratio of 1.1, calcined at 400 °C exhibited the highest catalytic activity and attributed to the synergistic effect of Au and Pd. The authors also reported efficient catalytic performance even at low temperatures and high dye concentrations. The kinetic study revealed that dye degradation followed pseudo-first-order kinetics and the catalyst also exhibited good reusability and catalytic stability after five cycles. The study also found that superoxide radical ($\bullet O^{2-}$) is the primary active oxidative species during the CWAO of dyes. Wang& Wang (2021) studied the influence of inorganic anions like chloride, carbonate, phosphate, sulfate, and nitrate on advanced oxidation processes (AOPs) commonly used in water treatment to form radicals, which influence the transformation of organic pollutants. The authors studied the catalytic activity of catalysts, the formation and transformation of reactive species, the stability

of oxidants (H_2O_2 and persulfate), and the degradation of intermediate products of organic pollutants. Zhang et al. (2023) explored the treatment of high-salinity and high-organic wastewater through the combination of CWAO and desalination technologies such as membrane distillation (MD), membrane bioreactor (MBR), ultrafiltration (UF), nanofiltration (NF), etc. The authors synthesized RuO_2/TiO_2 catalysts with different calcination temperatures for CWAO of maleic acid wastewater with a theoretical chemical oxygen demand (COD) value of 20,000 mg L^{-1}. The authors reported that RuO_2/TiO_2 series catalysts demonstrated remarkable salt resistance, with over 80% Total Organic Carbon (TOC) removal rates in the CWAO system containing 5 wt.% Na_2SO_4. RuO_2/TiO_2-350 exhibited the best degradation performance in both non-saline and Na_2SO_4-containing conditions. Various characterization techniques confirmed the physicochemical structure of RuO_2/TiO_2 catalysts and their impact on pollutant degradation. Calcination temperature directly influenced specific surface area, pore volume, oxygen vacancies, and acid sites, affecting catalytic activity. The study also investigated the catalyst's performance in treating acids, alcohols, and aromatic compounds with added NaCl or Na_2SO_4, demonstrating universality and excellent salt resistance. Additionally, the relationship between the structure of three types of organic compounds and the degradation effect in the CWAO system was explored. Zhang et al. (2024) developed a liquid-phase wet-washing process for effective toluene removal by advanced oxidation with persulfate (PMS). They synthesized a composite catalyst (CFQ/AC) with a high surface area to facilitate continuous PMS activation by providing abundant surface-active sites and it was achieved through a one-step process depositing 0 D $CoFe_2O_4$ onto low-cost activated carbon. They reported that Co(III)/Fe(III) species produced in the reaction, captured electrons from PMS, thus enabling Co(II)/Fe(II) regeneration and completing two redox cycles of Co(III)/Co(II) and Fe(III)/Fe(II). They reported that the CFQ/AC/PMS system consistently showed a stable toluene removal efficiency surpassing 96% within 2 hours, with over 80%

selectivity for CO_2, indicating high mineralization capability and reduced gaseous intermediates. They also reported changes in the valence of transition metals and the formation of charge transfer intermediates by analyzing through electrochemical and in-situ Raman spectroscopy. Zhao et al. (2022) explored the treatment of high-concentration N-methyl diethanolamine (MDEA)-containing wastewater, characterized by strong alkalinity, high COD, and toxic organics, using CWAO with commercial activated carbon (AC). The study investigated the influence of operational parameters (temperature, reaction pressure, and residence time) on the removal ratios of COD and MDEA. The wastewater had initial concentrations of 18.92 $g \cdot L^{-1}$ MDEA, 61.2 $g \cdot L^{-1}$ COD, 21.34 $g \cdot L^{-1}$ total organic carbon (TOC), and 5.65 $g \cdot L^{-1}$ total nitrogen (TN). The contribution of MDEA concentration to COD reached 89.8%. At optimal conditions (230 °C, 5.0 MPa, and 90 min residence time for 168 hours of continuous running), the removal ratios for MDEA and COD exceeded 98% and ~90%, respectively. The researchers reported that surface carboxylic acid groups on AC played a crucial role in generating hydroxyl radicals (•OH) through the adsorption of O_2, which then attacked the C-N bond of MDEA, forming intermediate products that were further oxidized to NH_4^+, CO_2, and H_2O. This study presents a promising pretreatment technology for high-concentration MDEA-containing wastewater. Zhou et al. (2019) investigated the remarkable durability and activity of a polymetallic Ru-doped Fe-Co-Ce/γ-Al_2O_3 nanocatalyst for the treatment of landfill leachate. They synthesized nanocatalysts with a carefully designed combination of ruthenium (Ru), iron (Fe), cobalt (Co), and cerium (Ce) supported on γ-Al_2O_3, which contributed to its superior catalytic performance. The study explored the synergistic effect observed in the nanocatalyst, arising from the presence of multiple metal components. The authors reported that the unique interplay between Lewis acid and base sites on the catalyst's surface played a crucial role in promoting catalytic activity and stability during the treatment of landfill leachate. The reaction mechanism underlying the enhanced catalytic

activity was elucidated, with a focus on the interfacial Lewis acid-base pair interactions that facilitate the degradation of organic pollutants in landfill leachate. Furthermore, the study evaluated the durability and stability of the nanocatalyst under harsh landfill leachate conditions, ensuring its potential for long-term application in wastewater treatment. The investigation included a comprehensive analysis of the performance of the nanocatalyst in the degradation of various organic pollutants present in landfill leachate, providing valuable insights into its versatility and efficiency. In conclusion, this study presented a polymetallic Ru-doped Fe-Co-Ce/γ-Al_2O_3 nano-catalyst with a synergistic effect, demonstrating remarkable durability and catalytic activity for landfill leachate treatment. The interfacial Lewis acid-base pair-dependent reaction mechanism offers a fundamental understanding of the catalyst's enhanced performance, contributing to the development of efficient and sustainable solutions for landfill leachate remediation.

CHAPTER 3

EXPERIMENTAL PROCEDURES

CHAPTER 3

EXPERIMENTAL PROCEDURES

3.1. Synthesis of catalyst

3.1.1. Excess Solution Impregnation (ESI) method

ESI is a commonly used technique for the synthesis of heterogeneous catalysts. The active metal precursor is dissolved in an aqueous or organic solution. Then the metal-containing solution is added to a catalyst support containing the same pore volume as the volume of the solution that was added. Capillary action draws the solution into the pores. Solution added in excess of the support pore volume causes the solution transport to change from a capillary action process to a diffusion process, which is much slower. The catalyst can then be dried and calcined to drive off the volatile components within the solution, depositing the metal on the catalyst surface. The maximum loading is limited by the solubility of the precursor in the solution. The concentration profile of the impregnated compound depends on the mass transfer conditions within the pores during impregnation and drying.

Single metal catalyst (Fe) was synthesized by excess solution impregnation method (ESI method) using preconditioned γ-Al_2O_3 as support. Alumina was first dried in a hot air oven for one hour to remove moisture and impurities. Iron (Iron III Nonahydrate-$Fe(NO_3)_3.9H_20$), acetic acid, and double distilled water were used in the experiment. Different weight percentage of iron (0.5,1.0,1.5,2.0) was taken and mixed with 100mL of distilled water and stirred for thirty minutes for dissolving in a magnetic stirrer. After thirty minutes 10 grams of preconditioned γ-Al_2O_3 was added and stirred continuously for four hours in the magnetic stirrer. After four hours the mixture is dried in a hot air oven overnight (12 hours) at 110º C. Then the residue left is to be calcined in a crucible in a calcination chamber at 400º C for 4 hours.

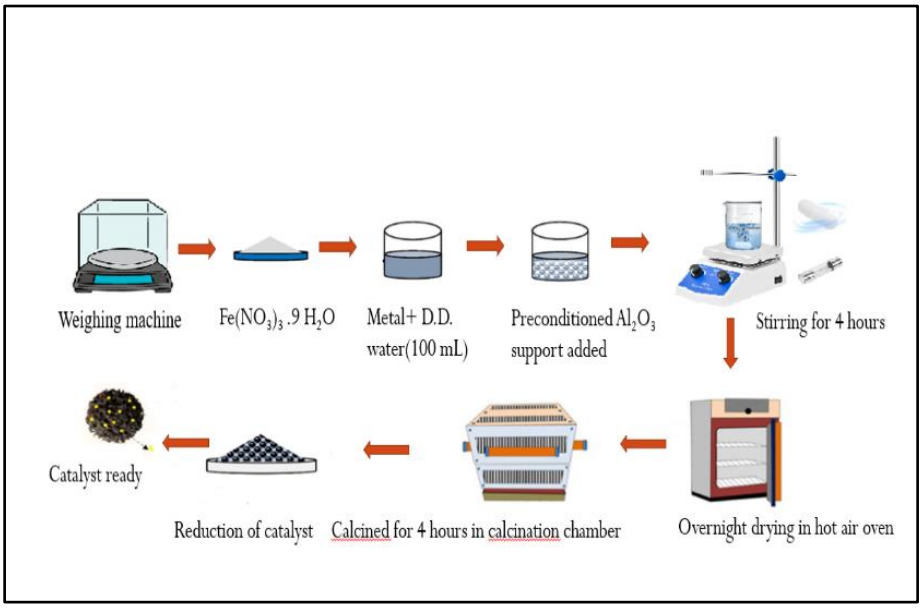


Fig.30. Schematic diagram of ESI method

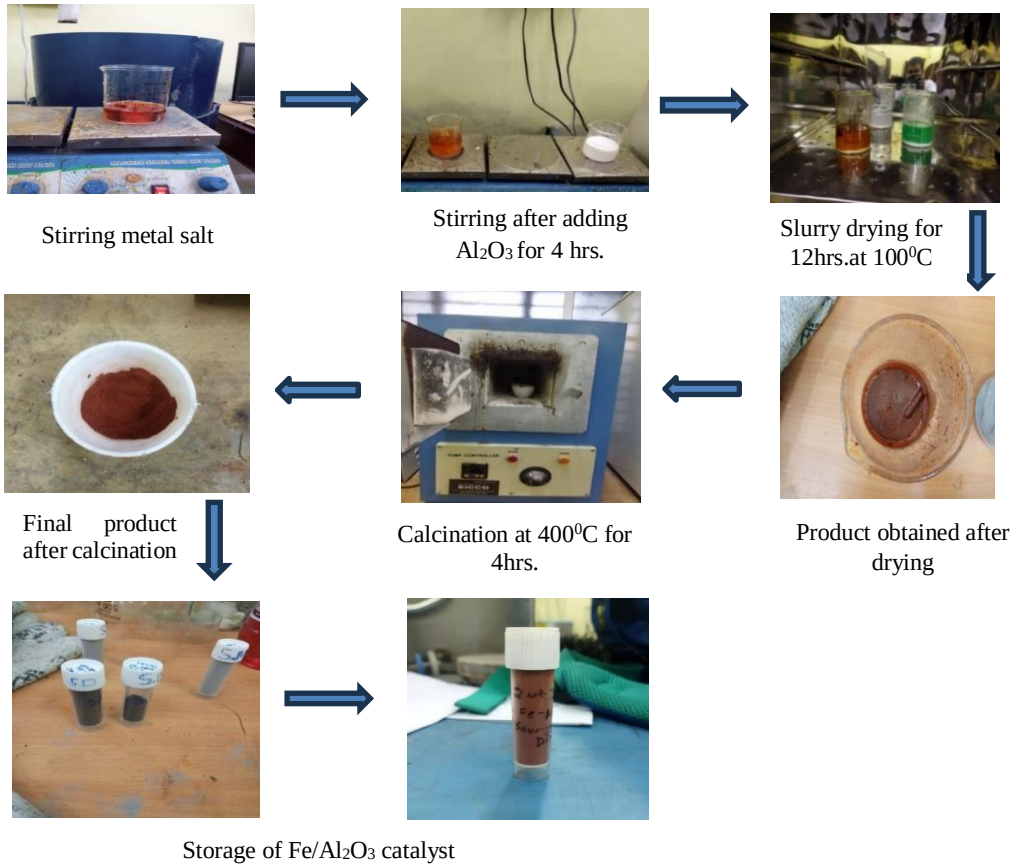


Fig.31. Excess Solution Impregnation (ESI) Method For Catalyst Synthesis

After removing the mixture from the calcination chamber, the catalyst is brought to room temperature and reduced. Finally, the catalyst is ready in its oxidized form for use in the reaction.

3.2. Characterization Techniques

3.2.1. Brunauer-Emmett-Teller (BET) Surface Area Measurement Technique

Brunauer-Emmett-Teller (BET) theory aims to explain the physical adsorption of gas molecules on a solid surface and serves as the basis for an important analysis technique for the measurement of the specific surface area of materials. In 1938, Stephen Brunauer, Paul Hugh Emmett, and Edward Teller published the first article about the BET theory in the Journal of American Chemical Society. The BET theory applies to systems of multilayer adsorption and usually utilizes probing gases that do not chemically react with material surfaces as adsorbates to quantify specific surface area. Nitrogen is the most commonly employed gaseous adsorbate used for surface probing by BET methods. For this reason, standard BET analysis is most often conducted at the boiling temperature of N_2 (77K). Specific surface area is a scale-dependent property, with no single true value of specific surface area definable, and thus quantities of specific surface area determined through BET theory may depend on the adsorbate molecule utilized and its adsorption cross section. The optimum temperature to carry out BET desorption can be known by preliminary calculations from Temperature Programmed Desorption (TPD).

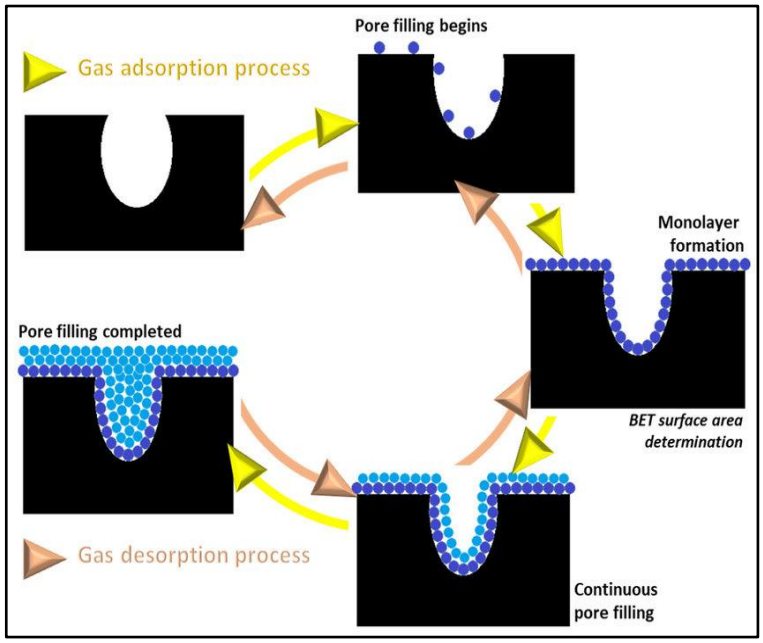


Fig.32. Underlying scientific principle of BET technique (Mohtar et al. 2021)

A non-reactive probing gas like N_2 is first allowed to get adsorbed on a catalyst support surface by the application of high pressure. Physisorption is generally preferred as it is reversible and can be easily carried out without causing any alterations to the microstructure of the support pores. After sufficient time (about 3-4 hrs.) has been allowed for the adsorption of the gas onto the substrate, we gradually reduce the pressure and start increasing the temperature, since low pressure and high-temperature favor desorption. As the temperature gradually increases, the topmost layer of physisorbed N_2 or the probe gas first starts to break the Van der Waals' bond and is released. This outlet is directed to a gas flowmeter or mass spectrometer, where the no. of desorbed gas molecules can be calculated. This is mainly the experimental part, which is followed by the calculation of Sg (effective specific area of catalyst available per unit weight of catalyst).



Fig.33. BET Instrument

We know that at room temperature, the volume occupied by 1 mole of a gas is approximately 22.4 L. By measuring the volume of the desorbed gas from the flow meter reading, the total no. of moles of N_2 released can be estimated.

3.2.2. Thermogravimetric analysis (TGA)

Thermogravimetric analysis (TGA) is a versatile analytical technique utilized in fields such as chemistry, materials science, and engineering to comprehensively understand the thermal properties and behavior of a wide range of substances. It's a cornerstone method for investigating the relationship between temperature and the physical and chemical changes that occur within materials. TGA involves subjecting a small sample of the material under investigation to a controlled temperature ramp in a specially designed furnace while continuously measuring its weight. The temperature ramp can be linear or stepwise, depending

on the requirements of the analysis and the characteristics of the material being studied. This heating process is conducted under an inert atmosphere (such as nitrogen or argon) or in the presence of a reactive gas to prevent unwanted oxidation or other chemical reactions.

With an increase in temperature, various thermal events may occur, leading to changes in the mass of the sample. Many materials contain moisture or other volatile components that can evaporate when heated. TGA can quantify the amount of moisture present in a sample and determine its thermal stability. Organic materials, polymers, and other complex substances may undergo degradation or decomposition when exposed to elevated temperatures. TGA can identify the onset temperature, rate, and extent of decomposition, providing insights into the material's stability and potential applications. Some materials may undergo oxidation or reduction reactions at high temperatures, leading to changes in their composition and mass. TGA can elucidate these reactions and their kinetics, aiding in the optimization of processes and the development of new materials. Changes in crystal structure, melting, sublimation, or other phase transitions can be detected and characterized using TGA, helping researchers understand the thermal behavior of materials under various conditions. The data obtained from TGA experiments are typically presented as thermograms, which plot the change in sample mass as a function of temperature or time. Analysis of these thermograms can provide valuable information such as thermal stability as the temperature at which significant mass loss or decomposition occurs can indicate the thermal stability of a material. Different components within a sample may exhibit distinct weight loss profiles, allowing for the identification and quantification of individual constituents. By analyzing the rate of mass change over time, kinetic parameters such as activation energy and reaction mechanisms can be determined. TGA can be used to assess the purity of a substance by measuring the amount of volatile impurities present. TGA is widely used in quality control and assurance processes to ensure consistency and reliability in manufacturing and product development. TGA is often employed in

conjunction with other analytical techniques such as differential scanning calorimetry (DSC), evolved gas analysis (EGA), or mass spectrometry (MS) to obtain complementary information and a more comprehensive understanding of the material under investigation. TGA instruments are used for a wide range of applications, including material characterization by assessing thermal stability and composition, decomposition studies of polymers and pharmaceuticals, and analysis of oxidation and reduction behaviors in metals. They measure moisture and volatile content for quality control, analyze thermal decomposition in environmental waste management, and conduct kinetic studies for chemical reactions. Additionally, TGA is used to evaluate component analysis in composite materials, making it a vital tool in materials science, chemistry, pharmaceuticals, environmental science, and engineering.



Fig.34. TGA Instrument

3.3. Oxidation reactor set up

The experiments were performed in a three-neck round bottom glass flask of 1 L capacity. During the experiment, there was a possibility of water vapor escaping out of the flask at high temperatures. To avoid the escaping of water vapor from the flask, a condenser was placed at the top of the flask to reflux the water vapor. For a typical run, 1 L of acetic acid solution with specified concentrations was taken in a glass reactor and the temperature of the reactor was kept constant at a desired value with the help of a temperature control unit. After reaching the desired temperature, 1 gram of catalyst (Fe/Al_2O_3) was added to the reactor, and air (which was a source of oxygen) was passed from a compressor through a rotameter at a constant flow rate.



Fig.35. Three necked bottle flask

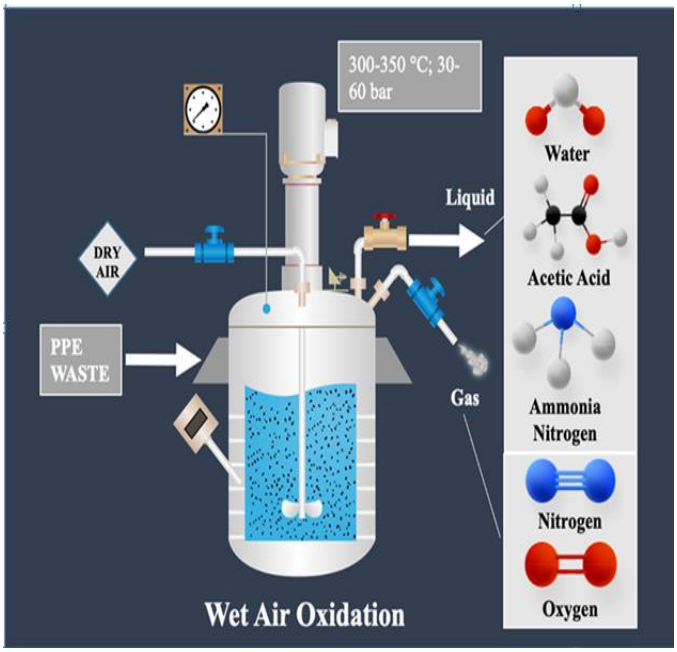


Fig.36. Schematic diagram of wet air oxidation

Oxygen, considered as excess in amount and acetic acid, considered as a limiting reactant were introduced immediately into the reactor while a magnetic agitator continuously stirred the solution at a certain speed.

3.4. Conversion measurement

The progress of the reaction was monitored by withdrawing samples of 5mL from the flask at regular time intervals using a pipette. The sample was titrated against 10^{-2} (M) NaOH solution using phenolphthalein as an indicator to determine the concentration of acetic acid in the sample.



Fig.37. Titration with Sodium Hydroxide (NaOH)

The percentage degradation of acetic acid at any time t, namely acetic acid conversion was calculated using eqn.

$$X_a = \frac{C_{ao} - C_a}{C_{ao}} * 100\%$$

Here C_{ao} is the initial concentration of acetic acid and C_a is the concentration of acetic acid at any time t.

CHAPTER 4

RESULTS AND DISCUSSIONS

CHAPTER 4

RESULTS AND DISCUSSIONS

4.1. Characterization techniques

4.1.1. Brunauer-Emmett-Teller (BET) Surface Area Measurement Technique

1.5 wt. % Fe/Al_2O_3 catalyst was outgassed at 300^OC for five hours under high vacuum conditions (10^{-5} mbar) before adsorption experiments. The nitrogen adsorption isotherm of Fe/Al_2O_3 catalyst sample is given in the figure below. The adsorption isotherm is of type III according to the IUPAC classification. The adsorption data were used to determine BET surface area.

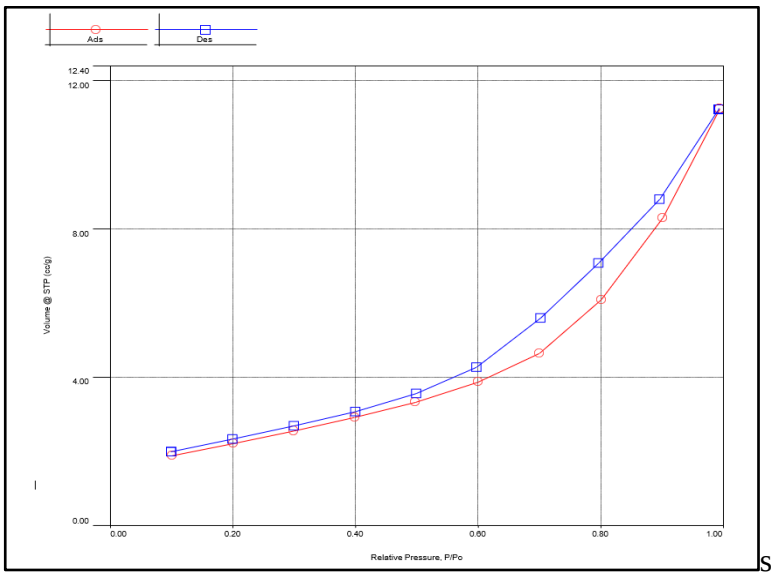


Fig.38. Adsorption-Desorption curve

The instrument used was Autosorb iQ Station 2. The weight of the sample was 0.8583 g. Nitrogen was used as an adsorbate. The temperature of the bath was 77.5 K. The outgas temperature was 377.5 K. For finding the surface area using BET, the governing equation used

was: $\frac{p}{V\,(p_0 - p)} = \frac{1}{V_m.c} + \frac{c-1}{V_m.c}\,\frac{p}{p_0}$. It represents the form of Y = mx + C where, Y = $\frac{p}{V\,(p_0 - p)}$, x = $\frac{p}{p_0}$, m = $\frac{c-1}{V_m.c}$ and, C = $\frac{1}{V_m.c}$ .The surface area was found to be 77.97 m^2/g. (Appendix B.3.)

Table 2. Post-reaction BET surface area for Cs-promoted Fe/Al_2O_3 catalysts (Luke et al. 2020)

Catalysts	**BET Surface area (m^2/g)**
Al_2O_3	124
0.1 Cs	122
0.25 Cs	129
0.5 Cs	144
1.0 Cs	112
2.0 Cs	70

Table 3. BET surface area of reduced catalysts as measured using N_2 physisorption (Ahmed et al. 2016)

Sample	**BET Surface area (m^2/g)**
$30\%Fe/Al_2O_3$	60.8
$30\%Fe\text{-}6\%Co/Al_2O_3$	43.4
$30\%Fe\text{-}15\%Co/Al_2O_3$	52.4
$30\%Fe\text{-}30\%Co/Al_2O_3$	72
$30\%Fe\text{-}6\%Ce/Al_2O_3$	56.25
$30\%Fe\text{-}15\%Ce/Al_2O_3$	52.1
$30\%Fe\text{-}30\%Ce/Al_2O_3$	95.3

Table 4. BET surface area of different catalysts (Laura et al. 2018)

Catalyst	BET Surface area (m^2/g)
Fe/Al_2O_3	174
1.0 % Cs Fe/Al_2O_3	168
2.5 % Cs Fe/Al_2O_3	153
5.0 % Cs Fe/Al_2O_3	149

4.1.2. Thermogravimetric analysis (TGA)

Thermal stability analysis of synthesized 1.5 wt.% of iron-alumina catalyst was investigated with TGA measurement in the temperatures 30^0C to 800^0C and the results are shown in below Fig.46.

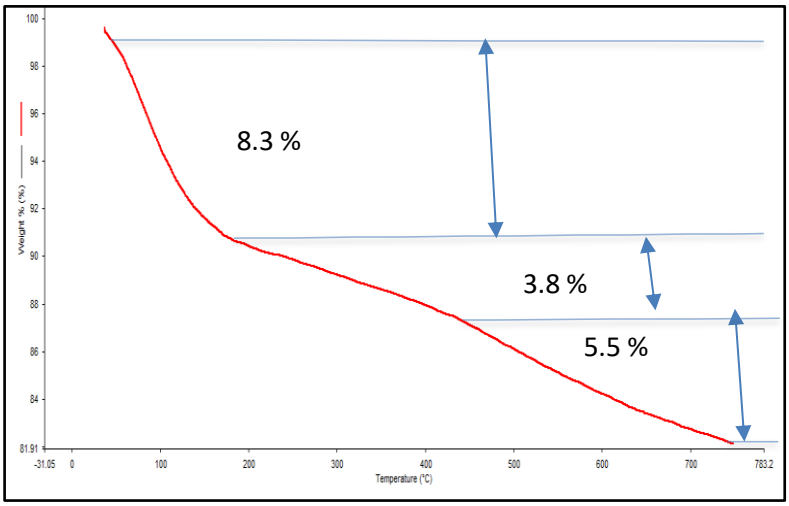


Fig.39. TGA image of fresh Fe/Al_2O_3 catalyst

In the TGA curve, the loss of weight was observed -8.3% in the temperature between 70^0C to 180^0C. In the temperature range of 180°C to 430°C, the TGA analysis indicates a weight loss of -3.8%, which is attributed to thermal decomposition processes. A similar weight loss of

-5.5% is observed between 430°C and 760°C, also corresponding to thermal decomposition. Beyond 760°C, the TGA curve exhibits no further change in weight, suggesting that a phase transition of the product has taken place, stabilizing the material (Appendix B.6.)

The TGA (Thermogravimetric Analysis) curve indicates three distinct weight loss events. The first weight loss occurs around 150°C and is attributed to desorption processes. The second weight loss, which is -0.92%, happens in the temperature range of 300°C to 540°C and is likely due to the oxidation of carbon, either free or combined with iron. The third weight loss, which is -1.35%, occurs at around 540°C and is significantly higher than the previous losses. This analysis is based on the study by Valdirene et al. (2009).

4.2. Effect of reaction temperature on acetic acid degradation

The experiment was carried out at atmospheric pressure and the initial concentration of acetic acid was 1000 ppm, initial mixing speed was 200 rpm. The temperatures were varied from 60ºC to 90ºC (333K-363K) at an interval of 10ºC.

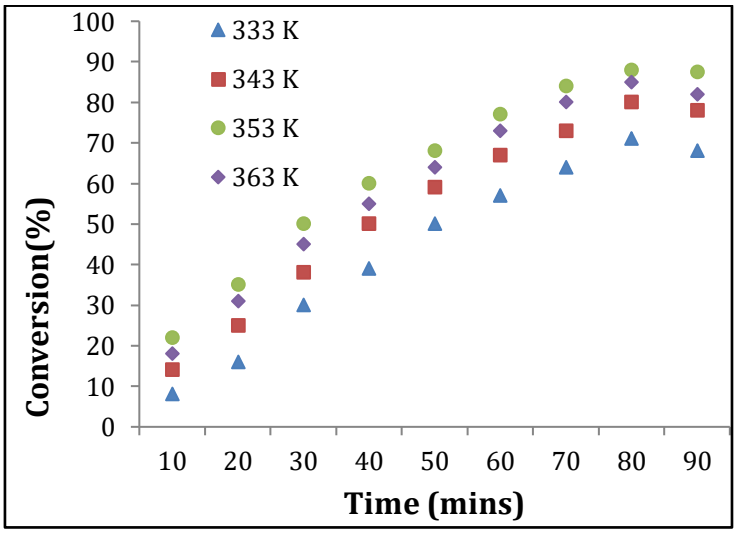


Fig.40. Effect of temperature on AA degradation. Catalyst: Fe (1.5 wt. %) /Al_2O_3, RPM: 400, Air flow rate: 1.0 LPM, Initial concentration of AA: 1000 ppm, Catalyst dosage: 1gm/L.

The corresponding Conversion vs Time graph was plotted where the experiment was carried out for 90 minutes (1.5 hours). An increase in acetic acid degradation can be noticed with an increase in reaction temperature to 80ºC or 353K beyond which the degradation decreases or remains constant in both cases. Increasing the reaction temperature is found to amplify the degradation of acetic acid, due to an increase in rate constant associated with the reaction. This phenomenon underscores the kinetic control governing the process. However, intriguingly, this augmentation in acetic acid degradation reaches a peak of around 353 K, after which any further increase in temperature leads to a decline in degradation rates. The observed decline in oxalic acid degradation beyond 363 K is proposed to originate from a decrease in the adsorption of acetic acid molecules onto the catalyst's surface. Moreover, as temperature rises, the solubility of oxygen in the reaction medium decreases, although the solubility of air in water remains consistently low. Despite this, the overall consequence of increasing the reaction temperature is a significant enhancement in the value of the reaction rate constant for kinetically controlled chemical reactions. However, although these discoveries reveal some aspects of how the system behaves on a larger scale, the fine details of how the reaction actually works is not revealed.

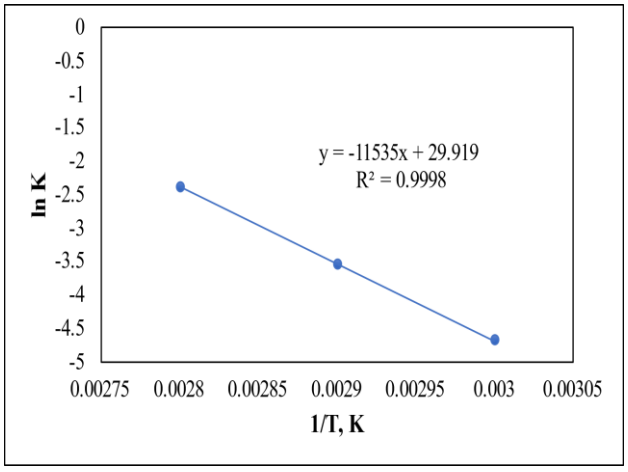


Fig.41. Arrhenius plot for the reaction

Increasing the temperature of a reaction generally speeds up the process (increases the rate) because the rate constant increases according to the Arrhenius Equation,

$$k = A.e^{(-Ea/RT)}$$

where k = rate constant, E_a = activation energy, T = Temperature (K), A = pre-exponential factor, R = universal gas constant, and e = mathematical constant.

As T increases, the value of the exponential part of the equation becomes less negative thus increasing the value of 'k'. Consequently, an increase in reaction temperature leads to a higher value of the reaction rate constant for kinetically controlled chemical reactions.

The activation energy was found to be 95.901 kJ/mol. (Appendix B.4.)

4.3. Effect of stirring speed (rpm) on degradation of acetic acid

The experiment was carried out at atmospheric pressure and the initial concentration of acetic acid was 1000 ppm, reaction temperature was 80º C. The mixing speed was varied between 200rpm & and 400rpm. The corresponding Conversion vs Time graph was plotted where the experiment was carried out for 90 minutes (1.5 hours).

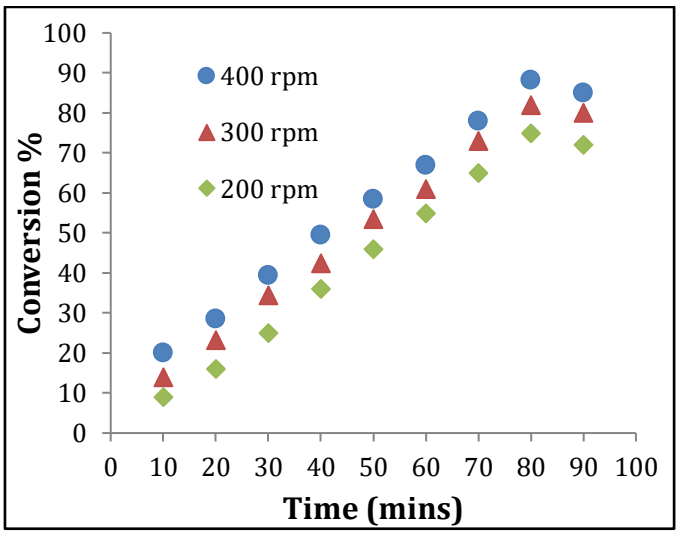


Fig.42. Effect of rpm on AA degradation. Catalyst: Fe (1.5 wt. %) /Al_2O_3, RPM: 400, Air flow rate: 1.0 LPM, Initial concentration of AA: 1000 ppm, Catalyst dosage: 1 gm/L.

The degradation of acetic acid increases with the increase in mixing speed till 400 rpm beyond which the degradation decreases or remains constant. It shows that if the mixing is good then the dissolution of oxygen in the solution will get enhanced which will result in a better oxidation reaction. There is an interface between two phases on the catalyst surface. So, the reactant has to diffuse through it to get oxidized on the catalyst and this interface provides an external resistance to the transfer. So, if the mixing speed is increased then the thickness of the interface film decreases which decreases the resistance, and the reaction rate increases.

4.4. Effect of loading of metal on acetic acid degradation.

The experiments were performed by varying the iron and cobalt content in the catalyst support by increasing the concentration of (Iron III Nonahydrate-Fe $(NO_3)_3.9H_20$). Fe loadings ranging from 0.5 wt.% to 2.0 wt. % were tested and the results showed an increase in acetic acid degradation with Fe loading up to 1.5 wt.%.

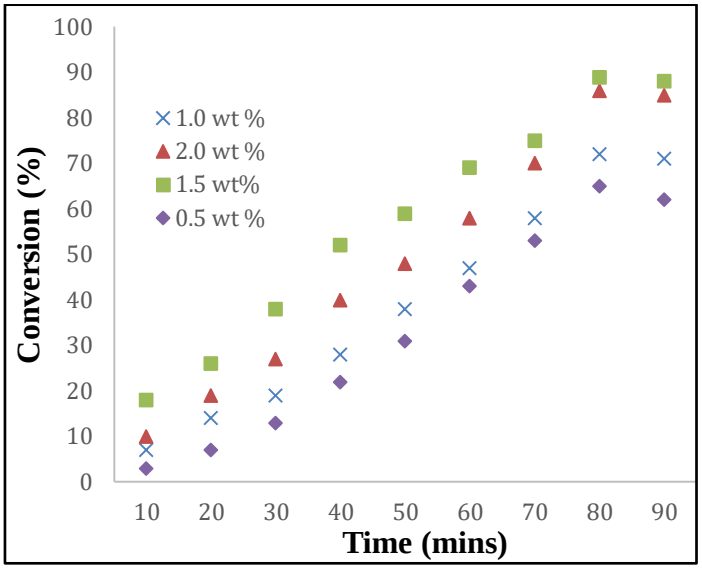


Fig.43. Effect of metal loading on AA degradation. Catalyst: Fe (1.5 wt. %) /Al_2O_3, RPM: 400, Air flow rate: 1.0 LPM, Initial concentration of AA: 1000 ppm, Catalyst dosage: 1 gm/L.

The maximum conversion, approximately 88.5%, was achieved at 1.5 wt.% Fe loading (Appendix B.2.). However, beyond 1.5 wt.% Fe, there was no significant degradation of acetic acid which suggests that sufficient active catalyst sites are available at 1.5 wt.% Fe and further increases in catalyst loading do not improve the degradation.

4.5. Effect of initial concentration of acetic acid on the degradation of acetic acid.

The experiment was carried out at atmospheric pressure and the initial mixing speed of the acetic acid solution was 200 rpm, and the reaction temperature was 80^0C. The initial concentration of acetic acid was varied at 1000 ppm & 2000 ppm. The corresponding Conversion vs Time graph was plotted where the experiment was carried out for 90 minutes (1.5 hours).

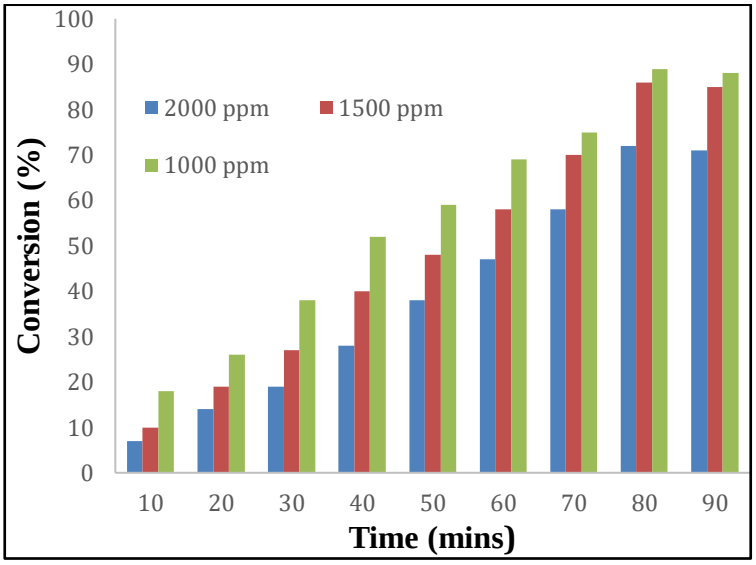


Fig.44. Effect of initial concentration of acetic acid (AA) on AA degradation. Catalyst: Fe (1.5 wt. %) /Al_2O_3, RPM: 400, Air flow rate: 1.0 LPM, Initial concentration of AA: 1000 ppm, Catalyst dosage: 1 gm/L.

An intriguing observation reveals that when the initial concentration is raised to 2000 ppm, the degradation of acetic acid diminishes over time. This suggests that the surface reaction occurring on two neighboring iron active sites, following Langmuir-Hinshelwood kinetics, could be the rate-determining step. The decrease in degradation efficiency with higher initial acetic acid concentrations is likely due to competition among reactant molecules for active sites on catalyst particles.

4.6. Modelling of the reaction: Power Law Model

The power law model is a mathematical expression used to describe the kinetics of a chemical reaction. It represents the rate of reaction as a power function of the concentrations of the reactants involved. In the case of the oxidation of acetic acid, the power law model takes the following form: $r = k.[O_2]^n.[AA]^m$

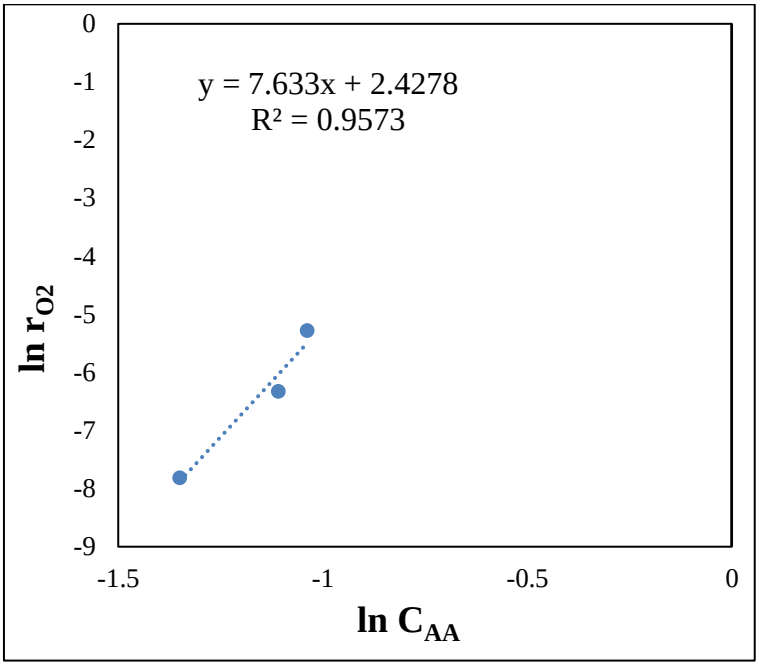


Fig.45. Rate of oxygen vs. Concentration of Acetic acid

r: Rate of the reaction, k: Rate constant, [AA]: Concentration of acetic acid, [O_2]: The concentration of oxygen, m: Reaction order concerning acetic acid, n: Reaction order concerning oxygen. Similar to m, this parameter indicates how the concentration of oxygen influences the rate of the reaction and is determined experimentally.

The reaction was of second order considering optimum parameters like temperature (80^{o}C), and mixing speed (400 rpm). (Appendix B.5.)

4.7. Mechanism of the reaction

The oxidation of acetic acid (CH_3COOH) by an iron catalyst typically involves the use of molecular oxygen (O_2) as the oxidizing agent. The reaction occurs in the following steps.

1. Formation of Iron Acetate Complex.

$Fe^{3+}+3CH_3COOH \rightarrow Fe\ (CH_3COO)_3+3H^+$

2. Activation of Molecular Oxygen.

$Fe^{n+} + O_2 \rightarrow Fe^{(n-1)+} + O^{2-}$

3. Oxidation of Acetic Acid.

$Fe^{(n-1)+} + O^{2-} + CH_3COOH \rightarrow Fe^{n+} + CH_3COO^- + H_2O_2$

4. Regeneration of Iron Catalyst.

$Fe^{n+} + O_2 \rightarrow Fe^{(n-1)+} + O^{2-}$

The overall reaction can be represented as the oxidation of acetic acid by molecular oxygen with the iron catalyst, producing carbon dioxide and water.

CHAPTER 5

CONCLUSIONS AND FUTURE WORK

CHAPTER 5

CONCLUSIONS AND FUTURE WORK

5.1. Conclusions

The objective of this project was to find optimum operating conditions for the Catalytic Wet Air Oxidation of Acetic Acid within the taken parameters. The reaction temperature being the first parameter was evaluated using experiments and 80º C was set to be the temperature where the maximum conversion of 88.5% was observed for 1.5 wt.% Fe. After the temperature, the mixing speed was changed and at 400 rpm, the degradation of acetic acid was maximum at 1.5 wt.% Fe. After optimization, the conversion % was seen to be the maximum at 1000 ppm concentration of acetic acid. The BET surface area was calculated as 77.97 m^2/g. The catalyst showed maximum degradation of acetic acid at a temperature of 80º C or 353 K, mixing speed of 400 rpm, and metal loading weight of 1.5 wt. %, and a concentration of 1000 ppm. The alumina-supported iron (Fe/Al_2O_3) catalyst proved to be efficient in acetic acid removal by CWAO. The prepared catalyst was very stable under the reaction conditions, and no significant leaching of the metal phase was observed. Single metal catalysts are simpler to synthesize and can be more cost-effective compared to double metal catalysts. It must be noted that the efficiency of a catalyst depends on the specific requirements of the reaction and the characteristics of the catalyst itself. Single metal catalysts can be more straightforward to work with, cost-effective, and suitable for certain reactions. The choice between single metal and bimetallic catalysts should be based on a careful consideration of the reaction conditions, desired outcomes, and the specific advantages each type of catalyst offers for a given application.

5.2. Future Work

The experiments were carried out at atmospheric pressure in this study. So in future, the reaction will be carried at higher pressure. There will be detailed work on catalyst and support characterization and synthesis of bi-metallic and tri-metallic catalysts. Different metals will be tested as metal precursors and different support will be used as catalyst support. The effect of calcination temperature and initial concentration of acetic acid on the degradation of acetic acid will be studied further.

REFERENCES

Abu, R.; Patchigolla, K.; Simms, N.; Anthony, E.J. Natural Gas Flaring Management System: A Novel Tool for Sustainable Gas Flaring Reduction in Nigeria. *Appl. Sci.* **2023**, 13(3), 1866.

Ahmed, E.M. Hydrogel: Preparation, characterization, and applications: A review. *J. Adv. Res.* **2015**, 6(2), 105-121.

Al-Fatesh, A.S.; Amin, A.; Ibrahim, A.A.; Khan, W.U.; Soliman, M.A.; Al-Otaibi, R.L.; Fakeeha, A.H. Effect of Ce and Co addition to Fe/Al_2O_3 for catalytic methane decomposition. *Catal.* **2016**, 6(3), 40.

Al-Sanabani, F.A.; Madfa, A.A.; Al-Qudaimi, N.H. Alumina ceramic for dental applications: A review article. *Am. J. Mater. Res*. **2014**, 1(1), 26-34.

Amor, C.; Rodriguez-Chueca, J.; Fernandes, J.L.; Dominguez, J.R.; Lucas, M.S.; Peres, J.A. Winery wastewater treatment by sulphate radical based-advanced oxidation processes (SR-AOP): Thermally vs UV-assisted persulphate activation. *Process Saf. Environ. Prot*. **2019** 122, 94-101.

Amrute, A.P.; De Bellis, J.; Felderhoff, M.; Schüth, F. Mechanochemical synthesis of catalytic materials. *Chem. Eur. J*. **2021**, 27(23), 6819-6847.

Andrigo, P.; Bagatin, R.; Pagani, G. Fixed bed reactors. *Catal. Today*. **1999**, 52(2-3), 197-221.

Anushree; Sheetal; Kumar, S. Nanocatalysts in Wet Air Oxidation. *J Water Environ Nanotechnol*. **2020**, 285-313.

Archila, K.; Campos, A.; Lugo, L.; Celis, C.; Moreno, S.; Reina, T.; Pérez-Flórez, A. Influence of the Active Phase (Fe, Ni, and Ni–Fe) of Mixed Oxides in CWAO of Crystal Violet. *Catal*. **2020**.

Ashiq, M.N.; Ehsan, M.F.; Iqbal, M.J.; Gul, I.H. Synthesis, structural and electrical characterization of Sb^{3+} substituted spinel nickel ferrite ($NiSb_xFe_{2-}xO_4$) nanoparticles by reverse micelle technique. *J. Alloys Compd*. **2011**, 509(16), 5119-5126.

Azman, N.S.; Marliza, T.S.; Mijan, N.A.; Yun Hin, T.Y.; Khairuddin, N. Production of biodiesel from waste cooking oil via deoxygenation using Ni-Mo/Ac catalyst. *Process.* **2021**, 9(5), 750.

Baloyi, S. J.; Moma, J. A. Catalytic wet air oxidation of phenol by cordierite honeycomb wash coated with Al/Zr pillared bentonite in a plug flow reactor. *J. Environ. Chem. Eng.* **2020**, 8(5), 104186.

Bao, Y.; Lee, W. J.; Lim, T. T.; Wang, R.; Hu, X. Pore-functionalized ceramic membrane with isotropically impregnated cobalt oxide for sulfamethoxazole degradation and membrane fouling elimination: Synergistic effect between catalytic oxidation and membrane separation. *Appl. Catal. B: Environ.* **2019**, 254, 37-46.

Bao, Y.; Lee, W. J.; Wang, P.; Xing, J.; Liang, Y. N.; Lim, T. T.; & Hu, X. A novel molybdenum-based nanocrystal decorated ceramic membrane for organics degradation via catalytic wet air oxidation (CWAO) at ambient conditions. *Catal.Today*. **2021**, 364, 276-284.

Bartolomeu, M.; Neves, M.G.P.M.S.; Faustino, M.A.F.; Almeida, A. Wastewater chemical contaminants: Remediation by advanced oxidation processes. *Photochem. Photobiol. Sci.* **2018**, 17(11), 1573-1598.

Bashir, A.; Malik, L.A.; Ahad, S.; Manzoor, T.; Bhat, M.A.; Dar, G.N.; Pandith, A.H. Removal of heavy metal ions from aqueous system by ion-exchange and biosorption methods. *Environ. Chem. Lett.* **2019**, 17, 729-754.

Bhatia, D.; Malik, S.; Jaiswar, V.K.; Saroha, A.K. Treatment of Highly Alkaline Industrial Organic Raffinate Containing Pyridine and Its Derivatives by Coupling of Catalytic Wet Air Oxidation and Biological Processes. *Ind. Eng. Chem. Res.* **2023**, 62(41), 16676-16685.

Bhatia, S.K.; Yang, Y.H. Microbial production of volatile fatty acids. current status and future perspectives. *Rev. Environ. Sci. Biotechnol.* **2017**, 16, 327-345.

Bhoite, G.M.; Vaidya, P.D., 2018. Improved biogas generation from biomethanated distillery wastewater by pretreatment with catalytic wet air oxidation. *Ind. Eng. Chem. Res.* **2018**, 57.7. 2698-2704.

Bokov, D.; Turki Jalil, A.; Chupradit, S.; Suksatan, W.; Javed Ansari, M.; Shewael, I.H.; Valiev, G.H.; Kianfar, E. Nanomaterial by sol-gel method. synthesis and application. *Adv. Mater. Sci. Eng.* **2021**, 1-21.

Boretti, A.; Rosa, L. Reassessing the projections of the World Water Development Report. *NPJ Clean Water*. **2019**, 2(1), 15.

Bourassi, M.; Lafaye, G.; Gombert, B.; Klusoň, P.; Barbier Jr, J. Catalytic wet air oxidation of sulfamethoxazole and tetracycline using platinum-based catalysts at eco-operating conditions. *J. Clean. Prod.* **2023**, 429, 139453.

Burey, P.; Bhandari, B.R.; Howes, T.; Gidley, M.J. Hydrocolloid gel particles. formation, characterization, and application. *Crit. Rev. Food Sci. Nutr.* **2008**, 48(5), 361-377.

Carneiro, R.B.; Mukaeda, C.M.; Sabatini, C.A.; Santos-Neto, Á.J.; Zaiat, M. Influence of organic loading rate on ciprofloxacin and sulfamethoxazole biodegradation in anaerobic fixed bed biofilm reactors. *Environ. Manag.* **2020**, 273, 111170.

Chai, Y.; Zhang, Y.; Tan, Y.; Li, Z.; Wei, H.; Sun, C.; Jin, H.; Mu, Z.; Ma, L. Life cycle assessment of high concentration organic wastewater treatment by catalytic wet air oxidation. *Chin. J. Chem. Eng.* **2023**, 56, 80-88.

Chaturvedi, N.K.; Katoch, S.S., Remedial technologies for aniline and aniline derivatives elimination from wastewater. *J. Health. Pollut.* **2020**, 10(25), 200302.

Chávez, A.M.; Gimeno, O.; Rey, A.; Pliego, G.; Oropesa, A.L.; Álvarez, P.M.; Beltrán, F.J. Treatment of highly polluted industrial wastewater by means of sequential aerobic biological oxidation-ozone based AOPs. *J. Chem. Eng.* **2019**, 361, 89-98.

Cheng, J.; Yu, B.; Zheng, R.; Wang, X.; Liu, J.; Wu, X.; Qin, L. Applications of advanced oxidation technologies for sludge treatment. In *IOP Conference Series: Environ. Earth Sci.* **2019**, 252, 4, 042044

Chohan, J.S.; Kumar, R.; Yadav, A.; Chauhan, P.; Singh, S.; Sharma, S.; Li, C.; Dwivedi, S.P.; Rajkumar, S. Optimization of FDM printing process parameters on surface finish, thickness, and outer dimension with ABS polymer specimens using Taguchi orthogonal array and genetic algorithms. *Math. Probl. Eng.* **2022**, 1-13.

Cozzens, R.F.; Fox, R.B. Infrared laser ablation of polymers. *Polym. Eng. Sci.* **1978**, 18(11), 900-904.

Crini, G.; Lichtfouse, E. Advantages and disadvantages of techniques used for wastewater treatment. *Environ. Chem. Lett.* **2019**, 17, 145-155.

Danks, A.E.; Hall, S.R.; Schnepp, Z.J.M.H. The evolution of 'sol–gel'chemistry as a technique for materials synthesis. *Mater. Horiz.* **2016**, 3(2), 91-112.

De Iuliis, S.; Migliorini, F.; Dondè, R. Laser-induced emission of TiO_2 nanoparticles in flame spray synthesis. *Appl. Phys. B*. **2019**, 125(11), 219.

de Magalhães, L.F.; da Silva, G.R.; Peres, A.E.C. Zeolite application in wastewater treatment. *Adsorpt. Sci. Technol.* **2022**, 1-26.

de Mora, A.; de Tuesta, J.D.; Pariente, M.I.; Segura, Y.; Puyol, D.; Castillo, E.; Lissitsyna, K.; Melero, J.A.; Martínez, F. Chemically activated hydrochars as catalysts for the treatment of HTC liquor by catalytic wet air oxidation. *Catal. Today*. **2024**, 429, 114462.

de Resende, V.G.; Peigney, A.; De Grave, E.; Laurent, C. In situ high-temperature Mössbauer spectroscopic study of carbon nanotube–Fe–Al_2O_3 nanocomposite powder. *Thermochim. Acta*. **2009**, 494(1-2), 86-93.

Dükkancı, M.; Gündüz, G. Catalytic wet air oxidation of butyric acid and maleic acid solutions over noble metal catalysts prepared on TiO_2. *Catal. Commun.* **2008**, 10, 913-919.

Duraisamy, S.; Murugesan, S.; Palanichamy, M.; Antony Raj, R. Restoration of critical dielectric properties of waste/aged transformer oil using biodegradable biopolymer-activated clay composite for power and distribution transformers. *Biomass Conv. Bioref.* **2022**, 12. 4817–4833.

Dursun, N.; Gülşen, H. Evaluation of industrial waste black cumin (Nigella Sativa) for biohydrogen production without pretreatment. *Environ. Dev. Sustain.* **2022**, 24(10), 12182-12202.

Feijoo, S.; Yu, X.; Kamali, M.; Appels, L.; Dewil, R. Generation of oxidative radicals by advanced oxidation processes (AOPs) in wastewater treatment. a mechanistic, environmental and economic review. *Rev. Environ. Sci. Biotechnol.* **2023**, 22(1), 205-248.

Feng, B.; Hao, L.; Deng, C.; Wang, J.; Song, H.; Xiao, M.; Huang, T.; Zhu, Q.; Gai, H. A highly hydrothermal stable copper-based catalyst for catalytic wet air oxidation of m-cresol in coal chemical wastewater. *Chin. J. Chem. Eng.* **2023**, 57, 338-348.

Feng, S.H.; Li, G.H. Hydrothermal and solvothermal syntheses. In *Mod. Inorg. Synth. Chem.* **2017**, 73-104.

Fernandes, F.A.; Lona, L.M. Fluidized bed reactor for polyethylene production. The influence of polyethylene prepolymerization. *Braz. J. Chem. Eng*. **2000**, 17, 163-170.

Ganbaatar, A.; Tsogbadrakh, N.; Baynjargal, O.; Ganbold, T. First-Principles Study of Adsorption of Hazardous Atoms on the Silica Surface. *In 5th International Conference on Chemical Investigation and Utilization of Natural Resource (ICCIUNR).* **2021**, 15-20.

Gao, R.; Mosquera-Romero, S.; Ntagia, E.; Wang, X.; Rabaey, K.; Bonin, L. Electrochemical separation of organic and inorganic contaminants in wastewater. *J. Electrochem. Soc.* **2022**, 169(3), 033505.

Geng, L.; Chen, B.; Yang, J.; Shui, C.; Ye, S.; Fu, J.; Zhang, N.; Xie, J.; Chen, B. Synergistic effect between Mn and Ce for active and stable catalytic wet air oxidation of phenol over MnCeOx. *Appl. Catal.A.* **2020**, 604, 117774.

Ghuge, S.P.; Saroha, A.K. Catalytic ozonation for the treatment of synthetic and industrial effluents-Application of mesoporous materials: A review. *Environ. Manag.* **2018**, 211, 83-102.

Girish, C.R. Various impregnation methods used for the surface modification of the adsorbent: A review. *Int. J. Eng. Technol.* **2018**, 7(4.7), 330-334.

Gizaw, B.A.; Habtu, N.G. Catalytic wet air oxidation of azo dye (reactive red 2) over copper oxide loaded activated carbon catalyst. *J. Water Process Eng.* **2022**, 48, 102797.

González, C.; Pariente, M.I.; Molina, R.; Espina, L.G.; Masa, M.O.; Bernal, V.; Melero, J.A.; Martinez, F. Increasing biodegradability of a real amine-contaminated spent caustic problematic stream through WAO and CWAO oxidation using a high specific surface catalyst from petcoke. *J. Chem. Eng.* **2023**, 460, 141692

Gopakumar, J.; Vold, S.; Enger, B. C.; Waller, D.; Vullum, P. E.; Rønning, M. Catalytic oxidation of NO to NO_2 for industrial nitric acid production using Ag-promoted MnO_2/ZrO_2 catalysts. *Catal. Sci. Technol.* **2023**, 13(9), 2783-2793.

Grace, J.R. Fluidized-bed catalytic reactors. *Multiphase Catalytic Reactors: Theory, Design, Manufacturing, and Applications*. **2016**, 80-94.

Gupta, P.; Pandey, K.; Verma, N. Augmented complete mineralization of glyphosate in wastewater via microbial degradation post CWAO over supported Fe-CNF. *J. Chem. Eng.* **2022**, 428, 132008.

Gupta, P.; Verma, N. Evaluation of degradation and mineralization of glyphosate pollutant in wastewater using catalytic wet air oxidation over Fe-dispersed carbon nanofibrous beads. *J. Chem. Eng.* **2021**, 417, 128029.

Gutiérrez-Sánchez, **P**.; Álvarez-Torrellas, S.; Larriba, M.; Gil, M.V.; Garrido-Zoido, J.M.; García, J. Efficient removal of antibiotic ciprofloxacin by catalytic wet air oxidation using sewage sludge-based catalysts: Degradation mechanism by DFT studies. *J. Environ. Chem.* **2023**, 11(2), 109344.

Hammedi, T.; Bensouilah, R.; Ouakouak, A.; Llorca, J.; Cabello, F.M.; Ksibi, Z. Study of the catalytic wet air oxidation of p-hydroxybenzoic acid on a fresh ruthenium catalyst supported by different oxides. *Heliyon*. **2023**, 9(10).

Hou, P.; Zhang, H.; Zi, Z.; Zhang, L.; Xu, X. Core-shell and concentration-gradient cathodes prepared via co-precipitation reaction for advanced lithium-ion batteries. *J. Mater. Chem. A.* **2017**, 5(9), 4254-4279.

Javid, F.; Xin, X.; Anderson, W. A.; Derraik, J. G.; Anderson, Y. C.; & Baroutian, S. Deconstruction of waste personal protective equipment (PPE) using subcritical wet air oxidation. *J. Supercrit. Fluids.* **2023**, 196, 105900.

Jiang, B.; Hao, L.; Zhang, L.; Sun, Y.; Xiao, X. Numerical investigation of flow and heat transfer in a novel configuration multi-tubular fixed bed reactor for propylene to acrolein process. *Heat and Mass Transfer*. **2015**, 51, 67-84.

Jiang, L.; Yuan, X.; Zeng, G.; Liang, J.; Chen, X.; Yu, H.; Wang, H.; Wu, Z.; Zhang, J.; Xiong, T. In-situ synthesis of direct solid-state dual Z-scheme WO_3/g-C_3N_4/Bi_2O_3 photocatalyst for the degradation of refractory pollutant. *Appl. Catal. B. Environ.* **2018**, 227, 376-385.

Jing, Q.; Li, H. Hierarchical nickel cobalt oxide spinel microspheres catalyze mineralization of humic substances during wet air oxidation at atmospheric pressure. *Appl. Catal. B. Environ.* **2019**, 256, 117858.

Kale, M.B.; Borse, R.A.; Gomaa Abdelkader Mohamed, A.; Wang, Y. Electrocatalysts by electrodeposition: recent advances, synthesis methods, and applications in energy conversion. *Adv. Funct. Mater.* **2021**, 31(25), 2101313.

Kanekol, T.; Tsuruminel, Y.; Poon, J.; Onuki, Y.; Dai, Y.; Kawabata, K.; Matsubara, T. Learning deep dynamical models of a waste incineration plant from in-furnace images and process data. In *2019 IEEE 15th International Conference on Automation Science and Engineering (CASE).* **2019**, 873-878.

Kaur, A.; Bajaj, B.; Kaushik, A.; Saini, A.; Sud, D. A review on template assisted synthesis of multi-functional metal oxide nanostructures. Status and prospects. *Mater. Sci. Eng.: B,* **2022**, 286, 116005.

Khatri, I.; Garg, A., 2021. Use of heterogeneous activated carbon supported copper catalyst for catalytic wet oxidation of biomethanated spent wash: Reaction kinetics, catalyst stability, catalyst deactivation kinetics and biochemical methane potential. *J. Water Process Eng.* **2021**, 44, 102387.

Kumar, O.P.; Ashiq, M.N.; Ahmad, M.; Anjum, S.; Rehman, A.U. Silver and yttrium-doped bismuth vanadate for photoluminescent activity and boosted visible light-induced photodegradation. *J. Mater. Sci.: Mater. Electron*. **2020**, 31(23), 21082-21096.

Kumari, M.; Saroha, A.K. Performance of various catalysts on treatment of refractory pollutants in industrial wastewater by catalytic wet air oxidation: A review. *Environ. Manag.* **2018** 228, 169-188.

Kurian, M. Advanced oxidation processes and nanomaterials-a review. *Clean. Eng. Technol.* **2021**, 2, 100090.

Kurian, M.; Remya, V.; Kunjachan, C. Catalytic wet oxidation of chlorinated organics at mild conditions over iron doped nanoceria. *Elsevier.* **2017**.

Li, L.; Liu, S.; Cheng, M.; Lai, C.; Zeng, G.; Qin, L.; Liu, X.; Li, B.; Zhang, W.; Yi, Y.; Zhang, M. Improving the Fenton-like catalytic performance of MnOx-Fe_3O_4/biochar using reducing agents: a comparative study. *J. Hazard. Mater.* **2021**, 406, p.124333.

Li, Y.; Lin, B.; Ge, L.; Guo, H.; Chen, X.; Lu, M. Real-time spectroscopic monitoring of photocatalytic activity promoted by graphene in a microfluidic reactor. *Sci. Rep.* **2016**, 6(1), 28803.

Lin, L.; Li, R.H.; Li, Y.; Xu, J; Li, X.Y. Recovery of organic carbon and phosphorus from wastewater by Fe-enhanced primary sedimentation and sludge fermentation. *Process Biochem.* **2017**, 54, 135-139.

Ma, D.; Yi, H.; Lai, C.; Liu, X.; Huo, X.; An, Z.; Li, L.; Fu, Y.; Li, B.; Zhang, M.; Qin, L. Critical review of advanced oxidation processes in organic wastewater treatment. *Chemosphere*. **2021**, 275, 130104.

Makatsa, T. J.; Baloyi, J.; Ntho, T.; & Masuku, C. M. Catalytic wet air oxidation of phenol. Review of the reaction mechanism, kinetics, and CFD modeling. *Crit. Rev. Environ. Sci. Technol*. **2021**, 51(17), 1891-1923.

Manna, M.; Sen, S. Advanced oxidation process: A sustainable technology for treating refractory organic compounds present in industrial wastewater. *Environ. Sci. Pollut. Res.* **2023**, 30(10), 25477-25505.

Marquardt, A.E.; Breitung, E.M.; Drayman-Weisser, T.; Gates, G.; Phaneuf, R.J. Protecting silver cultural heritage objects with atomic layer deposited corrosion barriers. *Herit. Sci.* **2015**, 3, 1-12.

Mason, D.R.; Piret, E.L. Continuous Stirred Tank Reactor Systems. *Ind. Eng. Chem. Res.* **1951**, 43(5), 1210-1219.

Miklovicz, T. Investigation on the potential of combined heat, power and metal extraction in Hungary (Doctoral dissertation, University of Szeged) **2014**.

Mishra, S.; Cheng, L.; Maiti, A. The utilization of agro-biomass/byproducts for effective bio-removal of dyes from dyeing wastewater: A comprehensive review. *J. Environ. Chem. Eng.* **2021**, 9(1), 104901.

Mohtar, S.S.; Aziz, F.; Ismail, A.F.; Sambudi, N.S.; Abdullah, H.; Rosli, A.N.; Ohtani, B. Impact of doping and additive applications on photocatalyst textural properties in removing organic pollutants: A review. *Catal.* **2021**, 11(10), 1160.

Mustafa, R.; Asmatulu, E. Preparation of activated carbon using fruit, paper and clothing wastes for wastewater treatment. *J. Water Process Eng*. **2020**, 35, 101239.

Muzaffar, F.A.I.Z.I.; Singh, U.K.; Chauhan, L. Review on microemulsion as futuristic drug delivery. *Int J Pharm Sci*. **2013**, 5(3), 39-53.

Nair, D.S.; Kurian, M. Heterogeneous catalytic oxidation of persistent chlorinated organics over cobalt substituted zinc ferrite nanoparticles at mild conditions. Reaction kinetics and catalyst reusability studies. *J. Environ. Chem. Eng.* **2017**, 5(1), 964-974.

Nanda, S. Reactors and fundamentals of reactors design for chemical reaction. **2008**.

Ni'am, M.F.; Othman, F.; Sohaili, J. Fauzia, Z. Electrocoagulation technique for removal of COD and turbidity to improve wastewater quality. *Ultrapure water*. **2008**, 25(3)

Ogugua, S.N.; Ntwaeaborwa, O.M.; Swart, H.C. Latest development on pulsed laser deposited thin films for advanced luminescence applications. *Coatings.* **2020**, 10(11), 1078.

Okuyama, K.; Abdullah, M.; Lenggoro, I.W.; Iskandar, F. Preparation of functional nanostructured particles by spray drying. *Adv. Powder Technol.* **2006**, 17(6), 587-611.

Owusu-Agyeman, I. Systems for ammonium concentration for further removal in the partial nitritation/anammox technology, **2012.**

Pan, C.; Wang, W.; Fu, C.; Nam, J.; Wu, F.; You, Z.; Xu, J.; Li, J. Promoted wet peroxide oxidation of chlorinated volatile organic compounds catalyzed by FeOCl supported on macro-microporous biomass-derived activated carbon. *Elsevier*. **2013**.

Parker, L.A.; Carter, J.H.; Dummer, N.F.; Richards, N.; Morgan, D.J.; Golunski, S.E.; Hutchings, G.J. Ammonia decomposition enhancement by Cs-promoted Fe/Al_2O_3 catalysts. *Catal. Lett.* **2020**, 150(12), 3369-3376.

Parvulescu, V.I.; Epron, F.; Garcia, H.; Granger, P. Recent progress and prospects in catalytic water treatment. *Chem. Rev.* **2021**, 122(3), 2981-3121.

Pastor-Pérez, L.; Shah, M.; Le Saché, E.; Ramirez Reina, T. 2018. Improving Fe/Al_2O_3 catalysts for the reverse water-gas shift reaction: on the effect of Cs as activity/selectivity promoter. *Catal.* **2018**, 8(12), 608.

Roy, S.; Saroha, A. K. Ceria promoted γ-Al_2 O_3 supported platinum catalyst for catalytic wet air oxidation of oxalic acid. kinetics and catalyst deactivation. *RSC Advances*. **2014,** 4(100), 56838-56847.

Roy, S.; Vashishtha, M.; Saroha, A.K., 2010. Catalytic Wet Air Oxidation of Oxalic Acid using Platinum Catalysts in Bubble Column Reactor: A Review. *J. Eng. Sci. Technol. Rev.* **2010**, 3(1).

Rueda-Marquez, J.J.; Levchuk, I.; Ibañez, P.F.; Sillanpää, M. A critical review on application of photocatalysis for toxicity reduction of real wastewaters. *J. Clean. Prod.* **2020**, 258, 120694.

Samer, M. Biological and chemical wastewater treatment processes. *Wastewater treatment engineering*. **2015**, 150(10.5772), 61250.

Saroha, A.K. Effectiveness of fresh and used supported noble and non-noble metal based catalysts for industrial organic raffinate oxidation by catalytic wet air oxidation at low operating parameters. *J. Environ. Chem. Eng.* **2019**, 7(5), 103382.

Sassi, H.; Lafaya, G.; Amor, H.; Gannouni, A.; Jeday, M.; Barbier-Jr, J. Wastewater treatment by catalytic wet air oxidation process over Al-Fe pillared clays synthesized using microwave irradiation. *Front. Environ. Sci. Eng.* **2017**.

Sgroi, M.; Snyder, S.A.; Roccaro, P. Comparison of AOPs at pilot scale: Energy costs for micro-pollutants oxidation, disinfection by-products formation and pathogens inactivation. *Chemosphere*. **2021**, 273, 128527.

Shan, H.; Oh, R.; Fan, J.; Zhang, X.; Zhang, N.; Huang, X.; Park, G.S.; Zheng, Q.; Lu, H.; Chen, B. Developing Pt-M/C catalyst (M= Pb, Cu) for efficient catalytic wet air oxidation of phenol wastewater under mild conditions. *J. Environ. Chem. Eng.* **2023**, 11(3), 109854.

Shepelin, N.A.; Tehrani, Z.P.; Ohannessian, N.; Schneider, C.W.; Pergolesi, D.; Lippert, T. A practical guide to pulsed laser deposition. *Chem Soc Rev.* **2023**.

Singh, L., Rekha, P. and Chand, S., 2018. Comparative evaluation of synthesis routes of Cu/zeolite Y catalysts for catalytic wet peroxide oxidation of quinoline in fixed-bed reactor. *J. Environ. Manag.* **2018**, 215, 1-12.

Singh, V.P.; Jasrotia, R.; Kumar, R.; Raizada, P.; Thakur, S.; Batoo, K.M.; Singh, M. A current review on the synthesis and magnetic properties of M-type hexaferrites material. *World J. Condens. Matter Phys.* **2018**, 8(02), 36.

Sirkar, K.K.; Shanbhag, P.V.; Kovvali, A.S. Membrane in a reactor. a functional perspective. *Ind. Eng. Chem. Res.* **1999**, 38(10), 3715-3737.

Soliman, N.K.; Moustafa, A.F. Industrial solid waste for heavy metals adsorption features and challenges; a review. *J. Mater. Res. Technol.* **2020**, *9*(5), 10235-10253.

Sun, W.; Lv, H.; Ma, L.; Tan, X.; Jin, C.; Wu, H.; Chen, L.; Liu, M.; Wei, H.; Sun, C. Use of catalytic wet air oxidation (CWAO) for pretreatment of high-salinity high-organic wastewater. *J. Environ. Sci.* **2022**, 120, 105-114.

Taghizadeh, M.; Aghili, F. Recent advances in membrane reactors for hydrogen production by steam reforming of ethanol as a renewable resource. *Chem. Rev.* **2019**, 35(3), 377-392.

Tekin, G.; Ersöz, G.; Atalay, S. Efficient mineralization of sugar industry wastewater by catalytic wet air oxidation as an eco-friendly method and its kinetic modelling. *Can. J. Chem. Eng*. **2023**, 101(7), 4076-4091.

Teoh, W.Y.; Amal, R.; Mädler, L. Flame spray pyrolysis: An enabling technology for nanoparticles design and fabrication. *Nanoscale*. **2010**, 2(8), 1324-1347.

Tufail, A.; Price, W.E.; Hai, F.I. A critical review on advanced oxidation processes for the removal of trace organic contaminants: A voyage from individual to integrated processes. *Chemosphere*. **2020**, 260, 127460.

Verma, V.; Ghosh, P.; Singh, S.B.; Gupta, V.; Chaudhari, P.K. 2022. Kinetics of catalytic treatment of coking wastewater (COD, phenol and cyanide) using wet air oxidation. *Int. J. Chem. React. Eng.* **2022**, 20(3), 325-341.

Wang, J.; Wang, S. Effect of inorganic anions on the performance of advanced oxidation processes for degradation of organic contaminants. *J. Chem. Eng.* **2021**, 411, 128392.

Wang, J.; Zhuan, R. Degradation of antibiotics by advanced oxidation processes: An overview. *Sci. Total Environ.* **2020**, 701, 135023.

Wang, L.; Geng, C.; Yu, D.; Liu, D.; Sun, H.; Xiao, K.; Zhao, H. Catalytic performance and mechanism of PTFE modified $NiCo_2O_4$ in high-salt organic wastewater treatment during wet air oxidation at ambient pressure. *Appl. Catal. B. Environ.* **2023**, 334, 122786.

Wang, P.; Liang, Y. N.; Zhong, Z.; Hu, X. Nano-hybrid bimetallic Au-Pd catalysts for ambient condition-catalytic wet air oxidation (AC-CWAO) of organic dyes. *Sep. Purif. Technol*. **2020**, 233, 115960.

Xiao, F.X.; Pagliaro, M.; Xu, Y.J.; Liu, B. Layer-by-layer assembly of versatile nanoarchitectures with diverse dimensionality. a new perspective for rational construction of multilayer assemblies. *Chem. Soc. Rev.* **2016**, 45(11), 3088-3121.

Yang, X.; Wang, Z.; Shao, L. Construction of oil-unidirectional membrane for integrated oil collection with lossless transportation and oil-in-water emulsion purification. *J. Membr. Sci.* **2018**, 549, 67-74.

Yao, X.; Zhang, Y.; Du, L.; Liu, J.; Yao, J. Review of the applications of microreactors. *Renew. Sustain. Energy Rev.* **2015**, 47, 519-539.

Zhang, B.; Qin, Y., Interface tailoring of heterogeneous catalysts by atomic layer deposition. *ACS Catal*. **2018**, 8(11), 10064-10081.

Zhang, T.; Liu, Y.; Zhong, S.; Zhang, L. AOPs-based remediation of petroleum hydrocarbons-contaminated soils. Efficiency, influencing factors and environmental impacts. *Chemosphere*. **2020**, 246, 125726.

Zhang, W.; Sun, W.; Zhang, Y.; Yu, D.; Piao, W.; Wei, H.; Liu, X.; Sun, C. Effect of inorganic salt on the removal of typical pollutants in wastewater by RuO_2/TiO_2 via catalytic wet air oxidation. *Chemosphere*. **2023**, 312, 137194.

Zhang, X.; Zhang, M.; Liu, H.; Gu, J.; Liu, Y. Environmental sustainability: a pressing challenge to biological sewage treatment processes. *Curr. Opin. Environ. Sci. Health.* **2019**, 12, 1-5.

Zhang, X.; Zhang, W.; Li, J.; Wang, T.; Miao, H.; Fan, Q.; Zhu, H.; Yang, Z.; Kong, C. Nanosized Co-Fe spinel quantum dots anchored on activated carbon for enhanced VOCs mineralization via PMS-based AOPs coupled with wet scrubber. *Sep. Purif. Technol*. **2024**, 328, 125135.

Zhang, Z.; Gao, Y.; Wang, Q. Fabrication, activity and mechanism studies of transition metal molybdate/molybdenum trioxide hybrids as novel CWAO catalysts. *Sep. Purif. Technol.* **2018**, 191, 354-363.

Zhao, J.; Wei, Y.; Liu, Z.; Zhang, L.; Cui, Q. Wang, H. Study on heterogeneous catalytic wet air oxidation process of high concentration MDEA-containing wastewater. *Chem. Eng. Process.: Process Intensif*. **2022**, 171, 108744.

Zheng, Y.; Li, X.; Dutta, P.K. Exploitation of unique properties of zeolites in the development of gas sensors. *Sensors*. **2012**, 12(4), 5170-5194.

Zhou, Y.; Xu, S.; Zhang, Y.; Hu, X.; Li, F.; Chen, X.; Cai, H.; Wang, J.; Shi, L.; Chen, X. Synergistic effect over a remarkable durable and active polymetallic Ru-doped Fe-Co-Ce/γ-Al_2O_3 nanocatalyst: Interfacial Lewis acid-base pair dependent reaction mechanism for landfill leachate. *J. Chem. Eng.* **2020**, 382, 122938.

APPENDIX A

CONVERSION ANALYSIS OF ACETIC ACID

A.1. Data for conversion of acetic acid using 1.5 wt. % Fe/Al_2O_3

Table1. Conversion using 1.5 wt. % Fe/Al_2O_3

Sl. No.	Temp (ºC)	Time	Vol.(V_1) (mL)	Vol. (ΔV) = (V_2-V_1) (mL)	RPM	Flowrate (L/min)	Sample	C_{ao}	C_a	% conversion (C_{ao}- C_a)/ C_{ao}* 100%
1	60	4.05	5	20	200	1.0	A.A.	0.4	C_{ao}= C_a=0.4	0
1.1. a.	60	4.05	5	17.2	200	1.0	A.A.	0.4	0.344	14
1.1. b.	60	4.15	5	16.6	200	1.0	A.A.	0.4	0.332	17
1.c	60	4.25	5	14.5	200	1.0	A.A.	0.4	0.29	27.5
1.2. a.	70	4.40	5	11	300	1.0	A.A.	0.4	0.22	45
1.2. b.	70	4.50	5	8.5	300	1.0	A.A.	0.4	0.17	57.5
1.2. c.	70	5.00	5	7	300	1.0	A.A.	0.4	0.14	65
1.2. a.	80	5.10	5	4.5	400	1.0	A.A.	0.4	0.09	77.5
1.3. b.	80	5.20	5	2.3	400	1.0	A.A.	0.4	0.046	88.5
1.3.c	80	5.30	5	2.5	400	1.0	A.A.	0.4	0.05	87.5
1.4	90	5.45	5	3.5	400	1.0	A.A.	0.4	0.07	82.5

A.2. BET Data

Table 2. Data from BET instrument

Relative Pressure	Volume at STP	1/[W((Po/P) - 1)]
0.0494523	15.5221	2.3232
0.0475667	17.2567	2.7216
0.1008252	19.0585	4.9719
0.152094	22.7056	7.3365
0.232132	21.1993	9.8725
0.291979	22.6302	11.915
0.303104	24.3477	14.293
0.459036	24.9052	15.074
0.920284	93.358	76.441
0.904593	85.6772	41.355
0.700878	56.7331	32.463
0.606589	39.4304	29.482
0.568046	33.3471	22.128
0.456206	27.7588	20.257
0.417499	26.3561	16.912
0.192285	26.2923	9.3255
0.0927142	20.778	4.62551

A.3. Data of Arrhenius Plot

Table 3. Data for ln k and 1/T to estimate the slope and intercept from the graph and temperature varies from 60º-90ºC

lnk	$\frac{1}{T}$ (K^{-1})
-4.677	0.003
-3.55	0.0029
-2.37	0.0028

A.4. Data of power law model

Table 4. Data ln r_{O_2} vs. ln C_{AA} for power law model plot

ln r_{O_2}	ln C_{AA}
-6.32	-1.108
-7.8116	-1.35
-5.27	-1.0.38

APPENDIX B

SAMPLE CALCULATIONS

B.1. Sample Calculation of different weight percentages

Iron III Nonahydrate- $Fe(NO_3)_3 . 9 H_2O$

Molecular weight of Fe= 55.845 u

Molecular weight of N= 14.0067 u

Molecular weight of O= 15.999 u

Molecular weight of H=1.00784 u

$Fe(NO_3)_3 . 9 H_2O$ = 55.845 + (14.0067*3) + {(15.999*3)*3} + 9(1.00784*2+15.999)

= 403.99 g/mol ~ 404 g/mol.

0.5 wt. % Fe= (404/55.845) * 0.5= 3.6171g

1 wt. % Fe= (404/55.845) * 1 = 7.2349 g

1.5 wt. % Fe=(404/55.845) * 1.5 = 10.8514 g

2 wt. % Fe = (404/55.845) * 2 = 14.4698 g

B.2. Calculation for conversion percentage using 1.5wt. % Fe/Al_2O_3

At 80ºC;

Before the addition of the catalyst,

Sample(V_1) = 5 mL; V_2=20 mL; S_2=0.1 N

$V_1S_1=V_2S_2$

$5*S_1=20*0.1$

Molarity= Strength/Basicity

$S_1 = (20*0.1)/5=0.4$

$C_a=0.4/1=0.4=C_{ao}$

$C_{ao} = 0.4$

From Table. 1 (Appendix A.1.),

1.3.a.

$V_1S_1=V_2S_2$ Sample(V_1) = 5 mL; V_2=4.5; S_2=0.1 N

$5*S_1=4.5*0.1$

$S_1 = (4.5*0.1)/5=0.09$

C_a= S1/Basicity=0.09/1 V=1L

C_a=0.09

X_a (%) = {(C_{ao}-C_a) / C_{ao}} * 100% = {(0.4-0.09)/0.4} * 100%= 77.5%

1.3.b.

$V_1S_1=V_2S_2$ Sample(V_1) = 5 mL; V_2=2.3; S_2=0.1 N

$5*S_1=2.3*0.1$

$S_1 = (2.3*0.1)/5=0.046$

C_a= S1/Basicity=0.046/1 V=1L

C_a=0.046

X_a (%) ={(C_{ao}-C_a) / C_{ao}} * 100% = {(0.4-0.046)/ 0.4* 100% = 88.5%

1.3.c.

$V_1S_1=V_2S_2$ Sample(V_1) = 5 mL; V_2= 2.5 mL; S_2=0.1 N

$5*S_1=2.5*0.1$

$S_1 = (2.5*0.1)/5=0.05$

C_a= S1/Basicity=0.05/1 V=1L

C_a=0.05

X_a (%) ={(C_{ao}-C_a) / C_{ao}} *100%= {(0.4-0.05)/0.4* 100% = 87.5%

B.3. Surface area calculation using BET equation

$\frac{p}{V\,(p_0 - p)} = \frac{1}{V_m.c} + \frac{c-1}{V_m.c}\,\frac{p}{p_0}$, represents the form of,

Y = mx + C. where, Y = $\frac{p}{V\,(p_0 - p)}$, x = $\frac{p}{p_0}$, m = $\frac{c-1}{V_m.c}$ and, C = $\frac{1}{V_m.c}$

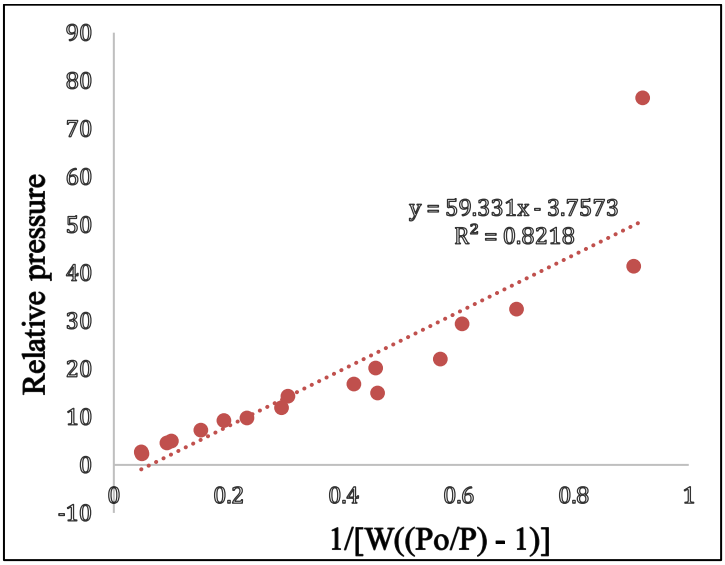


Fig.1. Relative Pressure vs. 1/[W((Po/P) - 1)]

From the above linear graph,

Slope (m) = 59.331, and intercept (C) = -3.7573

So,

$$V_m = \frac{1}{(Slope+Intercept)} = \frac{1}{(59.331-3.7573)} = 0.0179 \text{ cm}^3/\text{g}$$

and,

$$S_T = \frac{V_m \,.\, N \,.\, S}{v} m^2$$

or, $S_T = \frac{0.0179 \times 6.023\times10^{23} \times 0.162 \times 10^{-18}}{22.4}$

or, $S_{BET} = \frac{66.9224763}{0.8583} = 77.97 \text{ m}^2$

where, $S_{BET} = \frac{S_T}{a}$

V_m = monolayer volume in cm^3, N = Avogadro's No. (6.023×10^{23}), S = Cross-sectional area of a N_2 molecule (0.162 nm^2), v = molar volume of N_2 (22.4 L), V = amount of liquid N_2 adsorbed in cm^3/g of catalyst, p = vapour pressure of N_2 on the surface of material, p_0 =

Pressure at STP 1 atm or 760 mmHg, c = BET constant, S_T = total surface area (m^2), S_{BET} = BET surface area of the material (m^2/g)

B.4. Calculation of activation energy

We know,

$r_i = -\frac{dCa}{dt}$ and, $r_i = k.C_A$ (1st order assumption); $C_A = C_{A_0}.(1 - X_i)$

where, k= rate constant; C_{A_0} = initial concentration of Acetic acid=0.4

Now, to determine activation energy (E_a), we go for the expression,

$\ln k = \ln A - \frac{E_a}{RT}$

B.4.1. Determination of k_1

$r_i = \frac{(dca)}{dt} = -\frac{Caf-Cai}{dt} = -\frac{0.29-0.344}{20} = 0.0027$; $X_1 = 0.275$

$r_i = k.C_A = k.C_{A_0}.(1 - X_i) \Rightarrow 0.0027 = k_1 \times 0.4 \times (1 - 0.275)$

or, $k_1 = \frac{0.0027}{0.4\times(1-0.275)}$

or, $k_1 = 0.00931\ min^{-1}$

B.4.2. Determination of k_2

$r_i = \frac{(dca)}{dt} = -\frac{Caf-Cai}{dt} = -\frac{0.14-0.22}{20} = 0.004$ and $X_2 = 0.65$

or, $0.004 = k_2 \times 0.4 \times (1 - 0.65)$

or, $k_2 = \frac{0.004}{0.4\times(1-0.65)} = 0.02857\ min^{-1}$

B.4.3. Determination of k_3

$r_i = \frac{(dca)}{dt} = -\frac{Caf-Cai}{dt} = -\frac{0.05-0.14}{20} = 0.0045$; $X_3 = 0.885$

$r_i = k.C_A = C_{A_0}.(1 - X_i)$

or, $0.0043 = k_3 \times 0.4 \times (1 - 0.885)$

or, $k_3 = \frac{0.0043}{0.4 \times (1 - 0.885)}$

or, $k_3 = 0.093478$ 3 min

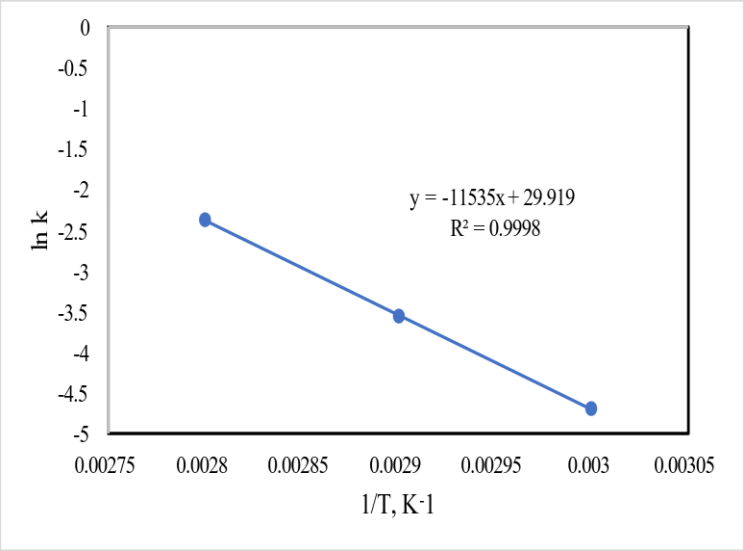


Fig.2. ln k vs 1/T

Slope $(-\frac{E_a}{R}) = -11535$ K

or, Ea = (11535 × 8.314) J/mol

or, Ea = 95901 J/mol = 95.901 kJ/mol.

B.5. Calculation of order for O_2 and acetic acid using the Power Law Model

Considering, T = 80^0C, k = 0.38043 min^{-1} (optimum value is taken, gives the maximum conversion of benzene), and ln k = -0.96645

To determine r_{O_2},

$$r = \frac{(\text{Oxygen flow rate} \times \text{density of oxygen} \times \text{Conversion})}{(\text{Mol.wt..of oxygen} \times \text{Mass of catalyst} \times \text{Mass percentage of impregnated metal})}$$

To determine the order for H_2 and benzene, the Power Law equation is, $r = k.C_{O_2}^{n}.C_{AA}^{m}$

Where, n = order of O_2

m = order of acetic acid

C_{O_2} = concentration of O_2

C_{AA} = concentration of AA

Since the presence of O_2 gas is higher as compared to acetic acid so, the flow rate is taken for O_2 gas only.

B.5.1. 1st data point for r_{O_2} and ln C_{AA}

$(r_{O_2})_1 = \frac{(0.209 \times 1.43 \times 0.275)}{(32 \times 1 \times 1.5)}$ = 0.0018 mol/g.min

and, lnr_{O_2} = n_1 ln C_{AA} + ln k

or, -6.32= -1.108 n_1 – 3.9654

or, n_{O_2} = 2.1

B.5.2. 2nd data point for r_{O_2} and ln C_{AA}

$(r_{O_2})_2 = \frac{(0.209 \times 1.43 \times 0.065)}{(32 \times 1 \times 1.5)}$ = 0.000405 mol/g.min

and, lnr_{O_2} = n_2 ln C_{AA} + ln k

or, -7.8116 = -1.35n_{O_2} –3.55

or, n_2 = 3.15

B.5.3. 3rd data point for r_{O_2} and ln C_{AA}

$(r_{O_2})_3 = \frac{(0.209\times1.43\times0.885)}{(32\times1\times1.5)}$ = 0.0051 mol/g.min

and, lnr_{O_2} = n_3 ln C_{AA} + ln k

or, -5.27=-1.038 n_2 -2.37 or, n_3 =2.79

B.6. Calculation of TGA weight loss

B.6.1. First stage weight loss calculation

Initial weight percentage from the Y-axis of graphical interpretation = 99.8%

Final weight % = 91.5 %

Change of % weight = 8.3 %

B.6.2. Second stage weight loss calculation

Initial weight percentage from the Y-axis of graphical interpretation = 91.5 %

Final weight % =88.023 %

Change of % weight = 3.8 %

B.6.3. Third stage weight loss calculation

Initial weight percentage from the Y-axis of graphical interpretation = 88.023 %

Final weight % = 83.18

Change of % weight = 5.5 %

APPENDIX C

IMAGES OF USED INSTRUMENTS AND CHEMICALS

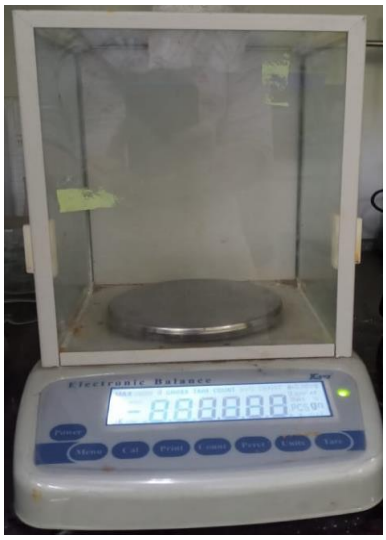


Fig.1. Weighing machine

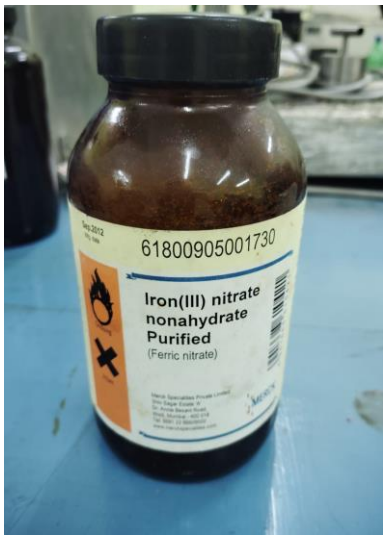


Fig.2. Iron (III) nitrate nonahydtrate

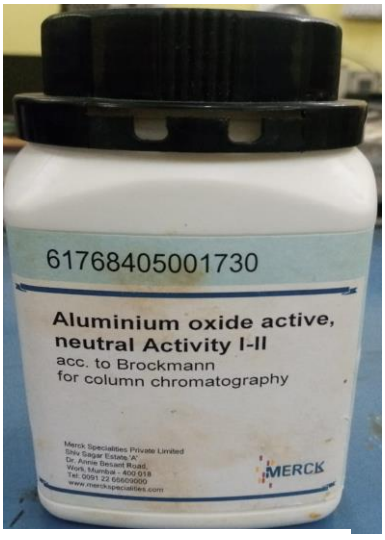


Fig.3. Al_2O_3 support salt



Fig.4. Magnetic hot plate



Fig.5. Hot air oven



Fig.6. Calcination chamber



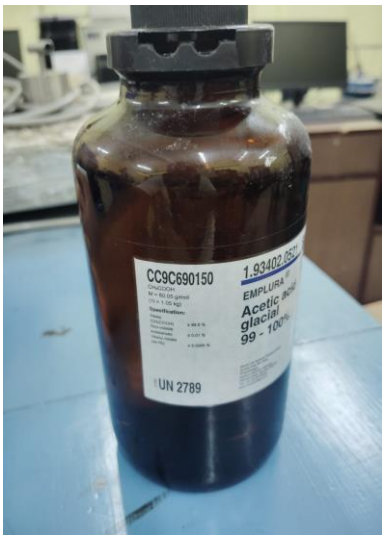


Fig.7. Three neck bottom glass reactor for oxidation reaction of acetic acid solution.

BIODATA

Name - Soumyajit Das

Father's Name - Sambhunath Das

Address- Nonatola Lane, Hatkhola, Chandannagar, Hooghly, West Bengal, Pin-712136.

Details of academic qualifications:

Name of Examination	**Name of School**	**Name of Board /University**	**% marks obtained**
Madhyamik Pariksha	Sri Aurobindo Vidyamandir	West Bengal Board of Secondary Education	84.14
Higher Secondary Examination	Kanailal Vidyamandir	West Bengal Council of Higher Secondary Education	67.9
B.E. (Chemical Engineering)	Jadavpur University	Jadavpur University	67.18
M.E. (Chemical Engineering)	Jadavpur University	Jadavpur University	82.5 (upto 2nd semester)